

INFORMATION TO USERS

This manuscript has been reproduced from the microfilm master. UMI films the text directly from the original or copy submitted. Thus, some thesis and dissertation copies are in typewriter face, while others may be from any type of computer printer.

The quality of this reproduction is dependent upon the quality of the copy submitted. Broken or indistinct print, colored or poor quality illustrations and photographs, print bleedthrough, substandard margins, and improper alignment can adversely affect reproduction.

In the unlikely event that the author did not send UMI a complete manuscript and there are missing pages, these will be noted. Also, if unauthorized copyright material had to be removed, a note will indicate the deletion.

Oversize materials (e.g., maps, drawings, charts) are reproduced by sectioning the original, beginning at the upper left-hand corner and continuing from left to right in equal sections with small overlaps.

Photographs included in the original manuscript have been reproduced xerographically in this copy. Higher quality 6" x 9" black and white photographic prints are available for any photographs or illustrations appearing in this copy for an additional charge. Contact UMI directly to order.

**Bell & Howell Information and Learning
300 North Zeeb Road, Ann Arbor, MI 48106-1346 USA
800-521-0600**

UMI[®]

**REGULATION OF GENE EXPRESSION AND CELL GROWTH BY
TRANSCRIPTIONAL PROTEINS OF THE INTERFERON SYSTEM**

by

Hannah Anh-Quan NGUYEN

A thesis submitted to the Faculty of Graduate Studies and Research
in partial fulfillment of the requirements for the degree of
Doctor of Philosophy

Department of Microbiology and Immunology

McGill University, Montreal

July 1998

© 1998 Hannah Anh-Quan Nguyen



National Library
of Canada

Acquisitions and
Bibliographic Services

395 Wellington Street
Ottawa ON K1A 0N4
Canada

Bibliothèque nationale
du Canada

Acquisitions et
services bibliographiques

395, rue Wellington
Ottawa ON K1A 0N4
Canada

Your file *Votre référence*

Our file *Notre référence*

The author has granted a non-exclusive licence allowing the National Library of Canada to reproduce, loan, distribute or sell copies of this thesis in microform, paper or electronic formats.

The author retains ownership of the copyright in this thesis. Neither the thesis nor substantial extracts from it may be printed or otherwise reproduced without the author's permission.

L'auteur a accordé une licence non exclusive permettant à la Bibliothèque nationale du Canada de reproduire, prêter, distribuer ou vendre des copies de cette thèse sous la forme de microfiche/film, de reproduction sur papier ou sur format électronique.

L'auteur conserve la propriété du droit d'auteur qui protège cette thèse. Ni la thèse ni des extraits substantiels de celle-ci ne doivent être imprimés ou autrement reproduits sans son autorisation.

0-612-44532-1

Canada

*To Ông Bà Ngoại and Ông Nội,
who are looking over me*

*To Bà Nội, for her wonderful smile, and
Chuong, for listening*

*To Dad and Mom, who taught me
perseverance, ambition and discipline*

*To Annette, for being there for me, and
Jean-Claude, pour les soirées de "Beigne"*

*et à Richard, pour sa capacité de donner,
comprendre et pardonner...*

ABSTRACT

The Interferon Regulatory Factors (IRFs) are a family of interferon-inducible proteins which play distinct roles in diverse processes such as pathogen response, cytokine signalling, cell growth regulation and hematopoietic development. The objective of this research was to investigate the mechanisms by which IRF-1 and IRF-2 regulate gene expression and cell growth. Structure-function analyses of the IRF-2 protein demonstrate that transcriptional repression by IRF-2 is contained within the first 125 N-terminal amino acids and correlates directly with IRF-2 DNA binding. Overexpression of functional IRF-2 deletion mutant proteins in NIH3T3 cells results in oncogenic transformation and tumorigenesis, suggesting that IRF-2 oncogenicity correlates directly with transcriptional repression. Similar structure-function analyses localize IRF-1 transactivation to the C-terminus. Like IRF-1, hybrid constructs which fuse the DNA binding domain of IRF-1 and IRF-2 to the transactivation domain of NF- κ B RelA(p65) are transcriptional activators. Inducible expression of IRF-1 and IRF/RelA in NIH3T3 cells results in reduced cellular growth and induction of apoptosis. Furthermore, expression of the PKR, STAT1(p91), and WAF1 growth regulatory proteins are elevated following induction of IRF-1 or IRF/RelA, correlating transactivation function and tumor suppressor activity of IRF-1 or IRF/RelA. By RNA fingerprinting, the secretory leukocyte protease inhibitor (SLPI) was identified as the first gene whose expression is downregulated by IRF-1 or IRF-1/RelA. A region in the SLPI promoter was identified that bound IRF-1, suggesting a direct mechanism for IRF-1 regulation of SLPI expression.

RESUME

Les protéines régulatrices IRFs (Interferon Regulatory Factors) appartiennent à la famille de protéines induites par les interférons et jouent des rôles distincts à différents niveaux : dans la réponse à des agents pathogènes, les cascades de transduction du signal induit par les cytokines, la régulation de la prolifération cellulaire et le développement hématopoïétique. L'objectif de ce travail a consisté en l'étude des mécanismes par lesquels IRF-1 et IRF-2 régulent l'expression génique et la prolifération cellulaire. L'analyse de la relation entre la structure et la fonction de la protéine IRF-2 démontre que la répression transcriptionnelle induite par IRF-2 dépend des 125 premiers acides aminés localisés dans le domaine N-terminal de la protéine. Ce domaine est également impliqué dans la fixation de IRF-2 à l'ADN. La surexpression de mutants de délétion fonctionnels de IRF-2 dans les cellules NIH3T3 déclenche la transformation oncogénique des cellules, ainsi que la tumorigénese suggérant que l'effet oncogénique de IRF-2 est en corrélation directe avec la répression transcriptionnelle. Une analyse similaire de la structure et de la fonction montre que l'activité transactivatrice de IRF-1 est localisée dans sa partie C-terminale. Des constructions hybrides contenant les domaines de fixation de IRF-1 ou de IRF-2 et le domaine de transactivation de NF- κ B RelA(p65), sont capables d'activer la transcription à un niveau comparable à celui de IRF-1. L'expression induite de IRF-1 et de IRF/RelA dans des cellules NIH3T3 est responsable de la diminution de la prolifération cellulaire et provoque l'apoptose de ces cellules. De plus, en réponse à l'induction de IRF-1 ou IRF/RelA, une expression plus élevée des protéines impliquées dans la prolifération cellulaire telles que la PKR, STAT1 (p91) et WAF1 est observée en corrélation avec les fonctions de transactivation et l'activité suppresseur de tumeurs de IRF-1 et de IRF/RelA. Au cours de ce travail, nous avons identifié grâce à la méthode de "RNA fingerprinting" la molécule SLPI (Secretory Leukocyte Protease Inhibitor), premier exemple d'un gène réprimé par IRF-1 et IRF/RelA. Cette étude a également montré que IRF-1 se fixe sur la région promotrice du gène SLPI, ce qui suggère un mécanisme direct de régulation de l'expression de SLPI par IRF-1.

ACKNOWLEDGEMENTS

I would like to express my deepest gratitude to Dr. John Hiscott for his utmost support and guidance not only as a PhD supervisor but also as a friend, psychologist and Swiss travel guide. I would also like to acknowledge John for his infinite attempts to convert me into a morning person.

My PhD would also not have been possible without my scientific bible, Dr. Rongtuan Lin. I will spend the rest of my life trying to be as technically efficient as he is. Among the many memories of Dr. Lin, I will especially remember his great sense of discipline, his numerous Ziploc bags filled with eppendorf tubes containing cloning intermediates, "Fig legs", and "There are no more BEAK!".

During my PhD studies I had the rare opportunity to meet a wonderful lab-mate. Louisa Petropoulos has been an unconditional listening ear and just being herself has added much fun and adventure in the lab. I would like to thank Louisa for her friendship and for constantly reminding me of all the letters in the alphabet.

I would also like to thank my lab neighbour and friend Dr. Michèle Algarté for having endured my complaining and for having taught me many "expressions françaises" such as "Je vais étudier mes Westernes et les autres manipe dans mon appart ce we pendant l'aprèm." I wish to acknowledge Michèle, Dr. Pierre Génin and Christophe Heylbroeck for the french translation of the Abstract. I am also indebted to Pierre for use of his portable computer during preparation of this thesis and will remember his practical jokes and his many attempts to become a godfather.

A special thank-you to Lindsay Teskey for a great second pair of hands. I was especially spoiled by her good nature and her enviable optimism.

I am thankful to all other past and present members of the lab for useful scientific discussions and for establishing a wonderful working atmosphere, particularly Dr. Pierre Beauparlant, Richard Bitar, Sonia Cisternas, Dr. Pascale Crépieux, Carmela DeLuca, Wai-gin Fong, Jenny Garoufalis, Ivy Kwan, Hakju Kwon, Raymond Lee, Yaël Mamane, Nadine Pelletier, Normand Pépin, Nicolas Solban, Will Spencer and Dana Zmeureanu. I would also like to thank Mrs. Mary Wiebe for being there when I needed her and for having kept us so organized.

I am grateful to the Fonds pour les Chercheurs et à l'Aide à la Recherche (FCAR) for supporting me financially during my PhD career. I am also indebted to Drs. Mark Wainberg and Antonis Koromilas for their support and good advice.

PREFACE

In accordance with the "Guidelines for Thesis Preparation", the candidate has chosen to present the results of her research in classical form. A general introduction is presented in chapter I and appears in part in the following review articles:

1. Hiscott, J., Nguyen, H., and Lin R. 1995. Molecular Mechanisms of Type I Interferon Induction, in: *Seminars in Virology*, vol. 6, Pitha, P. (ed.), Academic Press Ltd., London, pp. 161-173.
2. Nguyen, H., Hiscott, J., and Pitha, P. 1998. The Growing Family of IRF Transcription Factors. *Cyt. & Growth Fact. Rev.* 8, (*in press*)

The materials and methods used in this thesis are presented in chapter II. The results are described in chapters III to VI and appear in part in the following journal articles, in the same order:

3. Lin, R., Mustafa, A., Nguyen, H., Gewert, D., and Hiscott, J. 1994. Mutational Analysis of Interferon (IFN) Regulatory Factors 1 and 2: Effects on the Induction of IFN- β Gene Expression. *J. Biol. Chem.* 269, 17542-17549.
4. Nguyen, H., Mustafa, A., Hiscott, J. and Lin, R. 1995. Transcription Factor IRF-2 Exerts Its Oncogenic Phenotype Through the DNA Binding Transcription Repression Domain. *Oncogene* 11, 537-544.
5. Nguyen, H., Lin, R., Hiscott, J. 1997. Activation of Multiple Growth Regulatory Genes Following Inducible Expression of IRF-1 or IRF/RelA Fusion Proteins. *Oncogene* 15, 1425-1435.

6. Nguyen-Raymond, H., Teskey, L., Hiscott, J. Identification of the Secretory Leukocyte Protease Inhibitor (SLPI) as an IRF-1-Repressed Gene. (*manuscript in preparation*).

Chapter III presents the introductory studies leading to the basis for the work presented in Chapters IV to VI. Specific contributions to the work described in Chapter 3 are as follows:

Dr. Rongtuan Lin was responsible for the construction of the IRF-1/RelA and IRF-2/RelA fusion proteins represented in Figure 14, and contributed to the construction of the IRF-1 and IRF-2 deletion mutants.

Amir Mustafa was responsible for the construction of the IRF-1 and IRF-2 deletion mutants, as well as the results presented in Figures 9 and 11 to 14.

The candidate was responsible for the construction of the IRF-2 (100) mutant as well as the results presented in Figure 10.

All the research described in Chapters IV to VI was performed by the candidate with the following exception: Dr. Rongtuan Lin was responsible for the modification and subsequent perfection of the tetracycline-inducible system. The candidate wishes to acknowledge the excellent technical assistance of Lindsay Teskey for the work published in Chapter VI. A discussion is presented in Chapter VII. References for all chapters are grouped at the end of the thesis.

The candidate was also involved in collaboration with other researchers in the laboratory which resulted in the following publications:

7. Hiscott, J., Marois, J., Garoufalidis, J., D'Addario, M., Roulston, A., Kwan, I., Pépin, N., Lacoste, J., Nguyen, H., Benzi, G., and Fenton, M. 1993. Characterization of a Functional NF- κ B site in the Human Interleukin-1 β Promoter. *Mol. Cell. Biol.* 13, 6231-6240.
8. Lin, R., Heylbroeck, C., Nguyen, H., Algarté, M., Génin, P., Pitha, P.M. and Hiscott, J. 1998. The Role of the IRF-3 Transcription Factor in Interferon Gene Expression. *Biochimie (in press)*.
9. Algarté, M., Nguyen-Raymond, H., Lin, R., Hiscott, J. Differential Regulation of Interferon- β Gene Transcription by I κ B α and I κ B β . (*manuscript in preparation*).

TABLE OF CONTENTS

	Page
Abstract	i
Résumé	ii
Acknowledgements	iii
Preface	v
Table of Contents	viii
List of Figures and Tables	xv
List of Abbreviations	xviii
CHAPTER I GENERAL INTRODUCTION	1
1 The IFN- β Promoter: model of inducible gene expression.....	3
1.1 NF- κ B/Rel interactions with PRDII.....	7
1.1.1 Overview of the NF- κ B/Rel transcription factors....	7
1.1.2 I κ B regulation of NF- κ B activity.....	8
1.1.3 Virus-induced modulation of NF- κ B/I κ B activity: effect on IFN- β induction.....	10
1.2 IRF interactions with PRDI and PRDIII.....	15
1.3 ATF/CREB interactions with PRDIV.....	15
1.4 HMG protein interactions with PRDII and PRDIV.....	16
1.5 The IFN- β enhanceosome: synergism between PRDs.....	18

	Page
2 The Growing Family of Interferon Regulatory Factors.....	23
2.1 IRF-1 and IRF-2.....	35
2.1.1 The role of IRF-1 and IRF-2 in cell growth regulation.....	36
2.1.2 Involvement of IRF-1 and IRF-2 in immune regulation.....	38
2.1.3 IRF-1-dependent and -independent pathways for Type I IFN gene induction.....	39
2.2 IRF-3.....	45
2.3 ISGF3γ/p48.....	50
2.3.1 Role of p48 and ISGF3 in type I IFN activation.....	51
2.4 ICSBP.....	53
2.5 Pip/LSIRF/IRF-4/ICSAT.....	57
2.6 IRF-7.....	61
2.7 The viral IRFs.....	63
2.8 Cross-regulation of expression among the IRF family members.....	65
 RESEARCH OBJECTIVE AND SPECIFIC AIMS.....	 68
 CHAPTER II MATERIALS AND METHODS.....	 69
1 Plasmid construction.....	70
1.1 IRF deletion mutants.....	70
1.2 IRF/RelA fusion proteins.....	71
1.3 Recombinant IRF proteins.....	72
1.4 Tetracycline-regulated expression plasmids.....	72

	Page
2. Purification of IRF recombinant proteins.....	73
3. Preparation of IRF-specific antisera.....	73
4. Cell culture and generation of cell lines.....	74
4.1 Transient transfection and reporter gene assay.....	74
4.2 Generation of IRF-2 expressing cell lines.....	75
4.3 Generation of inducible IRF-1 and IRF/RelA cell lines.....	75
5. Analysis of growth phenotype.....	76
5.1 Measurement of growth rate.....	76
5.2 Determination of saturation density.....	76
5.3 Soft agar assay.....	76
5.4 Tumorigenicity in nude mice.....	77
5.5 Microscopic detection of apoptosis.....	77
6. Western blot analysis.....	77
7. Electrophoretic mobility shift assay.....	78
7.1 Oligonucleotide probes.....	78
7.2 Extract preparation and analysis.....	79
7.2.1 Detection of IRF DNA binding.....	79
7.2.2 Detection of STAT1 and ISGF3 DNA binding.....	81
8. RNA detection.....	82
8.1 RNA isolation.....	82
8.2 Reverse transcriptase-PCR assay.....	82
8.3 Northern blot analysis.....	82
8.4 RNA fingerprinting.....	83

	Page
9. DNase I footprinting.....	83
9.1 Preparation of DNA.....	83
9.2 Ladder formation and footprinting reactions.....	83
CHAPTER III MUTATIONAL ANALYSIS OF INTERFERON REGULATORY FACTORS-1 AND -2: EFFECTS ON THE INDUCTION OF INTERFERON-β GENE EXPRESSION.....	85
Construction of IRF-1 and IRF-2 deletion mutants.....	86
Repression by IRF-2 deletions.....	86
DNA binding activity of IRF-2 deletion mutants.....	87
Transcriptional activation by IRF-1 deletion mutants.....	90
Repression by IRF-1 deletion mutants.....	98
Activity of IRF/NF- κ B RelA fusion proteins.....	101
CHAPTER IV TRANSCRIPTION FACTOR IRF-2 EXERTS ITS ONCOGENIC PHENOTYPE THROUGH THE DNA BINDING/TRANSCRIPTION REPRESSION DOMAIN.....	109
IRF-1 and IRF-2 specific antisera.....	110
Establishment of NIH3T3 cells expressing full-length and deletion mutant IRF-2 proteins.....	111
Growth and tumorigenic properties of the full length and deletion mutant IRF-2 expressing clones.....	121
Virus and dsRNA inducibility of IFN- β mRNA in IRF-2 expressing cells.....	127
Displacement of IRF-1 by IRF-2 in DNA binding assays.....	130

CHAPTER V	ACTIVATION OF MULTIPLE GROWTH REGULATORY GENES FOLLOWING INDUCIBLE EXPRESSION OF IRF-1 OR IRF/RELA FUSION PROTEINS.....	134
	Establishment of NIH3T3 cells inducibly expressing IRF-1 and the IRF/RelA fusion proteins.....	135
	Growth-suppressive and apoptotic properties of the inducible IRF-1 and IRF/RelA cell lines.....	143
	Expression of PKR in the IRF-1 and IRF/RelA inducible cell lines.....	150
	Expression of STAT1 (p91) in the IRF-1 and IRF/RelA inducible cell lines.....	153
	Expression of WAF1 in the IRF-1 and IRF/RelA inducible cell lines.....	158
CHAPTER VI	IDENTIFICATION OF THE SECRETORY LEUKOCYTE PROTEASE INHIBITOR (SLPI) AS A TARGET OF IRF-1 REGULATION.....	162
	RNA fingerprinting of cell lines inducibly expressing IRF-1/RelA.....	163
	dsRNA activation of SLPI mRNA in the IRF-1 and IRF/RelA inducible cell lines.....	168
	IFN γ -inducible DNA binding to potential ISRE and NF- κ B sites in the human SLPI promoter.....	173
	Detection of IRF-1 binding activity at two regions of the SLPI promoter, distinct from BS1 and BS2.....	179
	Detection of IRF-1 binding to a -200 region in the SLPI promoter by DNase I footprinting.....	179

	Page
CHAPTER VII DISCUSSION.....	185
Structure-function analysis of IRF-1.....	186
Structure-function analysis of IRF-2.....	188
IRF-2 repression dominates IRF-1 activation.....	189
IRF-1/RelA and IRF-2/RelA mimic IRF-1 transactivation function.....	189
Localization of IRF-2 oncogenic activity.....	190
IRF-2 regulation of dsRNA and Sendai virus mediated IFN gene activation.....	191
Control of cell growth and expression of growth regulatory genes by IRF-1 and IRF/RelA.....	192
IRF-1 regulation of PKR expression.....	193
IRF-1 regulation of STAT1 (p91) expression.....	194
IRF-1 regulation of WAF1 (p21) expression.....	195
SLPI, a novel IRF-1-regulated gene	198
Model for the regulation of SLPI expression.....	201
 CONTRIBUTIONS TO ORIGINAL KNOWLEDGE.....	 204
 REFERENCES.....	 206

LIST OF FIGURES AND TABLES

Chapter I (General Introduction)

		Page
Figure 1	Nucleoprotein interactions contributing to positive and negative control of IFN- β gene expression.....	6
Figure 2	Virus-induced modulation of NF- κ B/I κ B activity and expression of the IFN- β gene.....	12
Figure 3	Model for synergistic activation of transcription by the IFN- β enhanceosome.....	22
Table 1	Genbank accession numbers of human, murine, avian and viral coding sequences of the IRF family members....	25
Figure 4	Schematic representation of the IRF proteins.....	27
Figure 5	Extensive homology among the IRF DNA binding domains.....	29
Table 2	Percent identities among the N- and C-termini of the IRF family members.....	31
Figure 6	Functional domains of previously characterized IRF family members.....	33
Figure 7	Schematic for the induction of Type I IFN genes by dsRNA and Newcastle Disease Virus.....	43
Figure 8	Model for virus-mediated activation of IRF-3.....	49
Table 3	Summary of IRF properties and functions.....	67

Chapter II (Materials and Methods)

		Page
Table 4	Description and sequence of EMSA oligonucleotide probes.....	80

Chapter III

Figure 9	Analysis of IRF-2 deletion mutants in repression assays..	89
Figure 10	DNA binding activity of the IRF-2 deletion mutants.....	92
Figure 11	Analysis of IRF-1 deletion mutants.....	94
Figure 12	Analysis of IRF-1 deletion mutants in activation and repression assays.....	97
Figure 13	Activation of the IFN- β promoter by NF- κ B and IRF-1 deletion mutants.....	100
Figure 14	Activity of IRF-1/RelA and IRF-2/RelA fusion proteins..	102

Chapter IV

Figure 15	IRF-1 and IRF-2 peptide specific antisera.....	113
Figure 16	Expression of IRF-2 RNA in full-length and deletion mutant IRF-2 clones.....	118
Figure 17	DNA binding activities of the full-length and deletion mutant IRF-2 clones.....	120
Table 5	Growth and tumorigenic properties of full-length and and deletion mutant IRF-2 clones.....	124

	Page
Figure 18 Soft agar colonies of FL and deletion mutant IRF-2 clones.....	126
Figure 19 IFN- β RNA levels in the IRF-2(FL), IRF-2 (160), and IRF-2 (100) cell lines.....	129
Figure 20 Displacement of IRF-1 by IRF-2 and IRF-2 (160) in mobility shift assays.....	133

Chapter V

Figure 21 Tetracycline-regulated expression of IRF-1 and IRF/RelA.....	137
Figure 22 Inducible expression of IRF-1 and IRF/RelA in NIH3T3 cells.....	139
Figure 23 DNA binding activities in rtTA-IRF-1 and rtTA-IRF/RelA expressing cells.....	141
Figure 24 Growth suppressive and apoptotic properties of IRF-1 and IRF/RelA.....	145
Figure 25 Expression of PKR in IRF-1 and IRF/RelA expressing cells.....	152
Figure 26 Expression of STAT1 (p91) in IRF-1 and IRF/RelA expressing cells.....	155
Figure 27 STAT1 binding activity in IRF-1 and IRF/RelA expressing cells.....	157
Figure 28 Expression of WAF1 in IRF-1 and IRF/RelA expressing cells.....	160

Chapter VI

	Page
Figure 29 The RNA fingerprinting method.....	165
Figure 30 RNA fingerprint of rtTA and rtTA-IRF-1/RelA cells.....	167
Figure 31 Expression of SLPI mRNA in rtTA-IRF-1/RelA cells.....	170
Figure 32 SLPI mRNA in dsRNA treated IRF-1 and IRF-1/RelA cells.....	172
Figure 33 IFN γ -inducible DNA binding activity to the SLPI promoter.....	176
Figure 34 Detection of IRF-1 binding to the SLPI promoter by mobility shift assays.....	181
Figure 35 Localization of IRF-1 binding to the SLPI promoter by DNase I footprinting.....	184

Chapter VII (Discussion)

Figure 36 Model for the regulation of SLPI expression.....	203
---	-----

LIST OF ABBREVIATIONS

-/-	knockout
aa	amino acid
bp	base pairs
CBP	CREB binding protein
CCE	cell-cycle element
CIP	calf intestinal phosphatase
CKII	casein kinase II
ConA	concanavalin A
CREB/ATF	c-AMP-responsive element binding factor/activating transcription factor
DBD	DNA binding domain
Dox	doxycycline
DSP-1	dorsal switch protein-1
dsRNA	double-stranded RNA
EBV	Epstein Barr virus
EMCV	encephalomyocarditis virus
EMSA	electrophoretic mobility shift assay
FL	full-length
GBP	guanylate-binding protein
H4	histone 4
HHV-8/KSHSV	Human herpes virus-8/Kaposi's sarcoma herpes simplex virus
HIV-1	human immunodeficiency virus-1
HMG	high mobility group
HSV	herpes simplex virus
HTLV-1	human T-cell leukemia virus-1
IAD	IRF association domain
ICS	interferon consensus site
ICSAT	interferon consensus binding protein in activated T-cells or in adult T-cell leukemia
ICSBP	interferon consensus binding protein
IFN	interferon
Ig	immunoglobulin
I κ B	inhibitory factor kappa B
IL-1, -2, -6, -12	interleukin-1, -2, -6, -12
IRF	interferon regulatory factor
IRF-E	interferon regulatory factor-element
ISGF	interferon stimulated gene factor
ISRE	interferon stimulated response element
JAK-STAT	Janus kinase-signal transducer and activator of transcription
LCMV	lymphocytic choriomeningitis virus
LIF	leukemia inhibitory factor

LPS	lipopolysaccharide
LSIRF	lymphoid-specific IRF
MDS	myelodysplastic syndrome
MEFs/EFs	mouse embryonic fibroblasts
MHC	major histocompatibility complex
NDV	NewCastles Disease Virus
NF- κ B	nuclear factor-kappa B
NK	natural killer
NES	nuclear export signal
NLS	nuclear localization sequence
NO	nitric oxide
iNOS	inducible nitric oxide synthase gene
NPM	nucleophosmin
NRE	negative regulatory element
nt	nucleotides
2'5'OAS	2'-5' oligoadenylate synthetase
Pip	PU.1 interaction partner
PMA	phorbol 12-myristate 13-acetate
PKR	double-stranded RNA dependent kinase
PRD	positive regulatory domain
RNA polII	RNA polymerase II
Ser	serine
SLPI	secretory leukocyte protease inhibitor
Thr	threonine
TNF	tumor necrosis factor
Tyr	tyrosine
VIF	virus-induced factor
VSV	vesicular stomatitis virus
VV	vaccinia virus

CHAPTER I

GENERAL INTRODUCTION

Interferons (IFNs) are a large family of multifunctional secreted proteins involved in antiviral defense, cell growth regulation and immune activation (reviewed in (210)). The biomodulatory activities pertinent to this group of cytokines have been extensively exploited at the clinical level, and are used in therapy for many hematological malignancies and multiple sclerosis (67). Interferons are classified into three distinct groups, designated IFN- α , IFN- β , (collectively grouped as Type I IFNs) and IFN- γ (Type II IFN). The alpha interferons consist of a multigene family with at least 20 genes and pseudogenes, while single IFN- β and IFN γ genes have been described (80,143).

Genes encoding the interferons are normally silent, but can be activated rapidly by a diverse group of natural and synthetic agents, such as viruses, synthetic polyribonucleotides and antigens (126,210). Infected cells produce a mixture of IFNs characteristic of the infected cell (7,82,126). Type I IFNs are produced by a variety of cell types, while type II IFN is produced by T-cells and natural killer (NK) cells (210). Newly synthesized IFN interacts with neighbouring cells through cell surface receptors, resulting in the rapid and efficient synthesis of over 30 new cellular proteins through the activation of the JAK-STAT family of cellular transcription factors (reviewed in (41,87,173)). These events represent the means by which IFNs induce the antiviral state that constitutes the primary host defense in innate immunity.

Among the many virus and IFN-inducible proteins are a growing family of transcription factors, the Interferon Regulatory Factors (IRFs). The IRF-1 and IRF-2 proteins, the best characterized members of this family, are the main focus of this thesis. Their discovery preceded the recent expansion of this group of IFN-responsive proteins to over 10 members.

This introduction is divided into two main sections. Since IRF-1 and IRF-2 were originally identified by studies of the transcriptional regulation of the human IFN- β gene (55,58,72,138), the first section describes the IFN- β gene promoter as a well characterized model of inducible gene expression. Analysis of this promoter delineates several interactive domains involving the NF- κ B/Rel, IRF, ATF/CREB and HMG protein families that contribute to a complex but elegant transcriptional switch from repression to induced synergistic activation of IFN- β gene expression. The second section provides a detailed description of previously characterized IRF family members. Studies analyzing IRF-expressing cell lines and IRF knockout mice reveal that each member of the IRF family exerts distinct roles in biological processes such as pathogen response, cytokine signalling, cell growth regulation and hematopoietic development. Understanding the molecular mechanisms by which the IRFs affect these important cellular events and IFN expression will contribute to a greater understanding of events leading to various viral, immune and malignant disease states and will suggest novel strategies for antiviral and immune modulatory therapy.

1 The IFN- β promoter: model of inducible gene expression

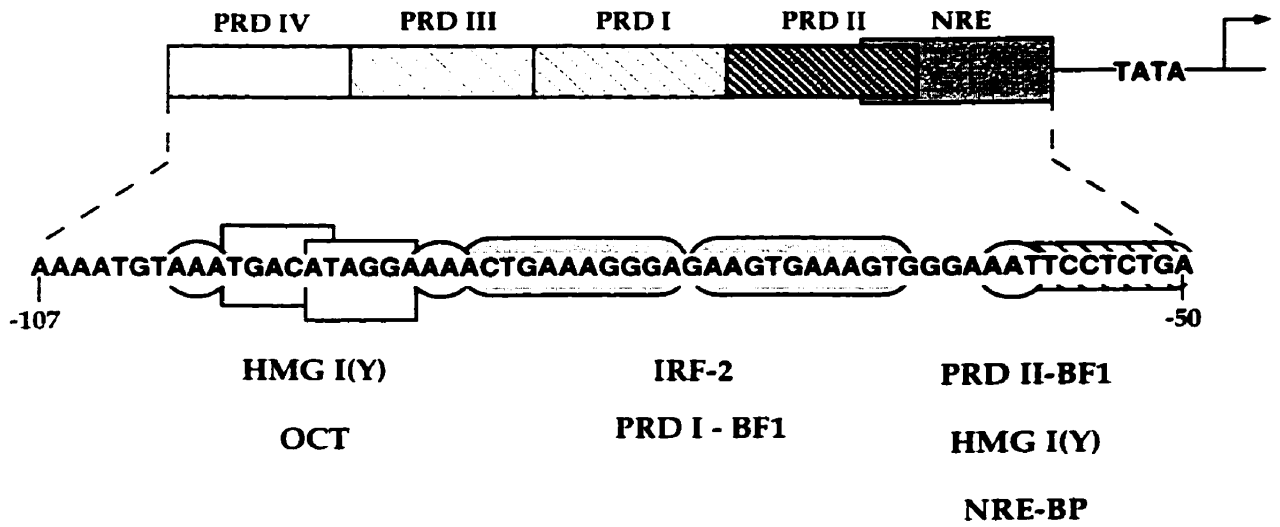
The Type 1 interferon genes (IFN- α and IFN- β) have served as a paradigm to examine the transcriptional mechanisms controlling virus inducible gene expression (125,126). The regulatory sequences which control the transcription of the human IFN- β gene are located within a 110 bp region immediately upstream from the transcription initiation site. Detailed mutational analysis of this enhancer reveals a complex organization of short overlapping 8 to 12 bp sequences that serve as recognition sites for multiple

DNA binding proteins (126). Four distinct regions, designated PRDI to PRDIV (positive regulatory domains I to IV) are required for maximum induction of the IFN- β promoter (54,56,59,62,109,210). PRDI (-77 to -64) and PRDIII (-94 to -78) serve as recognition sites for IRF-1 and IRF-2 (55,58,72,77,138) and the 88 kDa PRDI-BF1 protein (96). The PRDII domain (-64 to -55) binds the PRDII-BF1 protein and the NF- κ B/Rel transcription factors (56,81,114,126,212). PRDIV interacts with the ATF-2/CREB and octamer binding proteins (45,69). In the intact promoter, these 4 elements interact synergistically to activate transcription of the IFN- β gene. HMG I(Y) proteins bind to the minor groove of AT rich sequences within PRDII and PRDIV and stimulate the binding of NF- κ B and ATF-2 respectively to these elements (46,195). The IFN- β promoter also contains an 11 bp negative regulatory element (NRE) located at -60 to -50 which partially overlaps PRDII, is bound by NRE-BP and is able to repress PRDII mediated gene activity (151). Virus infected cells can overcome the silencing activity of the NRE by the cooperative effect of PRDI and PRDII.

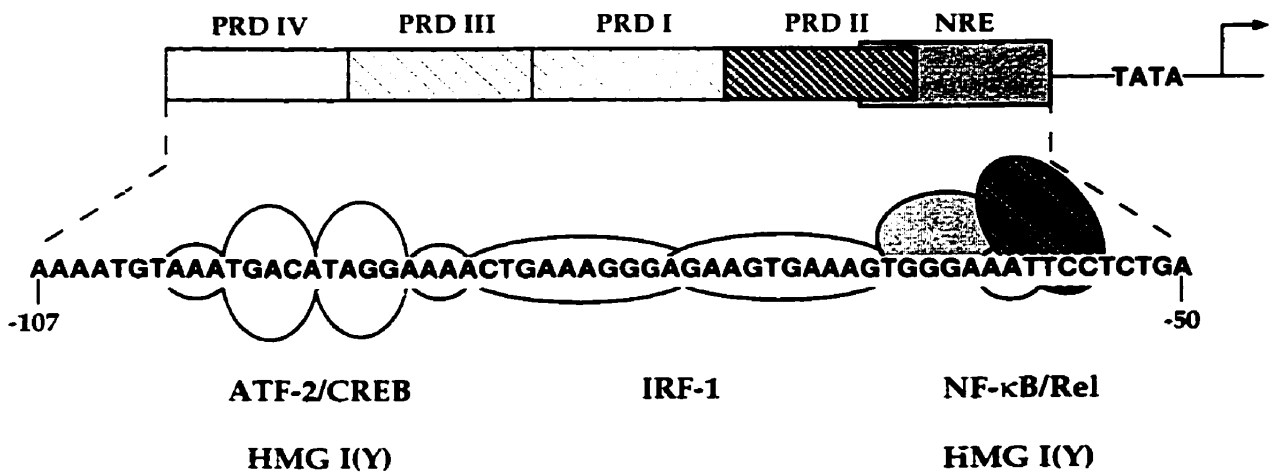
Much interest has been placed on the mechanisms of IFN- β gene activation and these studies are the focus of this section. However, repressor proteins belonging to the protein families mentioned above play an important role in suppressing expression of IFN- β prior to and post-induction. The multiple protein-DNA interactions contributing to positive and negative control of IFN- β expression is illustrated in Figure 1.

Figure 1. Nucleoprotein interactions contributing to positive and negative control of IFN- β gene expression. **A.** In uninduced cells, repressor NRE-BP binds to NRE, PRDII-BF1 binds to PRDII, IRF-2 and PRDI-BFI bind to PRDI and PRDIII and OCT binds to PRDIV; binding of these proteins contributes to transcriptional repression prior to or post-induction. **B.** After virus induction the repressors are replaced by transcriptional activators: the NF- κ B/Rel proteins bind to PRDII, IRF-1 binds to PRDI and PRDIII and ATF-2/CREB binds to PRDIV. HMG I(Y) binds to an AT-rich region within PRDII and to two sites flanking the ATF-2 binding site within PRDIV; HMG I(Y) interaction with DNA is constitutive.

A. Uninduced



B. Induced



1.1 NF- κ B/Rel interactions with PRDII

1.1.1 Overview of the NF- κ B/Rel transcription factors

The NF- κ B/Rel family of transcription factors binds to a decameric recognition sequence (consensus 5'-GGGRNNYYCC-3') and participates in the activation of numerous genes involved in immune regulatory functions including the acute phase proteins, cytokines, cell surface receptors involved in immune recognition, and enhancer domains of several viruses (13,123). Studies by Baeuerle and Baltimore demonstrate that a complex of three NF- κ B subunits exists in the cytoplasm of most cells: a DNA binding 48-55 kDa protein (p50), a DNA binding 65-68 kDa protein (p65), and a non-DNA binding regulatory subunit termed I κ B that interacts specifically with p65 (12). I κ B appears to be responsible for the cytoplasmic localization of the inactive NF- κ B complex (16,18,176). Molecular cloning of the NF- κ B1(p50) and RelA(p65) genes of NF- κ B reveals that the DNA binding, amino terminal portion of these proteins share strong homology with the *c-rel* proto-oncogene and with the *Drosophila* morphogen *dorsal* (61,98,148,166). The NF- κ B family members share a Rel homology domain that is responsible for DNA binding, nuclear localization and protein dimerization. DNA binding members of NF- κ B/Rel include: p50(NF- κ B1) (61,98); p65(RelA) (148,166), *c-Rel* (25), p52(NF- κ B2, *lyt-10*) (20,145,175), RelB(I-Rel) (167,169) and *dorsal* (12,13,123). p50 and p52 are synthesized as precursors of p105 and p100, respectively, and are proteolytically processed to generate active DNA binding p50 and p52 (20,61,98,145,175). The ubiquitin-proteasome pathway plays an essential role in the regulation of NF- κ B activity by processing the p105 precursor to p50 and by degrading I κ B α (154).

NF- κ B activity may be regulated at several distinct levels: at the level of transcription as an immediate early response to growth factors; at the post-transcriptional splicing level; at the post-translational levels of protein processing; at the level of phosphorylation and dissociation of protein subunits; and at the level of DNA binding site specificity. Furthermore, temporal variation in the nuclear appearances of NF- κ B DNA binding activities, distinct DNA affinities of individual subunits, and differences in homo- and heterodimer formation represent additional mechanisms which contribute to functional diversification of NF- κ B proteins. Finally, NF- κ B subunit genes may be subject to autoregulation by NF- κ B proteins, since the promoters of c-Rel, NF- κ B1, NF- κ B2 and I κ B α contain NF- κ B binding sites (12,13,16,123).

1.1.2 I κ B regulation of NF- κ B activity

The intracellular localization and posttranslational activity of NF- κ B/Rel proteins are regulated by the inhibitory I κ B protein family (16,78). All I κ B proteins possess multiple ankyrin repeat motifs that may play an important role in protein-protein dimerization and cytoplasmic anchoring of NF- κ B. Seven inhibitory subunits have been characterized: I κ B α (MAD3/pp40) (78); *bcl3* (147); I κ B γ (89,122); I κ B β (198) and I κ B ϵ (221), as well as the ankyrin containing precursors of NF- κ B1(p105) and NF- κ B2(p100), which also participate in the cytoplasmic localization of DNA subunits (16,123).

The cytoplasmic localization of both NF- κ B/Rel subunits is mediated via the masking of a nuclear localization sequence (NLS) in the *rel* homology domains of these subunits by I κ B (18,176). Phosphorylation and rapid degradation of I κ B α are the first detectable changes in NF- κ B/I κ B complexes after induction.

The mechanisms by which I κ B α is phosphorylated and subsequently degraded have been a subject of intense investigation. Phosphorylation of the I κ B α serines 32 and 36 in response to NF- κ B inducers represents a signal for ubiquitination and degradation by the 26S proteasome (5,6,17,24,28,121,202). The kinases which are specifically responsible for phosphorylation of the serine residues in I κ B α have recently been identified. I κ B α kinase (IKK)- α /IKK-1/CHUK and IKK- β /IKK-2 are the two kinases which interact and form a multiprotein complex of about 500 to 900 kDa which directly or indirectly phosphorylates the critical degradation residues in I κ B α (29,42,134,170,226,232). Loss of I κ B α results in translocation of NF- κ B to the nucleus, where it activates transcription of target genes and stimulates I κ B α transcription *de novo* by an autoregulatory mechanism (17,24,108,139,185). The *in vitro* DNA binding activity of NF- κ B complexes can be inhibited or dissociated by I κ B α addition; in some cases, I κ B α addition can enhance DNA binding activity, depending on the NF- κ B subunits (117).

I κ B α and I κ B β share three properties: they display equal affinities to the same NF- κ B subunits (RelA and c-Rel), they are cytoplasmic proteins and they inhibit DNA binding and transactivation of the NF- κ B proteins. However, several aspects distinguish these two major I κ B isoforms. First, they respond to different inducers. Unlike I κ B α , I κ B β does not respond to TNF α or PMA. Second, the kinetics of degradation and resynthesis differ between the two inhibitors. LPS and IL-1 treatment initiates a rapid degradation and resynthesis of I κ B α . I κ B β is also affected; however the kinetics of degradation and resynthesis of I κ B β is much slower than that observed with I κ B α , resulting in persistent activation of NF- κ B. This finding suggests the existence of two overlapping phases of NF- κ B induction, an early transient

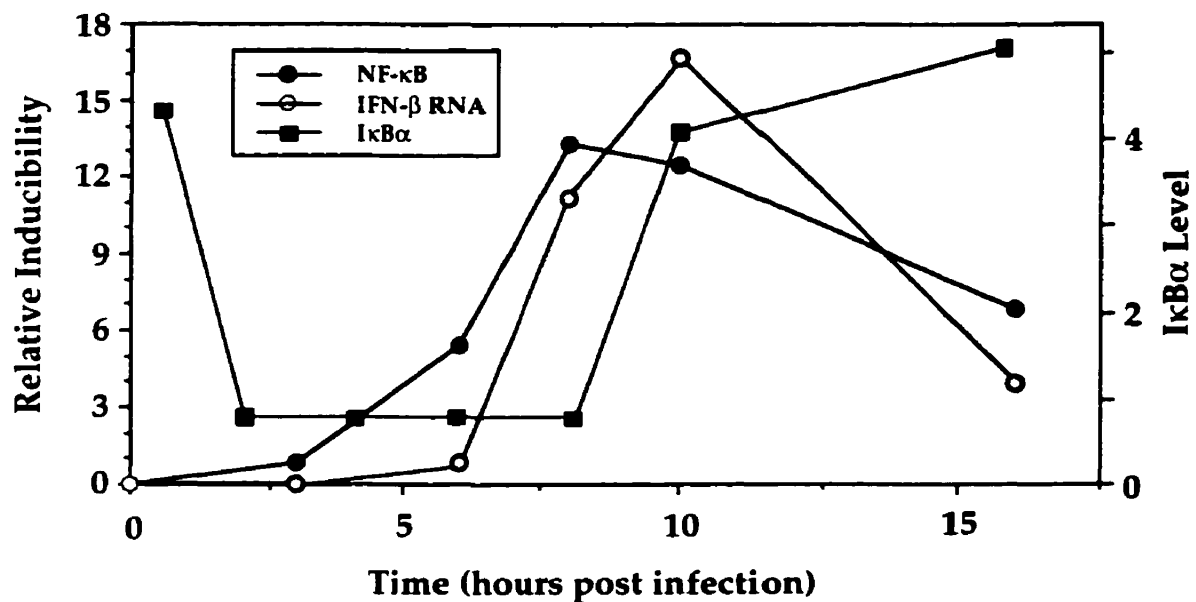
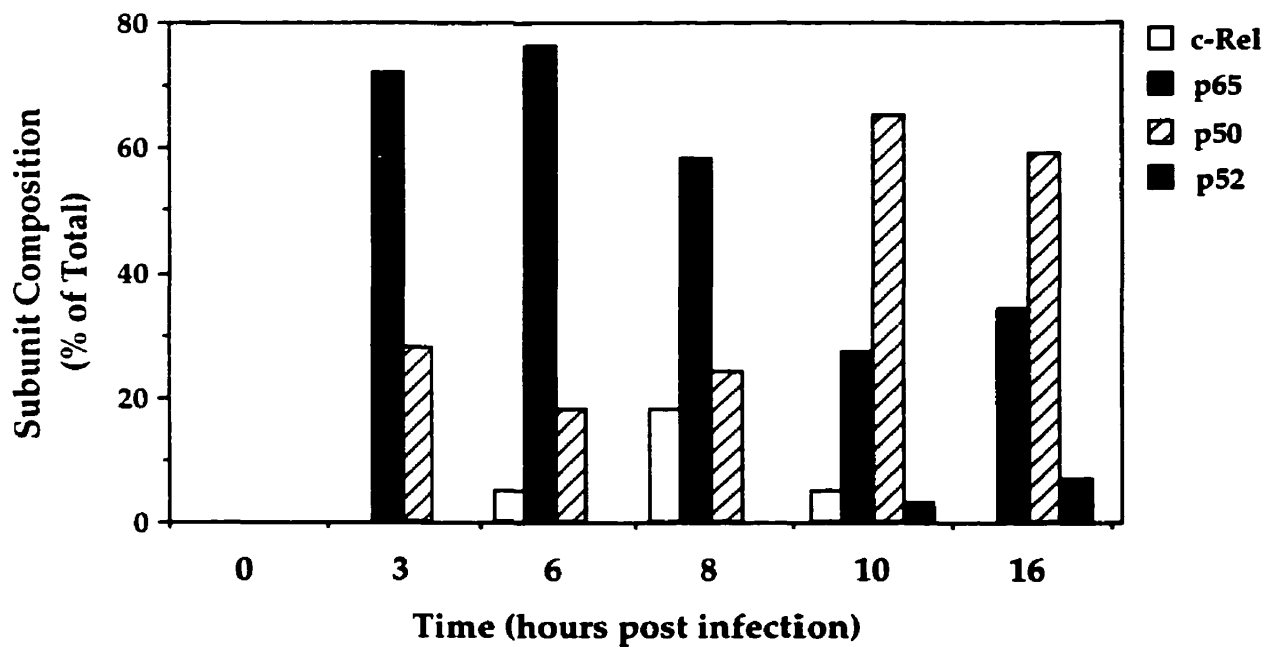
phase mediated by $\text{I}\kappa\text{B}\alpha$ and a latent, persistent phase in which $\text{I}\kappa\text{B}\beta$ predominates (198). Persistent activation of NF- κB is maintained as resynthesized $\text{I}\kappa\text{B}\beta$ appears in an unphosphorylated configuration which forms a stable complex with NF- κB in the cytoplasm. In this context, $\text{I}\kappa\text{B}\beta$ does not mask the NF- κB NLS or DNA binding domain, resulting in the nuclear translocation of NF- κB as a complex which is "protected" from inhibition by $\text{I}\kappa\text{B}\alpha$ and which can bind DNA (186,203).

1.1.3 Virus induced modulation of NF- κB / $\text{I}\kappa\text{B}$ activity: effect on IFN- β induction

The IFN- β PRDII region (-64 to -55) is a decamer sequence (5'-GGGAAATTCC-3') that serves as a recognition site for the NF- κB /Rel transcription factors (33,81,113,212). Base mutations or deletions which alter the PRDII domain cause a loss of virus inducibility, suggesting a critical role for this element in virus induction (62,195). Only the combination of p50 and RelA subunits are capable of activating transcription of the IFN- β promoter. Furthermore, virus-inducible complexes on the IFN promoter contain both p50 and RelA, implicating this NF- κB heterodimer responsible for NF- κB dependent activation of IFN- β (197).

During the induction of IFN- β gene expression in fibroblastic cells, alterations in the composition of NF- κB subunits associated with the PRDII domain occur as a function of time after virus infection (60). The formation of the PRDII specific complexes precedes the onset of detectable IFN- β transcription in Sendai virus infected cells (Figure 2A). Early after infection (3 and 6 hours), RelA is the main NF- κB component in the nucleus whereas by 10 hours after

Figure 2. Virus-induced modulation of NF- κ B/I κ B activity and expression of the IFN- β gene. **A.** Sendai virus induction of I κ B α degradation, NF- κ B DNA binding activity and IFN- β mRNA transcription. The relative intensities of PCR products (IFN- β mRNA), the protein-DNA complexes (NF- κ B binding activity) and immunoblots (I κ B α protein) were scanned by laser densitometry and plotted as a function of time (modified from (60)). **B.** Temporal shift in NF- κ B protein-DNA complexes during virus infection. Nuclear extracts from 293 cells infected with Sendai virus for the indicated times were used in supershift EMSA with NF- κ B subunit-specific antisera. The intensity of the shifted protein-DNA complexes was evaluated by laser densitometry and expressed as a percent of the shifted complexes.

A**B**

infection a shift in the relative abundance of these subunits occurs; both p50 and RelA are present in the specific complexes (Figure 2B).

The level of I κ B α is also dynamically altered by virus infection; by 2 hours after infection the amount of I κ B α decreases about five fold relative to cytoplasmic extracts from control cells. At 10 hours after infection, *de novo* synthesis of I κ B α restores the level of this inhibitory protein, coincident with the decrease in IFN- β mRNA accumulation (Figure 2A). These results are consistent with Sendai virus-induced degradation of I κ B α . Previous studies with Sendai virus infected cells demonstrate that *de novo* synthesized I κ B α can be chased into an immunoprecipitable complex with RelA (165). Thus, *de novo* synthesis of I κ B α may contribute to the post-induction shut-off of transcription by sequestering RelA-p50 (60).

It is thought that virus induction of the double stranded RNA dependent kinase (PKR) may mediate the early phosphorylation-dependent degradation of I κ B α since PKR has been shown to phosphorylate I κ B α and induce NF- κ B binding activity (106). However, the newly identified IKKs are potential key players. Surprisingly, I κ B α levels are decreased from two to eight hours after infection, a relatively long interval compared to other inducers such as tumor necrosis factor-alpha (TNF α) or phorbol 12-myristate, 13-acetate (PMA) that promote phosphorylation and degradation of I κ B α during the first hour after treatment. The heterogeneous nature of viral infection may contribute to the longer period of I κ B α decay than previously described for inducers such as cytokines or phorbol esters (17,24,108,139).

The effects of overexpression of the $\text{I}\kappa\text{B}\alpha$ and $\text{I}\kappa\text{B}\beta$ inhibitory proteins on the regulation of NF- κB dependent IFN- β gene transcription were recently investigated (4). $\text{I}\kappa\text{B}\alpha$ overexpression exhibits a strong inhibitory effect on virus induced activity of a construct containing the IFN- β promoter (-281 to +19) upstream of a CAT reporter gene. Furthermore, overexpression of a transdominant repressor $\text{I}\kappa\text{B}\alpha$ molecule which is point mutated at serines 32 and 36 (S32A, S36A; TD- $\text{I}\kappa\text{B}\alpha$) completely blocks IFN- β gene activation by Sendai virus. Strikingly, $\text{I}\kappa\text{B}\beta$ exerts an inhibitory effect only when expressed at high concentrations. Similar results were obtained in cell lines that inducibly express $\text{I}\kappa\text{B}\alpha$, $\text{I}\kappa\text{B}\beta$ or TD- $\text{I}\kappa\text{B}\alpha$ under the control of a tetracycline responsive promoter. Inhibition of IFN- β expression correlates with a reduction in binding of NF- κB (p50-RelA) complex to PRDII after Sendai infection in $\text{I}\kappa\text{B}\alpha$ expressing cells, while minimal decreases in IFN- β expression and NF- κB binding are observed in $\text{I}\kappa\text{B}\beta$ expressing cells. These experiments demonstrate a predominant role for $\text{I}\kappa\text{B}\alpha$ over $\text{I}\kappa\text{B}\beta$ in the regulation of NF- κB induced IFN- β gene activation (4), and supports the observed stronger inhibitory capacity of $\text{I}\kappa\text{B}\alpha$ compared to $\text{I}\kappa\text{B}\beta$ (203).

As will be elaborated later on, NF- κB binding to the PRDII element is enhanced by interaction with the HMG I(Y) protein. Interestingly, the presence of HMG I(Y) enhances the inhibitory activity of $\text{I}\kappa\text{B}\beta$ but not $\text{I}\kappa\text{B}\alpha$ on NF- κB binding. It is proposed that HMG I(Y) may alter the structure of NF- κB on the DNA such that $\text{I}\kappa\text{B}\beta$ can efficiently recognize and remove NF- κB from its target DNA (203).

1.2 IRF interactions with PRDI and PRDIII

PRDI, PRDIII and multimers of AAGTGA (Th) constitute binding sites for the Interferon Regulatory Factors IRF-1 and IRF-2 (58,72,138). The crystal structure of the IRF-1 DNA binding domain (DBD) bound to PRDI was recently resolved and reveals a new helix-turn-helix motif which binds to a GAAA sequence through three of the five conserved IRF tryptophans (52). The role of IRF-1 and IRF-2 in IFN- β gene regulation was demonstrated by the finding that expression of mouse and human IRF-1 genes increases transcription from reporter genes under the control of the IFN- β IRF-binding sites (58,72,138), and that this transactivation is abrogated with concomitant expression of IRF-2 (77). These studies indicate that IRF-1 behaves as a transcriptional activator of Type I IFN genes, whereas IRF-2 functions as an antagonistic repressor of transcription. In addition to IRF-2, a second repressor was cloned - PRDI-BF1 - that binds to the PRDI domain. PRDI-BF1 cDNA is unrelated to the IRFs and encodes an 88 kDa zinc finger protein involved in post-induction repression of the promoter (96).

IRF-1 and IRF-2 will be described in much greater detail in the latter part of this chapter. Despite the discovery of IRF-1 as a transactivator of IFN- β transcription, its role in IFN- β gene regulation has become increasingly controversial from studies in IRF knockout mice. These results will also be presented in Section 2.

1.3 ATF/CREB interactions with PRDIV

The sequence of PRDIV contains a binding site for members of the ATF/CREB family of transcription factors, a class of c-AMP inducible DNA binding proteins sharing homology within the C-terminal basic/leucine zipper

domains (211). The ATF/CREB site of the IFN- β promoter is required for virus induction in mouse L929 cells and mutations in PRDIV that disrupt or decrease the binding of the ATF-2/CRE-BP1 member of the ATF/CREB family significantly decreases virus induction of the intact IFN- β promoter *in vivo* (45). Antisense RNA inhibition experiments indicate that ATF-2 and c-Jun (another member of the ATF/CREB family) are required for virus induction (46). Reporter gene constructs containing multiple copies of PRDIV are inducible by both virus and cAMP, while a construct containing multiple copies of the ATF/CREB site from PRDIV is inducible by cAMP only, indicating that sequences immediately flanking the ATF/CREB site are also necessary for virus induction (46). Since ATF-2 interacts directly with p50, RelA, and HMG-I(Y) *in vitro*, ATF-2-NF- κ B association could stabilize the multiprotein complex required for transcriptional activation (46).

1.4 HMG protein interactions with PRDII and PRDIV

The HMG (high-mobility group) proteins are low-molecular-weight, highly charged chromatin-associated proteins. Based on their molecular masses, DNA binding characteristics and amino acid sequence motifs, these proteins can be classified into three families: the HMG 1/2, HMG I(Y) and HMG 14/17 families (26). The HMG I(Y) protein binds to the minor groove of double-stranded dA-dT rich sequences. In the PRDII region, HMG I(Y) binds to a centrally located AT-rich sequence while NF- κ B binds to the immediate flanking GC-rich sequences. The opposite configuration occurs in the PRDIV region; ATF-2 binds to the centre of PRDIV, while HMG I(Y) binds to AT-rich sequences at each end of this element. DNase I footprinting, methylation interference and *in vivo* transcriptional assays with deletion mutants of HMG I(Y) demonstrate that the two molecules of HMG I(Y) bind to PRDII and

PRDIV in a cooperative fashion. Cooperativity of binding requires correct helical phasing of the PRDII and PRDIV elements and within HMG I(Y) sites (229). Specificity of HMG I(Y) DNA binding is dependent on its acidic C-terminus.

Although it cannot activate transcription on its own, HMG I(Y) is necessary for virus induction from PRDII and PRDIV (195). The presence of either antisense RelA or antisense HMG I(Y) RNA significantly reduces virus induction from the IFN- β promoter. In addition, mutations that decrease binding of either NF- κ B or HMG I(Y) to PRDII and ATF-2 or HMG I(Y) to PRDIV *in vitro* decrease the level of virus induction of IFN- β *in vivo* (46,195). These observations suggest that both NF- κ B, ATF-2 and HMG I(Y) are required for virus induction from PRDII and PRDIV within the context of the IFN- β gene promoter.

Binding of NF- κ B and ATF-2 to their respective DNA target sites is increased by direct protein-protein interactions with HMG I(Y) (46,195). Phasing and circular permutation analyses reveal an intrinsic DNA bend in PRDII and PRDIV which are reversed upon binding by NF- κ B and ATF-2, respectively, and this effect is enhanced in the presence of HMG I(Y) (53). The solution structure of a truncated form of HMG I(Y) bound to its recognition site in PRDII was recently defined by multidimensional nuclear magnetic resonance spectroscopy (86). HMG I(Y) binds to a novel DNA minor groove motif which stabilizes the B-DNA form. It was suggested from the structural studies that HMG I(Y) DNA binding potentially prevents intrinsic distortions in DNA conformation and subsequently facilitates binding of NF- κ B and ATF-2 to the opposing major groove. As will be shown in the following section, the HMG

I(Y) protein is an “architectural factor” which plays an important role in the assembly and stabilization of the multiprotein complex required for transcriptional activation of the IFN- β promoter.

DSP1 (dorsal switch protein-1), a member of the HMG1 protein family from *Drosophila*, is an inhibitor of Dorsal, the *Drosophila* equivalent of NF- κ B (112). Cotransfection studies demonstrate that high levels of DSP1 block virus induction of the IFN- β promoter and inhibit activation by NF- κ B from a reporter construct containing the NRE adjacent to the PRDII sites. Inhibition by DSP1 requires the presence of the NRE as well as the NF- κ B p50 protein. An *in vitro* binding study shows that recombinant DSP1 stimulates binding of p50/RelA heterodimers and p50 homodimers to a probe containing two PRDII sites and an NRE, while DNA binding of RelA homodimers is not affected. In the presence of wild-type NRE, DSP1 switches p50 homodimers and the activators Dorsal and the p50/RelA heterodimer to repressors. Transactivation by RelA homodimers or RelA/c-Rel heterodimers is not affected by DSP1. Human HMG1 and HMG2 proteins are unable to convert Rel activators to repressors or to inhibit the activation by Rel proteins, suggesting that an unidentified HMG-like protein in human cells may function as a human equivalent of DSP1 (112).

1.5 The IFN- β enhanceosome: synergism between PRDs

When the entire IFN- β promoter (-281 to +19) is used in co-expression studies, the p50 and RelA combination only weakly increases IFN- β gene activity. Synergistic stimulation of IFN- β promoter activity is obtained when NF- κ B subunits are co-expressed together with the IRF-1 transcription factor (60). This result is consistent with a study demonstrating that efficient virus

induction of IFN- β requires the activation domains of IRF-1 and RelA (53). Furthermore, in addition to virus infection, individual PRDs respond to other inducers that activate the transcription factors binding to these domains (46,54,109). However, the entire IFN- β promoter does not respond to these inducers; rather, transcriptional synergy is specific to virus infection (196). Moreover, activation of the intact IFN- β promoter is at least an order of magnitude higher than that seen of each of the individual PRDs (196). These findings complement other studies illustrating the requirement of the synergistic activities of the different PRDs for maximum activation of IFN- β (54,62,109).

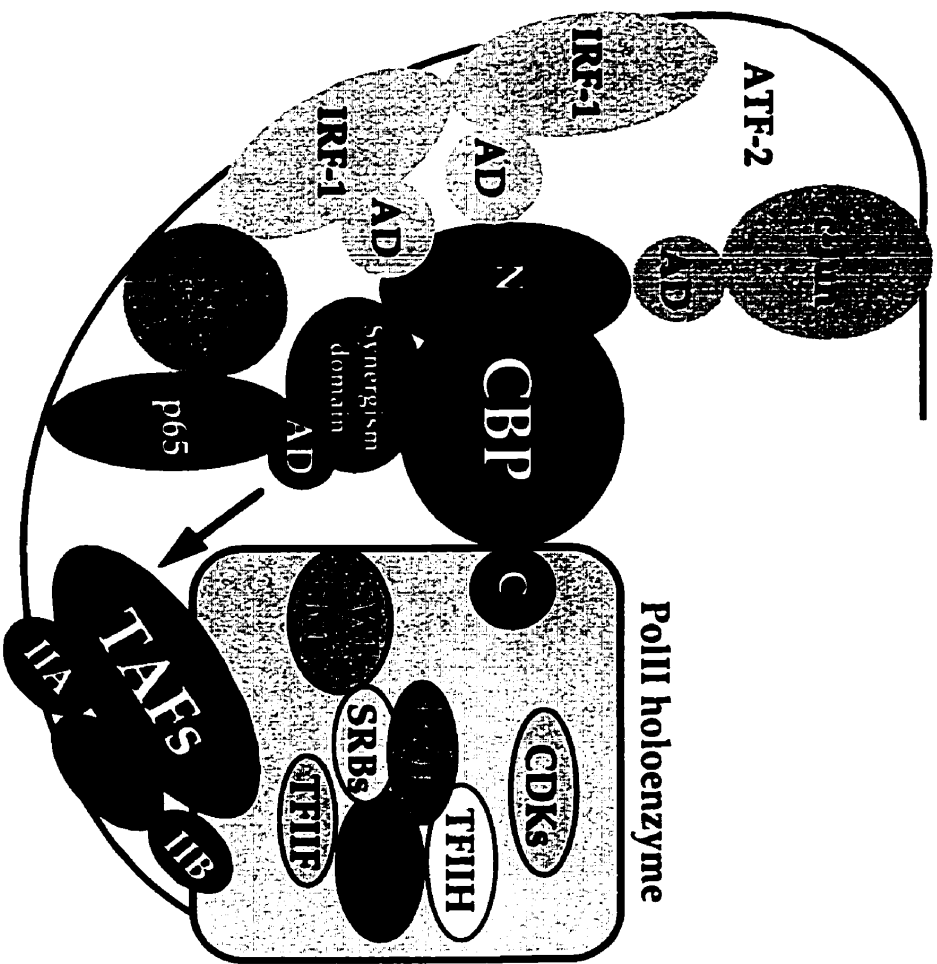
Extensive work by the Maniatis and Thanos groups reveals that the highly elevated virus induction of the IFN- β promoter is due to the assembly of a higher order transcription enhancer complex called an enhanceosome (53,99,135,196). Initial studies by Du *et al.* described earlier provide important insights into the synergistic activation of the IFN- β promoter since they demonstrate that HMG I(Y) plays an important role in establishing transcriptional synergy between PRDII and PRDIV through protein-DNA contact and protein-protein interaction with NF- κ B and ATF-2 (46). More recent studies show that HMG I(Y) also contributes to cooperative binding of IRF-1 to PRDI and allows for co-occupancy of PRDI and PRDII by IRF-1 and NF- κ B, respectively (196).

Many factors are involved in transcriptional synergy of IFN- β activation. First, the unique arrangement of the PRDs must be preserved for maximum virus inducibility of the IFN- β promoter; replacement of PRDIV by PRDII or reverse orientation of either or both domains (53,196) results in a dramatic

decrease in IFN- β promoter activation. Second, essential for *in vitro* assembly and *in vivo* transcriptional activity of the enhancer complex is specific helical phasing of the PRDs on the face of the DNA helix which optimizes interaction of the multicomponent complex with the basal transcriptional machinery. IFN- β promoters containing half-helical turns significantly reduce virus inducibility and this observation is reversed with the insertion of a full helical turn (196,203,229). Third, reconstitution experiments show that transcriptional synergy correlates with increasing cooperativity and stability of the promoter (53).

Interestingly, the transcriptional synergy involved in IFN- β activation also requires interaction of all transcription factor activation domains with CBP/p300 (135). CBP/p300 is a co-activator protein which plays a role in cell proliferation and differentiation through its interaction with many cellular activators (48,85,233) and is a component of the RNA polymerase II holoenzyme (95). A novel domain (aa 322-458) was identified in RelA - termed the synergism domain - which contains a potential leucine zipper domain present in CBP and CBP-interacting proteins. Through this domain, RelA associates with CBP and this interaction is essential for transcriptional synergy. The activation domains of the IFN- β transcription factors also interact with CBP *in vivo* and potentially stabilize the initial association between RelA and CBP. CBP recruitment to the enhanceosome is necessary but not sufficient for transcriptional synergy. Maximum activation requires the activation domain of RelA and IRF-1 (135). Interestingly, the enhanceosome is able to make contact with components of the transcriptional basal machinery *in vitro* (TFIID, TFIIA, TFIIB, and the USA coactivator) (99). Based on these findings, it was proposed that synergistic activation of IFN- β

Figure 3. Model for synergistic activation of transcription by the IFN- β enhanceosome. This schematic is adapted from Merika *et al.* (135). HMG I(Y) is omitted from the figure and only some of the protein-protein interactions involved in contact with the basal transcription machinery are illustrated for simplicity. The enhanceosome involves a 60 bp stretch of DNA where HMG I(Y) is bound to the minor groove and the IRF-1, NF- κ B and ATF-2/CREB transcription factors are bound to the major groove. Association of HMG I(Y) with NF- κ B and ATF-2 as well as DNA induces the conformational changes required to form this nucleoprotein complex. Formation of the enhanceosome results in recruitment of CBP through its N-terminus (N) by the activation domains (AD) and subsequent association of the complex with the PolII holoenzyme by contact with the C-terminus of CBP (C), implicating CBP as a bridge between transcriptional machinery and the IFN- β enhancer. The enhanceosome also makes contact with components of the transcriptional basal machinery (TFIID, TFIIA, and TFIIB). It is proposed that synergistic activation of IFN- β involves simultaneous recruitment of RNA polII and the basal transcriptional machinery by the enhanceosome.



Transcription

initially involves simultaneous recruitment of RNA polIII and the basal transcriptional machinery by the enhanceosome via CBP recruitment by RelA, implicating CBP as a bridge between transcriptional machinery and the IFN- β enhancer. A schematic representation of the IFN- β enhanceosome associated with the basal transcription complex is depicted in Figure 3.

2 The growing family of Interferon Regulatory Factors

The Interferon Regulatory Factors are a family of transcription factors originally consisting of the well-characterized IRF-1 and IRF-2 proteins and which now has expanded to include seven other members: IRF-3, ISGF3 γ /p48, ICSBP, Pip/ICSAT/ IRF-4, IRF-5, IRF-6 and IRF-7. Structurally, the Myb oncoproteins also share homology with the IRF family, although their relationship to the IFN system is unclear (209). Interestingly, recent evidence also demonstrates the existence of virally encoded forms of IRF proteins; the human herpes virus 8/Kaposi sarcoma herpes simplex virus (HHV-8/KSHSV) contains four ORFs encoding proteins (vIRFs) showing homology to the cellular IRFs (141,168). Genbank accession numbers for the human, murine, avian and viral coding sequences of the IRF family members are listed in Table 1.

This section provides a detailed description of the structures and known functions of the IRF family members. Several features highlight this family of transcription factors. As shown in Figure 4, all members of this family share significant homology in the N-terminal 115 amino acids (aa) which comprise the DNA binding domain (DBD); this region contains a characteristic conserved tryptophan repeat (five tryptophans spaced in 10-18 aa

Table 1. Genbank accession numbers of human, murine, avian and viral coding sequences of the IRF family members (N/A: non-applicable).

IRF Member	Human Sequence	Murine Sequence	Avian Sequence	Viral Sequence
IRF-1	X14454	M21065	L39766	N/A
IRF-2	X15949	J03168	X95478	N/A
IRF-3	Z56281	U75839	-	N/A
IRF-4	U52682	U34307 (Pip) U11692 (LSIRF)	-	N/A
ICSBP	M91196	M32489	L39767	N/A
ISGF3 γ	M87503	U51992	-	N/A
IRF-5	U51127	-	-	N/A
IRF-6	-	U73029	-	N/A
IRF-7	U73036	U73037	-	N/A
vIRF	N/A	N/A	N/A	U75698

Figure 4. Schematic representation of the IRF proteins. The IRF family consists of 10 members: nine cellular members (IRF-3 to -7, ISGF3 γ /p48, and ICSBP) and four virally encoded forms of IRF proteins (vIRFs). Based on transcriptional function, IRFs can be classified into three groups - activators (IRF-1, IRF-3 and ISGF3 γ), repressors (IRF-2, ICSBP, IRF-7 and vIRF) or both (IRF-4). Although IRF-5 and IRF-6 have been sequenced, their properties are not known. Extensive homology among the IRFs in the N-terminal 115 aa containing a conserved tryptophan (W) repeat with which the IRF proteins bind similar DNA binding motifs are depicted in red. For the ISGF3 γ , ICSBP, IRF-3 and IRF-4 proteins, homology extends to the IRF Association Domain (IAD; blue boxes) with which the IRFs interact with other family members or proteins. The amino acid size of each IRF protein is indicated.

IRF-1	W W W W W	325 aa	Activator
IRF-2	W W W W W	349 aa	Repressor
IRF-3	W W W W W IAD	427 aa	Activator
IRF-4	W W W W W IAD	450 aa	Act./Repr.
IRF-5	W W W W W IAD	504 aa	??
IRF-6	W W W W W	467 aa	??
IRF-7	W W W W W	457 aa	Repressor
ISGF3γ	W W W W W IAD	393 aa	Activator
ICSBP	W W W W W IAD	424 aa	Repressor
vIRF	W W W W W	449 aa	Repressor

intervals) which is also found in the DBD of the Myb oncoproteins. Through this DBD, the IRFs bind similar DNA motifs termed Interferon Stimulated Response Element (ISRE; found in most IFN-inducible gene promoters), Interferon Consensus Sequence (ICS; the ICSBP recognition site found in the MHC class I promoter) or Interferon Regulatory Factor Element (IRF-E or Positive Regulatory Domains (PRD) I and III in the IFN- β promoter; the IRF-1 and IRF-2 DNA binding sites). The similarity of the IRF homology DBD to that of Myb implies that IRF DNA binding activity may involve DBD formation of a helix-turn-helix structure as previously suggested for Myb (209). The relative homologies of the IRF and Myb DBD sequences and percent identities of the IRF N- and C-termini are represented in Figure 5 and Table 2, respectively. For the IRF-3, IRF-4, IRF-5, ISGF3 γ and ICSBP proteins, the homology extends into the C-terminus, at a region called the IRF association domain (IAD) by which these IRFs interact with other proteins or family members.

As shown in Figures 4 and 6, the IRFs can be classified into three groups - those that activate (IRF-1, IRF-3 and ISGF3 γ), those that repress (IRF-2, ICSBP, IRF-7 and vIRF) and those that both activate and repress (IRF-4) transcription of target genes. Although IRF-5 and IRF-6 have been sequenced, their properties have not yet been determined. Some IRFs are specific for hematopoietic cells (ICSBP and IRF-4), while others are expressed in multiple tissues and cell lines. Generally, IRF expression is either constitutive and/or induced upon treatment with IFNs or other cytokines or in response to viral infection. Interestingly, comparable to the IFN-inducible family of JAK-STAT proteins, IRF activity is regulated in part by post-translational modification and subsequent interaction between IRF family members. Studies

Figure 5. Extensive homology among the IRF DNA binding domains (DBDs).

This schematic was modified from Veals *et al.* (209). The N-terminal human or viral amino acid sequences of all known IRF family members (IRF-6 is only available in murine form) are depicted and compared to those of three imperfect repeats (R1 - aa 38 to 89; R2 - aa 90 to 141; R3 - aa 142 to 192) of human Myb. Amino acids found to be identical amongst at least 5 IRF members are depicted in pink. The blue-shaded amino acids are those found amongst at least 5 IRF members and share the same amino acid charge (apolar, uncharged polar or charged side groups). The tryptophan repeats (five in IRF; two in vIRF; three in Myb) are boxed and highlighted in yellow.

HIRF-1	MPITRMRMRPWL	LEMQINSNQI	PGLIWINKEEMI	FQI	HWKHA	AKHGWDINKDA	CLFRSW	58	
HIRF-2	MPVERMRMRPWL	EEQINSNTI	PGLKWLNKEKKI	FQI	HMHA	ARHGWDVEKDAPLFRNW		58	
HIRF-3	MGTPKPRI	LHWLVSQDL	LGQLEGVAVV	NKSRTRFRI	HWKH	GRLRODAQQE-DFGI	FQAW	57	
HIRF-4	MNLEGGGRGGEFGMS	AVSCGNGKLRQWL	IDQIDSGKY	PGLW	WENE	EKSIFRI	HWKHAGKQDYNREEDAALFKAW	74	
HICSBP	MCDRNGGGR	LRCWLIEQIDSS	MPYGLI	WENE	EKSIFRI	HWKHAGKQDYNQEV	DASIFKAW	60	
HISGF3G	MASGRARCTR	KLRN	VVEQVESGQF	PGVQWDDTAKT	MFR	I	HWKHAGKQDFREDQDAFFKAW	62	
HIRF-5	MNQSI	PVAPT	PPRRVRLK	HWLVAQVNSCQY	PGLQ	WVNGEKKLFCI	HWRHATR	HGPSQDGDNTIFKAW	67
MIRF-6	MALHPRRVRLK	HWLVAQVDSCLY	PGLI	WLHR	DSKR	FQI	HWKHATRHS	PQEEENTIFKAW	60
HIRF-7	MALAPERAA	PRVLFGEWLL	GEISSG	CYEGLQWL	DEARTCFR	V	HWKHIFARKDLSEAD-ARIFKAW	63	

vIRF 88 GKASIKDWIVCQVNSCKFFGVWEDEERTRFRI FVTPLADPCFEWRRDGE LGVY 141

C-MYB(R1)	38	LGKTRW	TREDEK	LKLLVEQ	NGTDDW	63
C-MYB(R2)	90	LIKGP	WTREEDQ	EVIELVQ	KYGP	KRW 115
C-MYB(R3)	142	VKKT	SWTEEDRI	IYQAH	KRLGNR	W 166

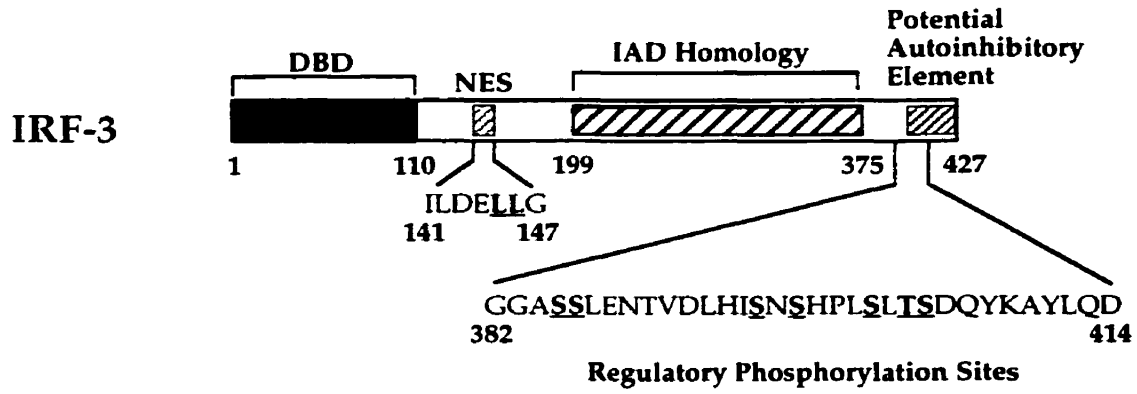
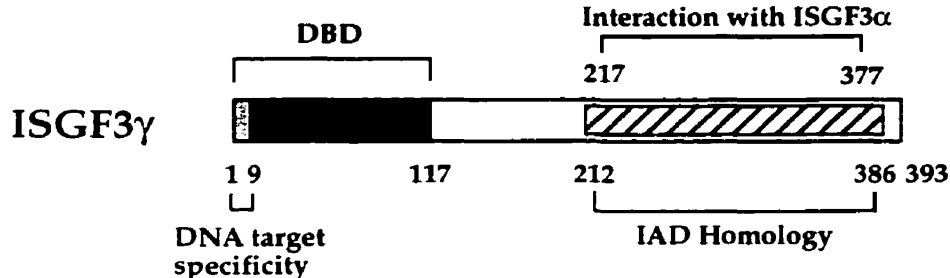
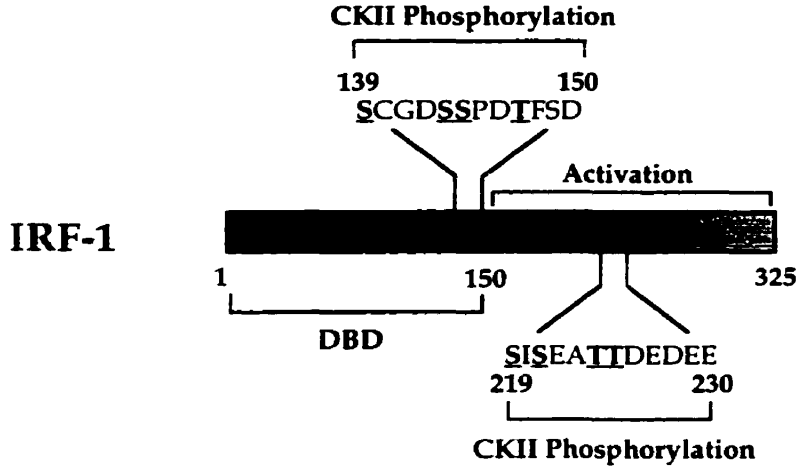
HIRF-1	AIHTGRYKAGEKEPDPK	-----	TWKAN	FR	CAMNSLPDIEEV	KDQSR	NRKGS	SAVRVYRMLPPLTKN	118
HIRF-2	AIHTGKHQPGVDKPDFK	-----	TWKAN	FR	CAMNSLPDIEEV	KDKS	IKKG	NAFRVYRMLPLSERP	118
HIRF-3	AEATCAYVPGRDKFDLP	-----	TWKR	NFR	SALNRKEGLRLAEDRSK	-DPHDP	HKI	YEFVNSGVGD	116
HIRF-4	ALFKGKFREGIDKPDPP	-----	TWKTR	LRCAL	NKSNDFEEL	VERSQ	LDISDPY	KVYRIVPEGAKK	134
HICSBP	AVFKGKFKEGDK-AEPA	-----	TWKTR	LRCAL	NKSPDFE	EVTD	RSQ	LISEPYKVYRIVPEEDQK	119
HISGF3G	AI FKGYKEG-DTGGFA	-----	VW	TR	LRCAL	NKSS	EFKEV	PERGRMDVAEPYEVYQLLPPGIVS	121
HIRF-5	AKETGKYTEGVDEADPA	-----	KWKAN	LRCAL	NKSRDFRLI	YDGP	PRDMP	PQFYKIYEVCSNGPAP	127
MIRF-6	AVETGKYQEGVDDPDPA	-----	KWKA	QLRCAL	NKSR	EFNL	MYDGTKEV	PMNPVKIYQVCDIPQPQ	120
HIRF-7	AVARGRWPPSSRGGGPPPEAETAERAG	WKTN	FR	CAL	RSTR	RFVMI	RDNSG	-DPAIDPHKVYALSRELCWR	132

vIRF IIRER 146

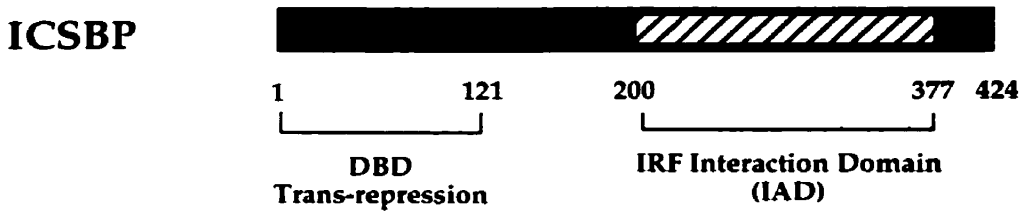
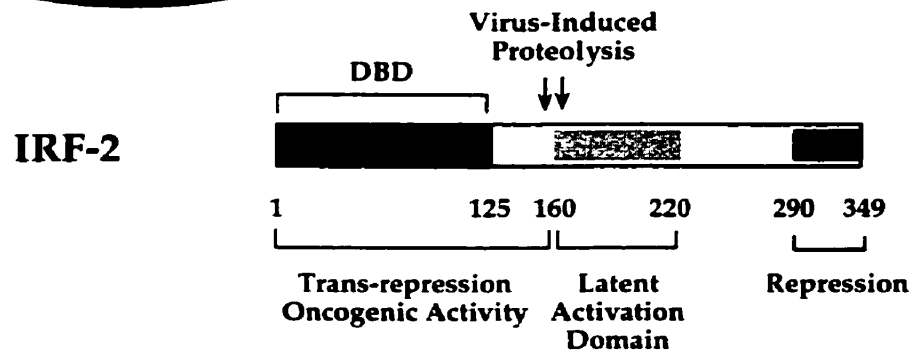
C-MYB(R1)	KVI	ANYL	PNRTD	VQCQ	H-----	RWOK	V	NPE	89
C-MYB(R2)	SVI	AKHL	KGRIG	KQCR	E-----	RWHN	H	L	NPE 141
C-MYB(R3)	AEI	AKLL	PGRT	DNAIK	N-----	HW	S	T	MRRK 192

Table 2. Percent identities among the N- and C-termini of the IRF family members. Some values were obtained from references (9,209,219,227). The remaining values were calculated using the Genbank BLAST algorithm; N-terminal identity (upper value) represents comparison within the homology DBD sequence, and C-terminal identity (lower value) represents comparison within the remaining IRF protein sequence. "-" is indicated where there is no identity between the respective IRF sequences.

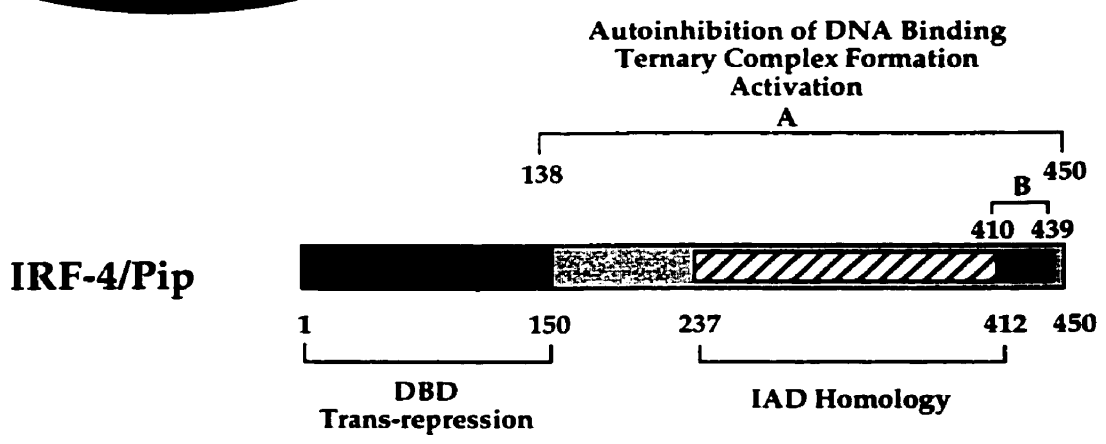
Figure 6. Functional domains of previously characterized IRF family members. DNA binding domain: DBD; purple shading. IRF Association Domain: IAD; gray hatched boxes. Activation domains are depicted in yellow, while repression domains are represented in blue. The N-terminal and C-terminal clusters of casein kinase II (CKII) sites in IRF-1 are expanded; serine and threonine aa found to be specifically phosphorylated by CKII are marked in bold. In ISGF3 γ , the first 9 aa of ISGF3 γ contributing to DNA binding affinity and target specificity are portrayed in pink. Serine and threonine residues present in the C-terminal domain and involved in DNA binding, increased transcriptional activation, cytoplasmic to nuclear translocation and virus-induced IRF-3 phosphorylation and degradation are marked in bold. Also present in IRF-3 is a nuclear export sequence (NES), represented in pink. Lysine residues essential for IRF-3 nuclear export are depicted in bold. The proposed element responsible for autoinhibition of DNA binding is illustrated in peach. DBDs of IRF-2, ICSBP and IRF-4 are able to trans-repress IFN- or IRF-1-mediated transactivation, presumably by binding to DNA and subsequently preventing entry of transactivator IRF protein. Arrows point to the site(s) where IRF-2 may be proteolytically cleaved into the 164 aa form following dsRNA or virus induction. Functional domains from studies characterizing both IRF-4 and Pip are represented together. Two regions of Pip responsible for autoinhibition of DNA binding and ternary complex formation are shown: domain A is a separate functional domain whose fusion to a heterologous IRF DBD prevents DNA binding and association with PU.1 and DNA, whereas domain B (orange box) is not a separable domain but is essential for this phenotype. Domain A also confers transactivation upon PU.1/Pip interaction.



Repressor



Activator/Repressor



characterizing IRF-expressing cell lines and IRF knockout mice reveal that each member of the IRF family exerts distinct roles in biological processes such as pathogen response, cytokine signalling, cell growth regulation and hematopoietic differentiation. Several characteristics of the various IRF family members are summarized at the end of this section (Table 3).

2.1 IRF-1 and IRF-2

IRF-1 and IRF-2 were originally discovered as transcription factors that play a role in the regulation of the IFN- β gene ((55,58,72,138); reviewed in (107,194)); however, they are also involved in the regulation of other virus- or IFN-inducible genes such as IFN- α (11) and MHC Class I (138), respectively. IRF-1 is expressed at low levels or is undetectable in a variety of cell types; however, its expression is inducible by virus infection, double-stranded RNA (dsRNA; poly (rI):poly (rC)), treatment with both Type I and II IFN as well as other cytokines and activators such as tumor necrosis factor (TNF), interleukin-1 (IL-1), IL-6, leukemia inhibitory factor (LIF), concanavalin A (ConA), calcium ionophore A23187 and phorbol 12-myristate 13-acetate (PMA; 3,57,72,138). In contrast, IRF-2 expression is constitutive in many cell types, but is also inducible by Type I IFN and virus infection (72).

Structurally, the IRF-1 and IRF-2 proteins are similar, sharing 76% identity in the first 154 N-terminal aa and 8% identity at the C-terminal end (72), but possess very different activities (58,72,138,163). IRF-1 serves as a transcriptional activator, whereas IRF-2 acts as an antagonistic

transcriptional repressor. The N-terminus of both proteins contains the DBD by which the IRF proteins recognize the virus-inducible IRF-elements (IRF-Es) present in the positive regulatory domains PRDI and PRDIII of the IFN- β promoter. Interestingly, DNA binding activity of IRF-1 and IRF-2 is enhanced by interaction with the TFIIB component of the basal transcription machinery (216).

2.1.1 The role of IRF-1 and IRF-2 in cell growth regulation

The functional differences between IRF-1 and IRF-2 extend further to include an important role in cellular growth regulation. IRF-1 and IRF-2 tumor suppressor and oncogenic activity were initially revealed by the hallmark experiment demonstrating IRF-2 induction of cellular transformation in NIH3T3 cells and tumor formation in nude mice, and reversal of the IRF-2-mediated tumorigenicity by IRF-1 (73).

Recent studies have further established the role of IRF-1 as a tumor suppressor. IRF-1 tumor suppressor activity is not only limited to IRF-2 overexpressing cells; IRF-1 expression also reverts the tumorigenic phenotype exerted by the *c-myc* and *fosB* oncogenes (193). The IRF-1 gene maps to chromosome 5q31.1, a region which is consistently deleted at one or both alleles in each of 13 cases of leukemia and preleukemic myelodysplasia (224). Furthermore, bone marrow and peripheral mononuclear cells from patients with myelodysplastic syndrome (MDS) or leukemia secondary to MDS preferentially express an "exon-skipped" IRF-1 mRNA which lacks exons 2 and 3; the protein product displays neither DNA binding nor tumor suppressive activities, suggesting a mechanism for inactivation of IRF-1 and

subsequent development of human hematopoietic malignancies (74). An alternative mechanism by which MDS or related human leukemias may develop through IRF-1 inactivation was recently proposed. Nucleophosmin (NPM)/B23/numatrin is a nuclear protein found to interact with IRF-1 and inhibit its DNA binding and transactivation (104). This non-ribosomal nucleolar phosphoprotein has potential oncogenic activity, since it induces cellular transformation when overexpressed in NIH3T3 cells. Furthermore, NPM levels are elevated in several cases of human leukemia and human-derived leukemic cell lines. Expression of both IRF-1 and NPM is regulated by the cell cycle, with levels highest in G1 phase, while IRF-2 expression is unaffected (73,104). However, IRF-1 and NPM expression patterns are inversely correlated; IRF-1 levels are highest in early G1 phase, while NPM levels peak during late G1 phase. These findings suggest that IRF-1 may play a role in cancer development by a novel mechanism involving its association and subsequent inactivation by NPM (104).

The tumor suppressor function of IRF-1 was further assessed in knockout mice deficient in IRF-1, IRF-2 or both IRF proteins. Cells from mice deficient in IRF-1 alone or both IRF-1 and IRF-2 are susceptible to transformation by the *ras* oncogene, whereas normal cells or cells from mice deficient in only IRF-2 are not transformed by *ras*. Interestingly, these non-transformed *ras*-expressing normal and IRF-2 deficient cells, unlike the *ras*-transformed IRF-1 deficient and IRF double knockout cells, die by apoptotic cell death under conditions of low serum, high density or exposure to anticancer drugs or ionizing radiation. These studies thus implicate IRF-1 as a critical tumor suppressor, regulating oncogene-induced cell transformation or apoptosis (192).

In contrast to IRF-1, the oncogenic activities of IRF-2 have not been elucidated to the same extent. Although IRF-2 is viewed generally as a transcriptional repressor, there are two reports that IRF-2 acts as an activator. First, the human histone H4 gene FO108 is found to be directly activated by IRF-2 through binding to a cell-cycle element (CCE) present in the H4 promoter (206). This histone gene is functionally coupled to DNA replication and cell-cycle progression at the G1/S transition, with mRNA levels peaking during early S phase. Interestingly, cells from IRF-2 knockout mice lose cell cycle control of H4 expression and demonstrate reduced endogenous levels of H4 mRNA. This phenotype is reversed following IRF-2 expression in IRF-2^{-/-} cells, implicating H4 as a target for IRF-2 mediated oncogenicity (207). Second, the Qp promoter region of the Epstein-Barr Virus (EBV)-encoded EBNA-1 gene is shown to be activated by IRF-2 (149). Furthermore, although both IRF-1 and IRF-2 can bind to the ISRE-like QRE-2 element in the Qp promoter, IRF-2 DNA binding is predominant in extracts derived from Burkitt lymphoma cells (149). These findings assign a physiological role for a latent activation domain previously mapped to the central region of IRF-2, and supports the proposed identity of IRF-2 as a dual transcription factor containing both activator and repressor functions (228).

2.1.2 Involvement of IRF-1 and IRF-2 in Immune Regulation

IRF-1 and IRF-2 are also implicated in the regulation of various immune processes - T-cell selection and maturation - as well as leukemogenic development, as demonstrated by several studies performed with knockout mice. Mice deficient in the IRF-1 gene demonstrate impaired CD8⁺ cell maturation. IRF-2 deficient mice suffer from bone marrow suppression of

hematopoiesis and B lymphopoiesis, and die following lymphocytic choriomeningitis virus (LCMV; *Arenavirus*) infection (129).

IRF-1 is involved in several immune processes. First, IRF-1 upregulates genes which are important for positive selection of CD8⁺ cells (155). TAP1 and LMP2 play an essential role in the function of MHC Class I and their expression is IFN γ -inducible. Interestingly, TAP1, LMP2 and surface Class I MHC levels are greatly reduced in IRF-1-deficient mice (220). Furthermore, *in vivo* footprinting and electrophoretic mobility shift assays reveal that IFN- γ treatment induces protein-DNA contacts at an IRF-E site present in both TAP1 and LMP2 genes, and that IRF-1 binds to the same site. These results may provide an explanation for the CD8⁺ T-cell deficiency observed in IRF-1^{-/-} mice. Second, IRF-1 plays a critical role in multiple stages of Th1 differentiation. Immune cells from IRF-1^{-/-} mice exhibit defective Th1 responses - impaired macrophage production of IL-12, deficient CD4⁺ T-cell response to IL-12, ablated NK cell development, and exclusive Th2 differentiation of macrophages and CD4⁺ T-cells *in vitro* (187). Last, IRF-1 is essential for the induction of NK cell-mediated cytotoxicity *in vivo*, since cytolytic activity of IRF-1^{-/-} NK cells is defective, even following induction by virus infection, dsRNA, IFN- β , IL-2 and IL-12 (47).

2.1.3 IRF-1-dependent and -independent pathways for Type I IFN gene induction

Despite the discovery of IRF-1 as a transactivator of IFN- β transcription, its role in IFN- β gene regulation has become increasingly controversial. Although forced overexpression of IRF-1 in COS cells results in increased

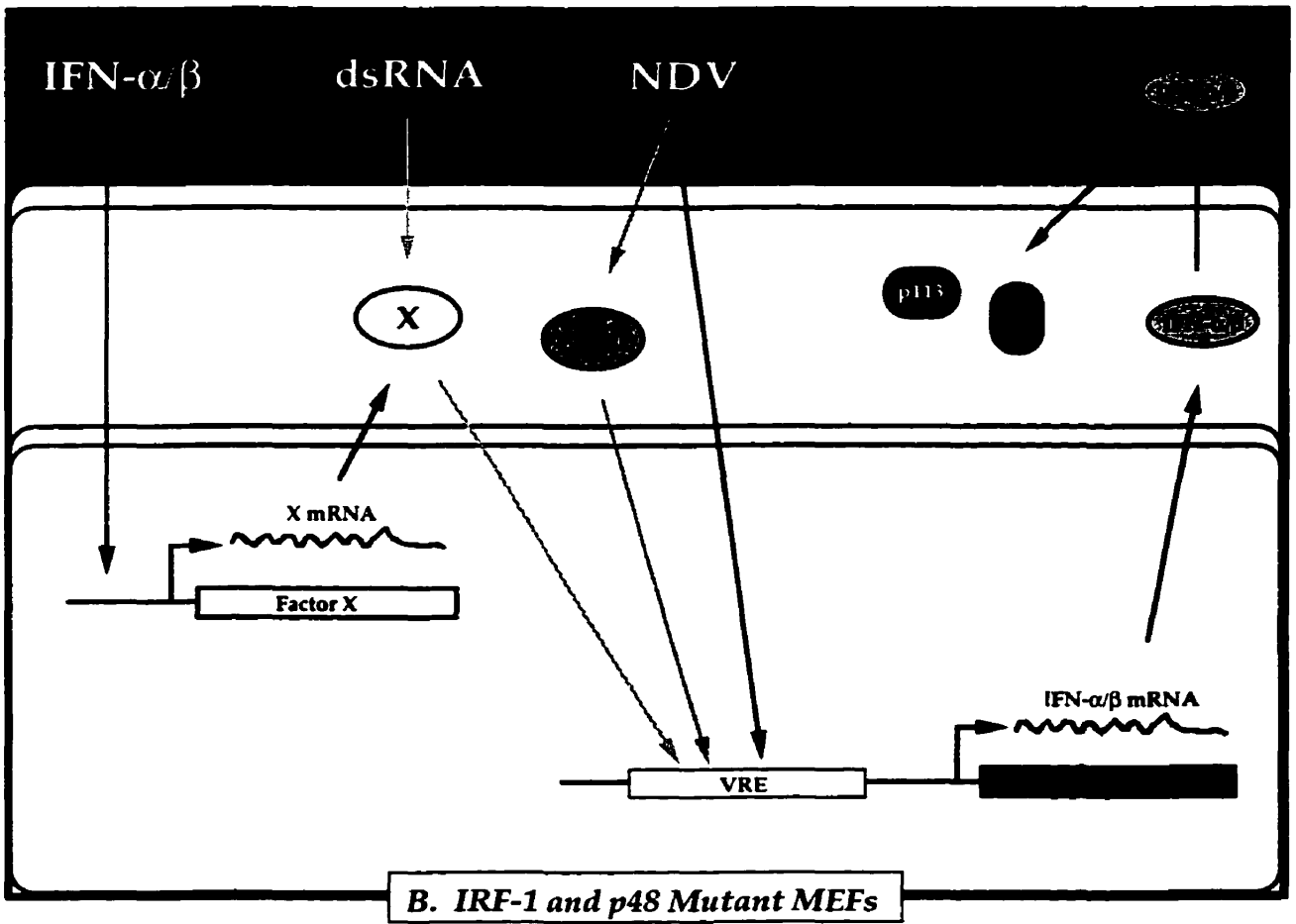
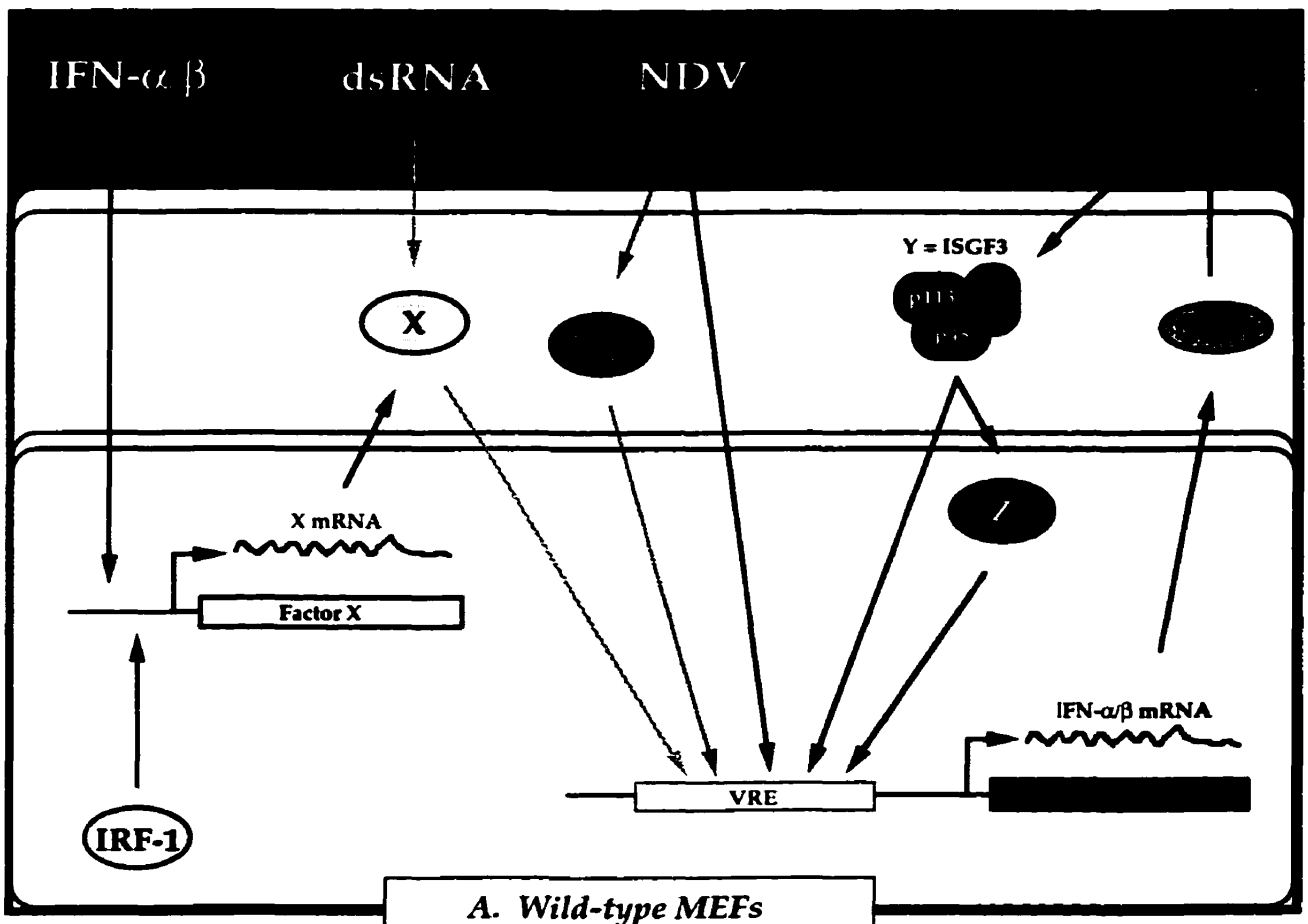
endogenous IFN- β expression in the absence of viral induction (72,77) and reduced IRF-1 expression correlates with decreased IFN- β expression in response to dsRNA or Newcastle Disease Virus (NDV; *Paramyxoviridae*) infection (163), other studies reveal that IFN- β gene expression is induced under conditions in which IRF-1 is absent (223). Conversely, in HeLa S3 cells, overexpression of IRF-1 does not result in IFN- β expression (159,223). Furthermore, in transient transfection assays, activation of an IFN- β -CAT construct is only weakly activated by IRF-1 but is strongly induced when NF- κ B RelA (p65) is cotransfected with IRF-1, suggesting that IRF-1 can serve as a co-activator of IFN- β transcription (120). The IRF binding site also plays an important role in the activation of IFN- α genes. A single mutation in this site abolishes virus-induced IFN- α 4 expression. Furthermore, overexpression of IRF-1 in L-cells stimulates transcriptional activation and enhances virus induction of IFN- α 4 expression (10).

Analysis of IFN expression in IRF knockout mice further extends these contradictions. In IRF-1^{-/-} embryonic fibroblasts (MEFs), type I IFN induction is completely impaired following dsRNA induction, but is reversed by priming with IFN- β . However, wild-type levels of IFN- α and IFN- β mRNA are observed in IRF-1^{-/-} MEFs in response to NDV infection (129). Analogous IRF-1^{-/-} mice generated by the Weissmann group display wild-type induction kinetics of type I IFN (IFN- α and IFN- β) and IFN-inducible genes in response to NDV infection; however, responses to dsRNA treatment demonstrate cell-type specificity (164). Serum and tissue levels of type I IFN after dsRNA treatment are comparable in wild-type and IRF-1^{-/-} mice. However, MEFs from the IRF-1 knockout mice are defective for IFN synthesis. Priming with IFN increases IFN production in IRF-1^{-/-} MEFs to normal levels. IFN

priming is a frequently used strategy to increase IFN expression (44,51,162,184). Although the molecular basis of IFN priming has not been established, the effects of priming are regulated at the transcriptional level (44) and are dependent on protein synthesis (164). Since IFN priming can compensate for the reduced type I IFN response to dsRNA in IRF-1^{-/-} MEFs, direct IRF-1 interaction with type I IFN promoters is not essential for the induction of type I IFN. These results suggest the existence of IRF-1-dependent and -independent pathways for the induction of Type I IFN and that NDV and dsRNA, at least in MEFs, may induce IFN gene expression through different mechanisms.

A model for IFN gene induction by virus infection and dsRNA treatment has been proposed by the Weissmann group (Figure 7). Induction by dsRNA requires the synthesis of a Factor X which is constitutively expressed at effective levels in the organs of both wild-type and IRF-1-deficient mice but not in IRF-1^{-/-} MEFs. The suggested expression pattern of Factor X would explain the cell-type specific response to dsRNA in IRF-1^{-/-} MEFs. Synthesis of Factor X in MEFs is dependent on IRF-1 (hence the reduced type I IFN levels in IRF-1^{-/-} MEFs compared to wild-type MEFs after dsRNA treatment); however, this factor can also be induced by IFN by an IRF-1-independent process - as shown by IFN priming of the IRF-1^{-/-} MEFs. The identity of factor X remains unclear (164); it could be a known IFN-inducible protein, or one of the many proteins found to bind to the IFN-β PRDI site by Whiteside *et al.* (223) . In contrast, viral infection by NDV proceeds through an independent mechanism which requires a Factor Y. Since the viral pathway is not inhibited by cycloheximide, Factor Y must be constitutively expressed and activated by virus infection. Two candidates have been suggested for Factor Y.

Figure 7. Schematic for the induction of Type I IFN genes by dsRNA and NewCastles Disease Virus (NDV) in wild-type MEFs (A) and mutant MEFs lacking both IRF-1 and p48 (B), presented as a combination of models proposed by the Weissmann (130) and Taniguchi (75) labs. A. Induction by dsRNA requires a Factor X whose synthesis in MEFs is dependent on IRF-1 (pink arrows). This factor can also be induced, or primed by IFN- α/β by an IRF-1-independent process (purple arrows). Factor X may be a known IFN-inducible protein or one of the many yet uncharacterized proteins found to bind to the IFN- β PRDI site (223). NDV infection proceeds through two independent mechanisms. The first mechanism requires a Factor Y which is constitutively expressed and activated by virus infection. NDV-mediated IFN- α gene induction may involve the Virus-Induced Factor (VIF) as Factor Y ((22,68); orange arrows). ISGF3 may be the other Factor Y involved in NDV-induced IFN- α and IFN- β gene expression, particularly in the absence of IRF-1 (75,94,100), and is the key player in the second, two-step mechanism of NDV induction. Viral infection initiates the first step of induction by inducing the synthesis of small amounts of IFN- α/β (black arrows). The secreted IFNs then stimulate the JAK-STAT pathway by both autocrine and paracrine mechanisms; the formation of ISGF3, the second step, results in maximum IFN- α/β activation (red arrows). ISGF3-mediated activation of type I IFN may proceed directly or indirectly through activation of another, yet unidentified, factor Z. B. In IRF-1^{-/-} cells, Factor X is still synthesized in the presence of IFN- α/β , such that dsRNA-mediated type I IFN activation remains unaffected. In p48^{-/-} cells, the ISGF3 complex cannot be formed and therefore NDV induction via ISGF3 is impaired, such that only small amounts of IFN are produced from the initial step of IFN- α/β activation by NDV.



NDV induction of IFN- α gene expression may involve the Virus-Induced Factor (VIF) as Factor Y, since it is activated within 1 hour of NDV infection, binds to two PRDI-like motifs present in the murine IFN- α 4 promoter, and its binding activity correlates with IFN- α gene activation. Although VIF recognizes an IRF-E DNA element, its identity is distinct from that of IRF-1, IRF-2 and ISGF3 γ (22,68). As will be discussed later, ISGF3 γ may be the other Factor Y involved in the positive regulation of both IFN- α and IFN- β gene expression following NDV infection in the absence of IRF-1 (75,94,100,231).

The existence of IRF-1-dependent and -independent pathways for IFN induction and the subsequent establishment of the antiviral state is further supported by studies revealing differential effects of viral infections on IFN induction in IRF-1^{-/-} MEFs (101). Inhibition of encephalomyocarditis virus (EMCV; *Picornaviridae*) replication by type I and II IFN is dramatically impaired in IRF-1^{-/-} mice, whereas infection by VSV (*Rhabdoviridae*) is well controlled. Although IRF consensus sites are present in the HSV Type I origins of replication and expression of Type I IFN and IRF-1 is upregulated upon reactivation of the herpes simplex virus (HSV; *Herpesviridae* (188)), the antiviral response to HSV infection is only minimally affected in these knockout mice (101). Interestingly, IFN- γ induction of IFN-inducible genes involved in antiviral response is affected to a larger degree than IFN- α -mediated induction of the same genes. While IRF-1^{-/-} MEFs demonstrate wild-type activation of MHC Class I, 2'5'oligoadenylate synthetase (2'5'OAS), 1-8 and PKR genes by type I IFN, the induction of the iNOS, guanylate-binding protein (GBP) and 2'5'OAS genes by IFN- γ is severely impaired in IRF-1^{-/-} MEFs (101,130). Taken together, these results demonstrate that IRF-1 is more

important in mediating the antiviral effects of IFN- γ than IFN- α , and that IRF-1-mediated antiviral action of IFNs is selective for particular viruses.

2.2 IRF-3

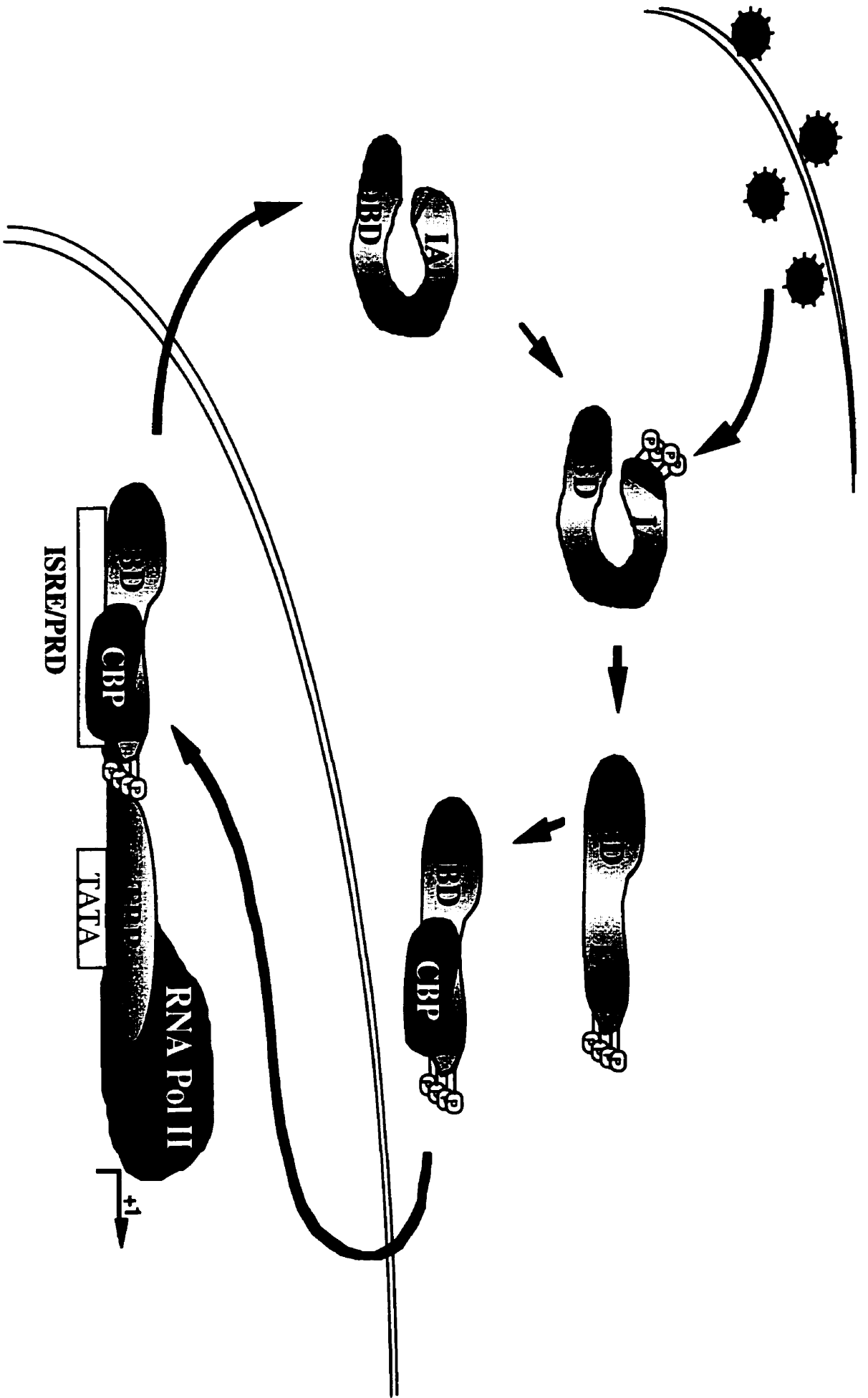
IRF-3 was recently identified and characterized by the Pitha group (9). This protein is distinct from cIRF-3, an avian protein which demonstrates homology to the IRF family members (65). As with IRF-2, the 55 kDa IRF-3 protein is expressed constitutively in all tissues. IRF-3 expression is not induced by viral infection or IFN treatment; however, it can be stimulated by phytohemagglutinin (PHA) and 12-*O*-tetradecanoyl-phorbol 13-acetate (TPA) in peripheral blood mononuclear cells (PBMCs) and macrophages, respectively (Shirazi and Pitha, *unpublished results*). At the amino acid level, IRF-3 has the highest homology to the ICSBP and ISGF3 γ IRF members, with the homology extending into the C-terminal domain. Although recombinant IRF-3 binds the ISRE and activates transcription of the ISG15 gene in transient transfection assays, it does not contain a well-defined transactivation domain. The ambiguous C-terminal domain is reflected by the inability of IRF-3 to activate transcription of the IFN- α 4 and IFN- β genes in transient transfection assays, despite IRF-3 binding to both Inducible Element (IE) and PRDIII regions within the respective promoters (172). Interestingly, in association with the NF- κ B family member RelA(p65), IRF-3 induces transcription of the IFN- β promoter but not the promoter of IFN- α gene that lacks the NF- κ B binding site (172). These results indicate that IRF-3 does not activate IFN gene transcription on its own but can cooperate with RelA to stimulate the IFN- β promoter.

IRF-3 demonstrates a unique response to viral infection (118,230). Following Sendai virus infection, IRF-3 is post-translationally modified by protein phosphorylation at multiple serine (Ser) and threonine (Thr) residues, located in the carboxy-terminus of IRF-3. A combination of IRF-3 deletion and point mutations localize the inducible phosphorylation sites to the region -ISNSHPLSLTSDQ- between amino acids 395 and 407; point mutation of Ser-396 and Ser-398 residues eliminates virus-induced phosphorylation of IRF-3 protein, although residues Ser-402, Thr-404 and Ser-405 are also targets. Phosphorylation results in the cytoplasmic to nuclear translocation of IRF-3, DNA binding and increased transcriptional activation. IRF-3 possesses a functional nuclear export signal (NES); deletion of aa 129 to 190 (230) or point mutation of lysine residues L145 and L146 (118) results in constitutive nuclear retention of IRF-3 following virus infection. Substitution of the Ser/Thr sites with the phosphomimetic aspartic acid (Asp) amino acid generates a constitutively active form of IRF-3 that functions as a very strong activator of promoters containing PRDI/PRDIII or ISRE regulatory elements. Phosphorylation also appears to represent a signal for virus mediated degradation, since the virus induced turnover of IRF-3 is prevented by mutation of the IRF-3 Ser/Thr cluster or by proteasome inhibitors. Interestingly, co-immunoprecipitation experiments reveal that virus infection leads to IRF-3 association with the CBP coactivator and this interaction is mediated by the C-terminal domains of both proteins. Mutation of residues Ser-396 and Ser-398 in IRF-3 abrogates its binding to CBP (118). An IRF-3 mutant lacking the DBD (aa 58-427) expectedly does not bind DNA but is phosphorylated and associates with CBP in response to virus infection. However, this DBD mutant functions in a dominant negative manner as it

blocks virus-mediated activation of IFN- α/β and other IFN-stimulated genes (230).

A model in which virus-inducible C-terminal phosphorylation of IRF-3 alters protein conformation to permit nuclear translocation, association with transcriptional partners and primary activation of IFN- and IFN-responsive genes is proposed ((118); Figure 8). IRF-3 exists in a latent state in the cytoplasm of uninfected cells. The IRF-3 C-terminus may physically interact with the DBD in such a way as to obscure both the DBD and the IAD regions of the protein; the presence of an autoinhibitory domain within the C-terminal 20 aa (407-427) would explain the activating effect of this deletion, as seen with IRF-4 ((23,49); discussed later). Virus induced phosphorylation at the Ser/Thr residues at the 396-405 aa cluster leads to a conformational change in IRF-3, exposing both the DBD and IAD and relieving C-terminal autoinhibition. Translocation to the nucleus, occurring via an unidentified nuclear localization sequence or in conjunction with a transcriptional partner associating through the IAD region, leads to DNA binding at ISRE- and PRDI/PRDIII-containing promoters. Phosphorylation is also necessary for IRF-3 association with the chromatin remodeling activity of CBP/p300. The presence of a NES element ultimately shuttles IRF-3 from the nucleus and terminates the initial activation of IFN responsive promoters. The phosphorylated form of IRF-3 exported from the nucleus may now be susceptible to proteasome mediated degradation. This scenario shares several features with the protein synthesis independent activation of NF- κ B, complements the finding that IRF-3 and CBP/p300 are components of the dsRNA-inducible complex DRAF (40,218), and suggests that IRF-3 may be the

Figure 8. Model for virus-mediated activation of IRF-3. IRF-3 exists in a latent state in the cytoplasm of uninfected cells. The IRF-3 C-terminus may physically interact with the DBD in such a way as to obscure both the DBD and the IAD regions of the protein. Virus induced phosphorylation of the Ser/Thr residues in the 396-405 aa cluster leads to a conformational change in IRF-3, exposing both the DBD and IAD and relieving C-terminal autoinhibition. Translocation to the nucleus, occurring via an unidentified nuclear localization sequence or in conjunction with a transcriptional partner associating through the IAD region, leads to DNA binding at ISRE- and PRDI/PRDIII-containing promoters. Phosphorylation is also necessary for IRF-3 association with the chromatin remodelling activity of CBP/p300 protein. The presence of a NES element ultimately shuttles IRF-3 from the nucleus and terminates the initial activation of IFN responsive promoters. The phosphorylated form of IRF-3 exported from the nucleus may now be susceptible to proteasome mediated degradation (not shown).



virus-inducible complex VIC (22,68). Interestingly, both DRAF and VIC play potential primary roles in the induction of IFN- or IFN responsive genes.

2.3 ISGF3 γ /p48

Interferon-stimulated gene factor-3 gamma (ISGF3 γ), or p48, generally exerts its transcriptional activities exclusively in association with signal transducer and activator of transcription-1 (STAT1 or p84/p91) and -2 (STAT2 or p113) proteins (the latter two are collectively termed ISGF3 α) activated through specific phosphorylation events by type I IFNs (19,209). This trimolecular complex, termed ISGF3, is formed within minutes of IFN treatment and participates in the transcriptional activation of a large number of IFN-inducible genes by binding to the ISRE; in this regard, p48 functions as an immediate early protein. p48 is constitutively expressed but is also inducible by IFN γ and viral infection (94,209). In untreated cells, this IRF member is both nuclear and cytoplasmic; however, following IFN- α treatment p48 protein levels accumulate in the nucleus (97). p48 recognizes and binds to the various ISREs and serves as an essential DBD subunit of ISGF3. Association with ISGF3 α increases p48 DNA binding affinity by 25-fold (97).

Deletion studies reveal that the IRF homology DBD of p48 is sufficient for DNA binding (208). However, like IRF-1 (159), treatment with calf intestinal phosphatase (CIP) inhibits p48 DNA binding, indicating that phosphorylation is essential for DNA binding activity. Removal of the N-terminal 9 aa of p48 dramatically decreases DNA binding affinity and specificity, demonstrating that the first 9 aa are essential for DNA target specificity. A 160 aa region

responsible for ISGF3 α -p48 interaction maps to the C-terminal aa 217 to 377 of p48; a chimeric protein consisting of the DBD of IRF-1 fused to this interaction domain associates with ISGF3 α and binds DNA in an IRF-1-specific manner (208). Interestingly, this domain is homologous to the IRF Association Domain of ICSBP, involved in ICSBP association with IRF-1 and IRF-2 (178).

2.3.1 Role of p48 and ISGF3 in Type I IFN Activation

Studies by the Taniguchi and Fujita groups have provided a new perspective on the regulation of IFN gene activity by the p48 protein (75,94,100,231). Based on the observation that MEFs from mice deficient in IRF-1 express reduced IFN- β mRNA levels in response to dsRNA but exhibit wild-type levels of IFN- β in response to NDV (129), the existence of IRF-1-dependent and -independent pathways leading to IFN- β gene expression has been proposed. The U2 cell line, which carries mutations within both p48 alleles, exhibits defective antiviral responses to type I and type II IFN (91). Interestingly, NDV infection of IRF-1^{-/-} and IRF-2^{-/-} MEFs results in the induction of p48 mRNA expression with kinetics similar to those of IFN- β . Furthermore, p48 and ISGF3 associate with the IRF-Es of the IFN- β gene. An independent study by the Fujita group shows that ISGF3 binds IRF-E with a higher affinity than IRF-1 and IRF-2 (231). Mutations within the IFN- β promoter that affect gene expression in response to NDV also prevent p48 DNA binding (94). These results support a novel role of p48 in the regulation of IFN- β gene expression in response to NDV infection.

The role of p48 in the transcriptional regulation of IFN- β was further analyzed in p48^{-/-} knockout and IRF-1^{-/-}p48^{-/-} double-knockout mice (75,100). As observed with the U2 cell line, the establishment of the antiviral state by p48^{-/-} and IRF-1^{-/-}p48^{-/-} EFs in response to type I and II IFN responses is severely impaired following infection by at least three viruses; the most dramatic impairment occurs with EMCV, and is less severe with VSV and HSV. This phenotype is similar to that seen in the type I IFN receptor (142) and STAT1 knockout mice (133), thus reinforcing the importance of ISGF3-mediated IFN signal transduction in the activation of IFN gene expression. The ISGF3 complex is detected in wild-type but not p48^{-/-} MEFs following induction by NDV. Interestingly, ISGF3 not only recognizes virus-inducible elements in the IFN- β promoter, it also interacts with the IE of the murine IFN- α 4 gene in response to NDV infection (75). Transient transfection of p48 in p48^{-/-} cells results in activation of a CAT reporter construct driven by the IE.

Type I IFN induction exhibits cell-type specificity in p48 deficient mice. First, in p48^{-/-} MEFs, NDV induction of IFN- α mRNA is reduced 40-fold, while IFN- β mRNA levels are decreased only two-fold. Residual IFN is still detected in the MEF culture supernatant, suggesting the involvement of a factor(s) - distinct from p48 - which binds to the IFN promoters and mediates IFN gene induction by NDV. To date, isolation of such a factor(s) has been unsuccessful; the availability of this factor appears to be protein synthesis independent but requires virus-induced tyrosine phosphorylation for activation (75). IFN priming does not occur in p48-deficient MEFs, thus implicating p48 in the priming process. Second, in contrast to the observations in p48^{-/-} MEFs, the decreases observed in macrophages of the

same mice are more drastic - 100-fold and 10-fold for IFN- α and - β , respectively. Third, p48^{-/-} splenocytes exhibit wild-type levels of type I IFN in response to NDV. No significant defect in IFN- β gene induction is found in p48 defective cell lines generated in the Stark laboratory (reviewed in (41)). In contrast, the Fujita group reports down-regulation of IFN- α and IFN- β gene induction in cells expressing a dominant negative mutant of p48 (231). Taken together, these results support a novel role of p48 and ISGF3 in the regulation of type I IFN genes.

A model by which p48 and ISGF3 mediate their regulatory effects has been proposed by the Taniguchi group and is illustrated together with the Weissmann model discussed earlier in Figure 7. The pathway consists of two steps. Viral infection initiates the first step of induction by stimulating the synthesis of small amounts of IFN- α/β . The secreted IFNs then stimulate the JAK-STAT pathway by both autocrine and paracrine mechanisms; the formation of ISGF3, the second step, results in maximum IFN- α/β activation. ISGF3-mediated activation of type I IFN may proceed directly or indirectly through activation of another, as yet unidentified, factor Z. The autocrine/paracrine second step would thus be impaired in p48^{-/-} cells, while the residual IFN observed in the p48^{-/-} MEFs corresponds to that produced during the unaffected first step of IFN- α/β activation.

2.4 ICSBP

Interferon consensus sequence binding protein (ICSBP) was originally isolated as the protein that recognized the ISRE motif present in the promoter region

of the MHC class I, H-2L^D gene (43,219). Sequence comparison studies reveal that ICSBP is more similar to ISGF3 γ than to IRF-1 and IRF-2. Unlike IRF-1, IRF-2, IRF-3 and ISGF3 γ , ICSBP exhibits a tissue-restricted pattern of expression and is expressed exclusively in cells of the immune system, particularly in the macrophage and lymphoid lineages. Expression of ICSBP is constitutive and can be dramatically enhanced by IFN- γ but not by IFN- α/β . Characteristic of an immediate early gene, induction of ICSBP expression is rapid and independent of *de novo* protein synthesis. Also unique to ICSBP is its very weak DNA binding affinity (43), which can only be detected using Southwestern assays. However, as will be discussed, ICSBP DNA binding is dramatically increased following interaction with IRF-1 and IRF-2 (21,178). By Southwestern assays, it was found that ICSBP not only recognizes the ISRE of MHC class I gene, but also of other IFN-inducible genes such as ISG54, 2'5' OAS and 6-16. Interestingly, this IRF member also demonstrates DNA binding to the PRDI element of the IFN- β gene (43). ICSBP can repress IRF-1-mediated induction of MHC class I and IFN- β reporters in the absence of IFN treatment (144). These ICSBP-mediated inhibitory effects are alleviated by either IFN- β or IFN- γ treatment, indicating that ICSBP has a role similar to IRF-2 in selectively repressing ISRE- and PRDI-containing promoters. ICSBP also inhibits the DNA binding activity of p48, although direct association between these two proteins has not been demonstrated (21). Using domain swap analyses, it was demonstrated that ICSBP has a modular structure that is comprised of two components, a DBD and a repression domain (177).

Stable expression of a truncated ICSBP consisting of the DBD interferes with IRF-1 transactivation, possibly through competitive binding to the ISRE. Furthermore, ICSBP DBD also inhibits expression of IFN-inducible genes such

as ISG54, 2'5'OAS, IRF-2, PKR and STAT1 (201). This inhibition is not observed in cells expressing full-length ICSBP. Strikingly, cell lines expressing ICSBP DBD grow slower than control cells, while the parental wild-type ICSBP clones exhibit control growth rates. Cell cycle analysis reveals that progression through S and G2/M stages is delayed in the DBD clones. Surprisingly, while control and ICSBP clones are predictably sensitive to the antiproliferative activities of type I and II IFNs, ICSBP DBD cell lines remain refractory to IFN growth regulation. The latter observation may be related to the finding that IFN- γ -mediated inhibition of phosphorylation of the retinoblastoma (Rb) protein results in G1 arrest and is prevented in ICSBP DBD cells. These results thus confer a growth regulatory activity to the ICSBP DBD (201).

ICSBP interacts with IRF-1 and IRF-2 both *in vivo* and *in vitro*, and this interaction greatly enhances the otherwise very low binding affinity of ICSBP to the ISRE (21,178). The region involved in IRF-ICSBP interaction is mapped to a 177 aa region (aa 200-377) in the C-terminal repressor domain of all three proteins. Interestingly, this region, now called the IRF association domain (IAD), is conserved amongst many IRF family members, including IRF-3, IRF-4, IRF-5 and p48 (178). Direct binding of ICSBP to DNA is prevented by tyrosine (Tyr) phosphorylation *in vitro* - hence its failure to be detected by EMSA (43). However, ICSBP in its Tyr-phosphorylated form strongly interacts with target DNA through its association with Tyr-phosphorylated IRF-1 and IRF-2 (178). Predictably, ICSBP, IRF-1 and IRF-2 are Tyr-phosphorylated *in vivo*. The ICSBP/IRF-2 complex binding is found to be constitutively expressed, while ICSBP/IRF-1 DNA binding is induced by IFN- γ . These results imply that like STATs, IRF activity is regulated in part by Tyr

phosphorylation and subsequent interaction with other family members. Strikingly, ICSBP also interacts with Tyr-phosphorylated PU.1 - the interacting partner of Pip/IRF-4 - and subsequently binds to the λ B site of the immunoglobulin light chain enhancer (23).

As with IRF-1 and IRF-2 deficient mice, ICSBP knockout mice exhibit immunodeficiencies and dysregulated hematopoiesis, demonstrating a role of ICSBP in the proliferation and differentiation of hematopoietic progenitor cells (84). Unlike IRF-1 and IRF-2 knockout mice, ICSBP^{-/-} and ICSBP^{+/-} mice display an obvious pathological change: a syndrome similar to human chronic myelogenous leukemia. These mice are also selectively sensitive to particular viral infections, demonstrating a critical role for ICSBP in the establishment of the antiviral state. Spleen cell extracts from ICSBP knockout mice predictably do not display ICSBP or ICSBP-IRF-2 complex DNA binding. Although IRF-1 and IRF-2 mRNA levels remain normal, no IRF-2 protein expression or DNA binding is detected in these cells, suggesting a defect in posttranscriptional and translational modification of IRF-2. Expression of virus- or IFN-regulated genes such as IFN- α , IFN- β , and MHC class I, as well as cellular responses to IFN- α and IFN- γ are not affected by the absence of ICSBP. VSV infection is well controlled in ICSBP^{-/-} mice, indicating that the B and T helper cell compartment as well as the IFN type I system are normal in these mice. However, a contrasting phenotype is observed following infection with vaccinia virus (VV; *Poxviridae*) and LCMV. Wild-type ICSBP mice survive VV or LCMV infections but ICSBP^{-/-} mice die within 10-20 days after infection. This result correlates with a dramatic decrease in cytotoxic T lymphocyte (CTL) activity, as well as deficient production of IFN- γ after stimulation of T-cells or macrophages. Impaired antiviral immunity to

LCMV is similarly observed in IRF-2 deficient mice, but not in IRF-1 deficient mice, suggesting a role of the two IRF repressor molecules in antiviral defense against LCMV (84).

The antiviral activity exhibited by ICSBP extends to infection by human immunodeficiency virus-1 (HIV-1; *Retroviridae*) (200). The ICSBP DBD strongly inhibits infection by VSV and HIV when stably expressed in monocytic U937 cells. The repressive effect of ICSBP DBD on HIV-1 infection may be mediated directly. The HIV-1 genome contains an ISRE-like sequence 3' of the transcription initiation site that binds IRF family proteins (50,115,200,205).

2.5 Pip/LSIRF/IRF-4/ICSAT

The birth of another member of the IRF family resulted from an effort to clone factors binding to the murine immunoglobulin (Ig) light chain enhancer E λ 2-4 (49). PU.1 interaction partner, or Pip (most likely identical to NF-EM5), was discovered as a novel murine transcription factor with an IRF-like N-terminal domain. Pip binds to DNA, but exclusively in association with PU.1, a member of the ETS family of transcription factors that in their own right contribute to lymphoid and myeloid lineage development (37). Serine phosphorylation at aa 148 of PU.1 is required for PU.1-Pip interaction and subsequent binding of the heterodimer to the ISRE-like λ B site in the Ig enhancer region. Pip most closely resembles ICSBP, sharing 80% homology at the N-terminal end and 48% homology over a 160 aa C-terminal region of Pip. Expression of Pip is restricted to the B and T cell lineages; however, PU.1

is exclusively expressed in B-cells, thus conferring B-cell specificity to the PU.1-Pip heterodimer. The PU.1-Pip dimer functions as a transactivator when bound to the enhancer but both factors display mutual co-dependence for activity. PU.1 is able to bind DNA on its own, but will not transactivate unless associated with Pip; therefore, PU.1 and Pip function as mutually dependent transcription factors.

Further studies map unique functional domains in the Pip protein (23). Pip's closest sibling, ICSBP, is also able to form a ternary complex with PU.1 and the λ B DNA sequence. However, unlike PU.1-Pip, PU.1-ICSBP does not modulate expression of a reporter CAT construct driven by λ B sites, indicating that the transactivation observed with PU.1-Pip results from an activation domain present in Pip. Indeed, the C-terminal region of Pip consisting of aa 150 to 450 stimulates transcriptional activity when fused to the heterologous GAL4 DBD. While IRF-1 and p48 recognize λ B and activate transcription of λ B-CAT constructs, a truncated Pip protein consisting of the DBD is able to trans-repress IRF-1 and p48-mediated transactivation in the absence of PU.1, suggesting that Pip is a "dichotomous regulator" with both activation and repression domains (23).

The Pip DBD is also able to bind DNA in the absence of its partner, suggesting a potential C-terminal inhibitory domain within Pip preventing DNA binding of the full-length protein which may be masked when Pip associates with PU.1 (49). Interestingly, Pip does possess a domain in its C-terminal end (aa 410 to 439) which inhibits its binding to DNA in the absence of PU.1 and is concomitantly required for high affinity ternary complex formation. When the region of Pip containing the DNA autoinhibitory domain (aa 138 to 450) is

fused to the DBD of p48, it prevents p48 binding to DNA and also allows PU.1-p48 ternary complex formation with λ B. A model for the regulation of Pip activity based on these results was proposed in which the C-terminal DNA binding autoinhibition domain of Pip folds over and interacts with the DBD of Pip (23). In the presence of PU.1 phosphorylated on serine 148, a PU.1-Pip heterodimer is formed that disrupts Pip autoinhibition and results in the formation of a high affinity ternary complex with DNA. Potential interaction between PU.1 and the DBD of Pip may further increase DNA binding activity.

Mutagenesis studies were performed defining the region of PU.1 required to recruit Pip to DNA (157,161). Three segments within the PU.1 PEST domain (aa 118-125, 133-139, and 141-147) are important for DNA recruitment of Pip by PU.1. Furthermore, the ETS domain of PU.1 (aa 170-255) and other ETS family members is also necessary and sufficient for interaction with Pip, but is not adequate for recruitment of Pip to DNA. It is thought that PU.1-Pip interaction occurs by a two-step mechanism. Interaction between PU.1 and Pip occurs first via the PU.1 ETS domain. Upon serine 148 phosphorylation, the PU.1 PEST domain undergoes a conformational change which then allows binding of Pip to DNA. The PU.1 PEST domain does not signal protein degradation. Taken together, these results indicate that conformational changes in both PU.1 and Pip proteins are essential for DNA binding of the PU.1-Pip heterocomplex.

Independently, another group cloned the same protein which they called lymphoid specific IRF (LSIRF), now termed IRF-4 (128). In contrast to Pip, LSIRF binds autonomously to the ISRE of the MHC class I promoter. LSIRF expression is low in primary lymphocytes and is not induced by IFN.

However, LSIRF levels are dramatically elevated by receptor-crosslinking stimuli such as plant lectins, CD3 or IgM.

Yamagata et al. also recently isolated the human equivalent of Pip/LSIRF/IRF-4 from an adult T-cell leukemia cell line, hence its name IFN consensus sequence- β -binding protein in adult T-cell leukemia cell lines or activated T-cells (ICSAT), also termed IRF-4 (227). IRF-4 possesses a very different function compared to its murine counterpart. While PU.1-Pip functions as a transactivator complex, IRF-4 exerts an IRF-2 and ICSBP-like repressive effect on IFN- and IRF-1-induced gene activation. Interestingly, IRF-4 expression is restricted to a specific subset of lymphocytes: only T-cells treated with PMA and calcium ionophore A23187 or infected with the human T-cell leukemia virus-1 (HTLV-1) express this IRF protein. Jurkat cells transiently transfected with the HTLV-1 Tax gene become induced to express IRF-4, indicating that Tax may function as a viral activator upstream of the IRF-4 gene. Since the oncogenic potential of HTLV-1 resides in the transactivation function of the Tax protein (reviewed in (83)), induction of IRF-4 expression by Tax may be an important cellular target implicated in HTLV-1-induced leukemogenesis (227). The induction of this unique IRF family member by another T-cell activation signal, PMA, furthermore implies that IRF-4 may function in the transduction of proliferative signals in response to T-cell activation.

IRF-4 deficient mice were generated, and like many other IRF^{-/-} mice, develop severe immunodeficiencies (137). While normal T- and B-cell distribution is observed at 4 to 5 weeks of age, with time IRF-4^{-/-} mice gradually exhibit severe lymphadenopathy. Both B- and T-cell activation is

profoundly affected; serum immunoglobulin concentrations and antibody responses are reduced and cytotoxic and antitumor responses are absent in IRF-4 knockout mice. Normal early T-cell events such as calcium influx and expression of the T-cell activation markers CD25 and CD69 in IRF-4^{-/-} T-cells indicate that IRF-4 may function at later stages of T-cell activation, possibly at the level of IL-2 production and/or IL-2 response. This hypothesis is further supported by the observation that the reduced T-cell proliferation in these mice is not reversed by exogenous IL-2 treatment.

In addition to exerting an immunomodulatory role, IRF-4 also plays a potential role in cell growth regulation. The IRF-4 gene maps to chromosome 14q32, a locus in juxtaposition with a translocation which is recurrent in cases of multiple myeloma. Furthermore, expression of IRF-4 in Rat-1 fibroblasts results in cellular transformation *in vitro*, implicating IRF-4 as a potential oncogene, designated the "multiple myeloma gene-1" (MUM1; (88)).

2.6 IRF-7

Most of the IRF family members so far identified appear to have specific and critical functions in lymphoid cells and/or their action is related to the signalling pathway induced by IFN or viruses. Interestingly, there is recent evidence indicating that the IRF(s) may also play a role in the transcriptional activation of viral promoters. The Q_p promoter region of the EBV-encoded gene EBNA-1 contains an ISRE-like element (QRE-2) that is responsive to IRF-1 and IRF-2 as well as to IFN- α (149,150,171). Using a yeast one-hybrid screen technique, a new factor was recently isolated that binds specifically to the QRE-2 (149,234). The amino acid sequence of this protein is identical to

the IRF-7 protein present in the Genbank database ((66); accession number U73036). By homology search of the HGF ETS cDNA library the Pitha group also found a novel IRF whose sequence is identical to that of IRF-7 (Au, Moore and Pitha, *unpublished results*). Several open reading frames (ORFs) of IRF-7 have been identified. Three shorter ORFs were identified by the Pagano's group (234), listed in the database as IRF-7A, B and C (accession nos. U53830, U53831 and U53832, respectively). Two IRF-7 cDNAs isolated by the Pitha group contain insertions in either the N- or C-termini, suggesting that this gene may undergo differential patterns of splicing.

Expression of IRF-7 is predominant in the spleen, thymus and both primary peripheral blood lymphocytes (PBLs) and PBL cell lines (234), and is also effectively induced by IFN- α in B-cells and other cells of lymphoid origin (149). Interestingly, IRF-7 expression is also coupled with EBV latency; while IRF-7 is undetectable in type I latency cells, levels of this IRF protein are consistently high in type III latency cells (234).

At the amino acid level, IRF-7 shows highest homology to IRF-3. *In vitro* translated IRF-7 encodes a protein of 68 kDa (66,149). IRF-7 binds to QRE-2 and is able to compete with IRF-1 for the Q μ ISRE site. In addition, IRF-7 also represses basal levels as well as IFN- α and IRF-1 mediated transactivation of a reporter gene construct containing Q μ ISRE sequences (234). Further studies ongoing in several laboratories are addressing the role of IRF-7 in the regulation of EBNA-1 gene expression, IFN- α -mediated signalling and expression of IFN- α -stimulated genes.

2.7 The viral IRFs

The presence of human herpes virus (HHV)-8 in Kaposi's sarcoma and plural effusion lymphoma suggests that this virus plays a role in these malignancies. In addition to genes required for viral replication, HHV-8 contains a unique set of nonstructural genes, some of which are homologous to cellular genes regulating the cell cycle, apoptosis and early inflammatory responses (141,168). These viral analogues potentially serve as components of viral mimicry and may be essential for viral replication and pathogenicity *in vitro*. Interestingly, the HHV-8 sequence contains four ORFs encoding proteins homologous to the IRF family members (141), termed viral IRFs (vIRFs). The role of HHV-8 encoded vIRFs in HHV-8 replication and oncogenicity is not known. Since the HHV-8 genome contains several DNA recognition domains that are identical to the ISRE, vIRFs may be involved in modulating both HHV-8 replication and HHV-8 associated tumorigenicity.

The HHV-8 encoded vIRF present in the genome between nucleotides 83 860 and 85 209 was cloned. This 55 kDa protein contains only two of the five conserved N-terminal IRF tryptophan repeats. An initial 5' 87 aa stretch unique to vIRF contains another tryptophan residue. This stretch is followed by a sequence of about 50 aa which shares extensive homology with the cellular IRF N-terminal DBDs. Whether this region also determines the DNA binding specificity of vIRF is not known; preliminary data indicate that recombinant vIRF protein does not bind efficiently to the ISRE of the ISG15 gene (Schafer and Pitha, *unpublished results*).

Overexpression of vIRF in 293 cells down-regulates both constitutive and IFN-stimulated transcriptional activities of ISRE-containing genes such as ISG15 and PKR (Schaffer and Pitha, *unpublished results*). Furthermore, while it has no significant effect on the expression of the EBV EBNA-1 gene through the Q_p promoter region, this vIRF down-regulates transcriptional activity of constructs driven by the HIV-LTR. Zimring *et al.* (235) demonstrate by reporter gene assays that vIRF represses transcriptional activation by Type I and Type II IFN and IRF-1. This is in accordance with the recent finding that NIH3T3 cells expressing vIRF are less sensitive to the antiviral effect of IFN (Pitha, *unpublished results* and Moore, *personal communication*). However, vIRF does not compete with IRF-1 for the ISRE site; rather, vIRF interferes with the transactivation function of IRF-1 (235). These results indicate that vIRF may interfere with IFN- α -mediated signalling and subsequently with IFN antiviral effects, and that vIRF mediated repression proceeds through a novel mechanism distinct from that involving DNA binding competition with IRF activators typical of other IRF repressor proteins.

The oncogenic potential of vIRF was analyzed by generating stable vIRF NIH3T3 cell lines. As seen with IRF-2, overexpression of vIRF induces growth in soft agar and tumor growth in nude mice (Pitha, *unpublished results* and Moore, *personal communication*). Whether vIRF-mediated oncogenicity can be reversed by IRF-1, as shown for IRF-2, remains to be elucidated.

Altogether, these results suggest that vIRF may play a dual role; it may (1) regulate HHV-8 gene expression and subsequent viral replication and (2) take part in viral mimicry by direct interference with the IFN signalling pathway.

Blockade of the IFN pathway by vIRF may affect not only the establishment of the antiviral state but also lead to the modulation of apoptosis and induction of an oncogenic phenotype. It would be interesting to see whether the other viral ORF-encoded IRF-like proteins induce similar effects.

2.8 Cross-regulation of expression among the IRF family members

In addition to participating in the regulation of many IFN-inducible genes, the IRFs also regulate the expression of each other. The IRF-2 promoter contains an IRF consensus site which is activated by IRF-1 when placed upstream of a CAT reporter construct (27). Furthermore, IRF-2 expression is inducible by transient or stable IRF-1 expression (76), suggesting that IRF-1 may play a role in the regulation of its partner IRF-2 gene. An IFN- γ -activated sequence was identified in the IRF-1 and murine ICSBP promoters and was shown to be bound by the STAT1 (p91) subunit of ISGF3 (93,158). Activation via Tyr-phosphorylation of STAT1 correlates with transcription of IRF-1 in response to IFN- γ treatment, thus establishing a direct link between the IFN JAK-STAT signal transduction pathway and induction of IRF expression (158). Furthermore, as will be shown in Chapter V, IRF-1 upregulates STAT1 expression as well (146), implying feedback regulation of STAT1 expression by IRF-1. Both IRF-1 and IRF-2 gene promoters contain the consensus binding site of the NF- κ B family of transcription factors (27,76,182). Cross-regulation of expression among the IRFs and interactions among the family members suggest a complex gene network in the regulation of the IFN system.

Table 3. Summary of IRF properties and functions. Relevant reference numbers are indicated. Generally, IRF expression is either constitutive and/or induced upon treatment with IFNs or other cytokines or in response to viral infection. Some factors are hematopoietic specific while other family members are expressed in multiple tissues and cell lines. While some members are IFN-inducible, all IRFs themselves are involved in the transcriptional regulation of type I IFN and/or IFN-inducible genes. IRFs vary in transcriptional activity, classified as activators, repressors, or both. Studies characterizing IRF-expressing cell lines and IRF knockout mice reveal that each member of the IRF family exerts distinct roles in biological processes such as pathogen response, cytokine signalling, cell growth regulation and hematopoietic differentiation.

IRF Member	Expression Pattern	Inducers of Expression	Transcriptional Role	Target Genes	Physiological Role(s)	Knockout Phenotype	Role in Resistance of
IRF-1	most cell types (138) low-level constitutive (138) inducible (138,57,3)	Type I IFN (57) Type II IFN (57,101) virus infection (138) dsRNA (57) TNF (57) IL-1 (57) IL-6 (3) LIF (3) ConA (138) Ca ionophore A23187 (57) PMA (57)	Activator (58,138,55,72)	IFN- α (138,11) IFN- β (58,138,55,72) 2'5'OAS (163,101,130) MHC Class I (138,163) GBP (101,130) INOS (92,127) PKR (102,106, Chapter V) ICE (189) WAF1 (152, Chapter V) STAT1 (Chapter V) Lysyl oxidase (190) IRF-2 (27,76) EBNA-1 (149,171) LMP-1 (220) TAP-1 (220) SLPI (Chapter VI)	tumor suppressor (73,193,224,74,104,192,102,106,189,152,190,36,70, Chapter IV) antiviral defense (129,155,220,187,47,92,127,164,101,130) immune regulation (129)	Impaired CD8 ⁺ cell maturation (129)	EMCV (Picornaviridae) (101)
IRF-2	most cell types (72) constitutive (72) inducible (72)	Type I IFN (72) virus infection (72)	Repressor (IFN- β) (72) Activator (H4, EBNA-1) (206,149,171)	IFNB (72) Histone H4 (206) EBNA-1 (206,171)	oncogene (73,206,Chapter IV) antiviral defense (129) immune regulation (129)	bone marrow suppression of hematopoiesis and B lymphopoiesis (129)	LCMV (Arenavirus) (129)
IRF-3	most cell types (9) constitutive (9) Inducible (118,230)	PHA (unpubl.) TPA (unpubl.)	Activator (9,118,230)	ISG-15 (172) IFN- α (172) IFN- β (172)	Unknown	N/A	N/A
ISGF3γ	most cell types (209,97) constitutive (209,97)	Type II IFN (209) virus infection (94)	Activator (114,209,19)	Many ISRE-containing IFN-inducible genes (114,41,19) IFN- α (75) IFN- β (94,100,75,231)	antiviral defense (100)	none	NDV (Paramyxoviridae) EMCV (Picornaviridae) VSV (Rhabdoviridae) HSV (Herpesviridae) (100)
ICSBP	cells of macrophage and lymphoid lineages (43,219) low-level constitutive (43,219) inducible (43,219)	Type II IFN (43)	Repressor (21,144,178,201)	MHC Class I (43,219) ISG-54 (43) 2'5'OAS (43) 6-16 (43) IFN- β (43)	antiviral defense (84,200) immune regulation (84)	deregulated hematopoiesis (84) human CML-like syndrome (84)	VV (Poxviridae) (84) LCMV (Arenavirus) (84) HIV (Retroviridae) (200) VSV (Rhabdoviridae) (200)
IRF-4	Activated T-cells ATL cells (227)	PMA (227) HTLV-1 Tax (227)	Repressor (227)	Unknown	immune regulation (137)	severe lymphadenopathy (137) Impaired T- and B-cell activation (137)	N/A

RESEARCH OBJECTIVE AND SPECIFIC AIMS

The objective of this research was to investigate the effects of IRF-1 and IRF-2 on the regulation of gene expression and cell growth. Initially, structure-function studies of the IRF proteins were performed through the analysis of C-terminal IRF deletion mutants in co-transfection studies. These studies localized IRF DNA binding to the N-terminus of both proteins, IRF-1 transactivation to the C-terminus, and IRF-2 repression to the N-terminal DNA binding domain. Identification of IRF-1 and IRF-2 as a tumor suppressor and oncogene, respectively, led to division of the research objective into three specific aims. The first specific aim was to analyze the effects of IRF-2 on oncogenic phenotype and IFN- β expression. A direct correlation between IRF-2 DNA binding/transcriptional repression and oncogenic transformation phenotype was revealed. This work prompted investigation of the relationship between IRF-1 transactivation function and tumor suppression. The second specific aim was to analyze the effects of IRF-1 on cell growth and expression of growth regulatory genes. In the process of these studies, tetracycline-responsive cell lines inducibly expressing IRF-1 and the IRF-1-like IRF/RelA proteins were established. The third specific aim was to take advantage of these inducible cell lines and RNA fingerprinting to identify novel IRF-1 gene targets and characterize their role in IRF-1-mediated activities. This work led to the identification of the secretory leukocyte protease inhibitor as an IRF-1-repressed gene, assigning a repressor function to IRF-1 and a novel role for IRF-1 in the modulation of inflammatory and antiretroviral responses.

CHAPTER II

MATERIALS AND METHODS

1 Plasmid Construction

1.1 IRF deletion mutants

Six IRF-1 and eight IRF-2 fragments containing different length deletions in the C-terminus were generated by 25 cycles of PCR amplification. DNA oligonucleotide primers were synthesized using an Applied Biosystems DNA/RNA Synthesizer. Both the N-terminal and C-terminal primers for IRF-1 deletion mutants were synthesized with *EcoRI* restriction enzyme sites at their ends for cloning into the CMV-BL expression plasmid, which contains the CMV promoter adjacent to the multiple cloning site of bluescript BL vector followed by a polyA site derived from SV40 (a kind gift from Dr. A. Cochrane). With the *EcoRI* site underlined, the sequence of the N-terminal IRF-1 primer is 5'-AGCAGAAATTCACATGCCCATCACTTG GATG-3' and the sequence of the IRF-1 C-terminal primers is as follows:

IRF-1(120): 5'-AGCAGAAATTCACCTATCTCTGGTTCTTGGTGAG-3'
IRF-1(150): 5'-AGCAGAAATTCACCTAATCAGAGAAGGTATCAGG-3'
IRF-1(170): 5'-AGCAGAAATTCACCTACATGTAGCCTGGAAGTGT-3'
IRF-1(200): 5'-AGCAGAAATTCACCTATTCCACTGGGATGTGCCA-3'
IRF-1(250): 5'-AGCAGAAATTCACCTAGTTTGTGGCTGCCACTC-3'
IRF-1(300): 5'-AGCAGAAATTCACCTAGTTCCTCAGATCTGTGAA-3'

Primers for the generation of the various IRF-2 deletion mutants had an *XbaI* site at their ends. With the *XbaI* site underlined, the sequence for the IRF-2 N-terminal primer is 5'-GTACTCTAGACCCATGCCGGTGGAACGGATG-3' and the sequence of the IRF-2 C-terminal primers is as follows:

IRF-2 (100): 5'-GTACTCTAGATTACTTTATGCTTCTGGTCCTTCAC-3'
IRF-2 (125): 5'-GTACTCTAGATTATGGTTTCTTTCTTTCTTGG-3'
IRF-2 (160): 5'-GTACTCTAGATTAGACCGCATACTCAGGAGA-3'
IRF-2 (200): 5'-GTACTCTAGATTAGCAGATGTCTGGCGGGTTA-3'
IRF-2 (240): 5'-GTACTCTAGATTAGGCCACACTGTCCGGTAGT-3'
IRF-2 (270): 5'-GTACTCTAGATTAGTTCCGTGTCCCATGTT-3'
IRF-2 (300): 5'-GTACTCTAGATTAAGGCATCGGACAGCTATC-3'
IRF-2 (320): 5'-GTACTCTAGATTACGTGGGGGTCACTGGGGC-3'

1.2 IRF/RelA fusion proteins

The IRF-1/RelA and IRF-2/RelA fusion proteins were generated and inserted into the CMV-BL expression vector by Dr. Rongtuan Lin using a four step process. First, a PCR-generated 1.3 kb *XbaI/XhoI* fragment containing the sequence encoding the C-terminus of RelA (aa 397 to aa 550) from SVK3/p50/RelA was inserted into the *XbaI/XhoI* backbone fragment of the pBluescript KS vector. Second, a 1.3 kb *NotI*(blunt)/*XhoI* fragment from the resulting plasmid was cloned into the *HindIII*(blunt)/*XhoI* backbone fragment of SVK3/IRF-1p1, an SVK3 based plasmid carrying an IRF-1 cDNA in which the sequence encoding aa 205 and aa 206 of IRF-1 was mutated to generate a *HindIII* site. Third, a 2.6 kb *EcoRI/BamHI* fragment from this intermediary plasmid was ligated to the *EcoRI/BglIII* backbone fragment of CMV-BL, resulting in the generation of CMV/IRF-1/RelA. Finally, the CMV/IRF-2/RelA plasmid was constructed by inserting a 0.6 kb *HindIII/AvaII*(blunt) fragment from CMV/IRF-2 into the *HindIII/XbaI*(blunt) backbone fragment of CMV/IRF-1/RelA.

1.3 Recombinant IRF proteins

IRF-1 and IRF-2 were inserted into the baculovirus pAcH6N1 vector for the generation of polyhistidine-tagged IRF recombinant proteins. The pAcH6N1/IRF-1 plasmid was a kind gift from Dr. Dirk Gewert. pAcH6N1/IRF-2 was constructed by Dr. Rongtuan Lin (117) by first inserting a ≈ 1.4 kb *XbaI-XhoI* fragment from CMV-BL/IRF-2 containing the IRF-2 gene into the *XbaI-XhoI* site of a pSVK3-based vector and then subcloning a ≈ 1.3 kb *Cfr10I*(blunt)-*KpnI* fragment from the resulting plasmid into the *BglII*(blunt)-*KpnI* site of the pAcH6N1 vector.

1.4 Tetracycline-regulated expression plasmids

CMV_t-rtTA contains the Moloney murine leukemia virus-based pBABE vector backbone, which contains a puromycin (puro) resistance gene under the control of the CMV promoter. Construction of the plasmid consisted of the consecutive insertion of three components into the polylinker site: the doxycycline-responsive promoter CMV_t from the CMV_tBL vector (a kind gift from A. Cochrane), the rtTA gene from the pUHD172-1neo plasmid (179), and the polyA fragment from the pSVK3 vector. neo CMV_t BL was constructed in two steps. First, an intermediary plasmid (neo BL) was generated by ligation of a 3 kb *XhoI/EcoRI* fragment from the pMV7 vector (contains the neomycin (neo) resistance gene) to a 3.8 kb *XhoI/EcoRI* fragment from the CMV BL vector (contains the poly A site and the ampicillin (Amp) resistance gene). Second, a 450 bp *XhoI*(blunt)/*NotI* fragment of CMV_t BL (contains the CMV_t promoter) was cloned into the *EcoRI*(blunt)/*NotI* sites of neo BL. CMV_t-IRF-1 was constructed by cloning of an *XbaI*(blunt) IRF-1 cDNA fragment downstream of CMV_t at the *BamHI*(blunt) site of neo CMV_t BL. Analogously, for the construction of the CMV_t-IRF-1/RelA and CMV_t-IRF-

2/RelA plasmids, *EcoRI/BamHI* IRF-1/RelA and *HindIII*(blunt)/*BamHI* IRF-2/RelA cDNA fragments were inserted into the *EcoRI/BamHI* (for IRF-1/RelA) or *EcoRI*(blunt)/*BamHI* (for IRF-2/RelA) sites of neo CMV_t BL.

2 Purification of IRF recombinant proteins

The pACh6N1/IRF-1 and pACh6N1/IRF-2 plasmids were expressed by Dr. Rongtuan Lin in baculovirus as polyhistidine-tagged proteins using a BaculoGold™ transfection kit as recommended by the manufacturer (Pharmingen). Insect SF9 cells were then infected with the recombinant baculoviruses and cultured for 4 days at 28°C. Infected cells were harvested, washed with PBS, and lysed in binding buffer (5 mM imidazole, 500 mM NaCl, 20 mM Tris-HCl, pH 7.9). Polyhistidine-containing recombinant proteins were isolated from the insect cell lysates under native elution conditions by rapid affinity purification using His-Bind metal chelation resin as recommended by the manufacturer (Novagen, pET system manual). The resulting purified recombinant proteins were then analyzed by SDS-polyacrylamide gel electrophoresis.

3 Preparation of IRF-specific antisera

Peptide sequences derived from the IRF proteins were chosen for highest degree of hydrophilicity and antigenic index. An additional cysteine residue was added at the N-terminus to facilitate coupling to the carrier protein. HPLC-purified synthetic peptides (Core Facility for Protein/DNA Chemistry, Queen's University, Kingston, Ontario) were dissolved in sterile water and coupled to preactivated Keyhole Limpet Hemocyanin (KLH) carrier (Pierce,

Rockford, IL) according to manufacturer's instructions. For the primary immunization, rabbits received 1 mg of coupled peptide in Freund's incomplete adjuvant (ICN Biomedicals Inc., Costa Mesa, CA) injected subcutaneously (sc) in the dorsocapular region. Boosts of 300 ug of peptide also in Freund's incomplete adjuvant were administered sc at 4, 8, 12, 16, 20 and 24 weeks after the primary immunization. Rabbits were bled 12 to 14 days following the third, fourth, fifth and sixth boosts and serum collected. Antisera were screened by Western blot and electrophoretic mobility shift assay for specificity and reactivity to the IRF proteins. Serum from animals receiving the fifth boost (IRF-1 #51 and IRF-2 #53) was used in these studies.

4 Cell culture and generation of cell lines

4.1 Transient transfection and reporter gene assay

Transient transfections were carried out in human embryonic kidney 293 cells grown in α -Modified Eagles Medium (α -MEM) supplemented with 10% fetal bovine serum, glutamine and antibiotics. Subconfluent cells were transfected with 5 μ g of CsCl purified chloramphenicol acetyltransferase (CAT) reporter (Th-CAT and SV₀ β CAT; (109)) and CMV-IRF expression plasmids by the calcium phosphate coprecipitation method as described previously (109). In some experiments, cells were infected with Sendai virus (500 hemagglutinating units per mL for 90 min) 24h post transfection for a period of 16 to 24 hrs. All transfections were performed 3-5 times. CAT activity was assayed using 100 μ g of total protein extract for 2-4h at 37°C.

4.2 Generation of IRF-2 expressing cell lines

To generate the IRF-2 expressing cell lines, 10 ug of the IRF-2 full-length or deletion mutant CMV-BL plasmids were co-transfected with 0.2 ug of the RSV-neo plasmid, which carries a neomycin resistance gene, into NIH3T3 cells (4 to 5 x 10⁵ cells per 100 mm dish) by the calcium phosphate method. Cells were selected in Dulbecco's modified Eagles Medium (DMEM; high glucose) supplemented with 10% heat-inactivated calf serum, glutamine, antibiotics and 500 ug/ml G418 (Life Technologies, Inc.) for 2 weeks. Single colonies were then isolated and maintained individually.

4.3 Generation of inducible IRF-1 and IRF/RelA cell lines

Plasmid CMV_t-rtTA was introduced into NIH3T3 cells by lipofection (Lipofectamine, Life Technologies, Inc.) according to manufacturer's instructions. Cells were selected beginning at 48h for one week in DMEM containing 10% heat-inactivated calf serum, glutamine, antibiotics and 2.5 ng/ul puromycin (Sigma). Resistant cells carrying the CMV_t-rtTA plasmid (rtTA cells) were then transfected with the CMV_t-IRF-1, CMV_t-IRF-1/RelA and CMV_t-IRF-2/RelA plasmids. Cells were selected beginning at 48h for a period of approximately 2 weeks in DMEM containing 10% heat-inactivated calf serum, glutamine, antibiotics, 2.5 ng/ul puromycin and 400 ug/ml G418. To induce expression by tetracycline, cells were cultured in the presence of 1 ug/ml doxycycline (Sigma).

5 Analysis of growth phenotype

5.1 Measurement of growth rate

The growth rate was determined using exponentially dividing cells. Experiments were performed either in complete medium (containing 10% heat-inactivated calf serum) or serum starved medium (containing 0.5% heat-inactivated calf serum). Cells were trypsinized and counted in Isoton II solution (Coulter Electronics of Canada) every 24 hrs during a 7-day period using the electronic Coulter cell counter (Coulter Electronics of Canada). Numbers are the average of three experiments performed on two independent isolated clones per cell line, initially plated at a density of 1×10^5 cells per 35 mm dish.

5.2 Determination of saturation density

Saturation density was determined in cell cultures in medium containing 2% heat-inactivated calf serum at 4 days post-confluence. Cells were trypsinized and counted using the Coulter cell counter. Numbers are the average of three experiments performed on two independent isolated clones per cell line, initially plated at a density of 1×10^5 cells per 35 mm dish.

5.3 Soft agar assay

For the soft agar assay, 5×10^5 cells were suspended in a 0.35% agar solution in DMEM containing 20% heat-inactivated fetal bovine serum (FBS), and overlaid onto 0.5% agar solution in DMEM containing 20% FBS in 100 mm plates. Cells grown in soft agar were counted 20 days after plating, and cloning efficiency was determined as the number of colonies $\times 100$ divided by the number of cells plated (average of two experiments, 2 to 3 individual clones per cell line).

5.4 Tumorigenicity in nude mice

To assay for tumorigenicity, 1×10^6 cells suspended into 100 μ l of phosphate-buffered saline were injected subcutaneously into the hind limbs of 4 to 8 week-old athymic mice (CD1 nu/nu; Charles River). The experiment was performed using two independently isolated clones per cell line; three mice per clone were injected. The time required to produce tumors of at least 5 mm diameter was considered the latency period. Mice were inspected for 60 days.

5.5 Microscopic detection of apoptosis

To identify apoptotic cells, adherent and floating cells were harvested after 24-48h culture in the absence or presence of 1 μ g/ml doxycycline, resuspended in DMEM containing 4 μ g/ml of the DNA intercalating dye acridine orange (Sigma). The mixture was then viewed under UV illumination using a Leica fluorescent microscope. To calculate percent apoptosis, a minimum of 200 cells were counted.

6 Western blot analysis

Cells were washed once with phosphate-buffered saline and resuspended in lysis buffer (10 mM Tris-Cl pH 8.0, 60 mM KCl, 1 mM EDTA, 1 mM dithiothreitol (DTT), 0.5% Nonidet P-40 (NP-40)) containing 0.5 mM phenylmethanesulfonyl fluoride (PMSF) and 2 μ g/ml leupeptin, pepstatin, and aprotinin as protease inhibitors. Equivalent amounts of whole cell extract (20 μ g) were subject to SDS-polyacrylamide gel electrophoresis (SDS-PAGE) in a 10% polyacrylamide gel. After electrophoresis, the proteins were transferred to Hybond transfer membrane (Amersham) in a buffer containing 30 mM

Tris, 200 mM glycine and 20% methanol for 1h. The membrane was blocked by incubation in phosphate-buffered saline (PBS) containing 5% dried milk for 1h and then probed with either IRF-1 (either kind gifts from Drs. T. Taniguchi, H. Harada and R. Pine, or rabbit antiserum #51, described in section 3 of this chapter, or IRF-1 (M-20)/(C-20) from Santa Cruz Biotechnology, Inc.), IRF-2 (rabbit antiserum #53, described in section 3 of this chapter, or IRF-2 (C-19) from Santa Cruz Biotechnology, Inc.), C-terminal NF- κ B RelA (rabbit antiserum #28 (156)), STAT1 (p91) (STAT1 α (p91) (C-111) from Santa Cruz Biotechnology, Inc.), PKR (a gift from John Bell) or WAF-1 (p21) (C-19) from Santa Cruz Biotechnology, Inc.) antibody in 5% milk/PBS, at a dilution of 1:1000. These incubations were done at 4°C overnight or at room temperature for 1-3h. After four 10 min washes with PBS, membranes were reacted with a peroxidase-conjugated secondary goat anti-rabbit or anti-mouse antibody (Amersham) at a dilution of 1:2500. The reaction was then visualized with the enhanced chemiluminescence detection system (ECL) as recommended by the manufacturer (Amersham Corp.).

7 Electrophoretic mobility shift assay (EMSA)

7.1 Oligonucleotide probes

Oligonucleotide probes used for electrophoretic mobility shift assay were either synthesized using an Applied Biosystems DNA/RNA synthesizer (PRDI, TH and iNOS), obtained from GIBCO BRL/Life Technologies, Inc. (BS1, BS2, and BS12) or offered as kind gifts (ISRE and GAS; by Dr. Antonis Koromilas). Complementary oligonucleotides (50 ug each) were mixed together, heated at 85°C for 5 min and slowly cooled down to room temperature to maximize proper annealing. Double-stranded

oligonucleotides were purified on a 1X TBE (50 mM Tris-HCl, pH 8.0; 50 mM boric acid; 1 mM EDTA) 12% polyacrylamide gel (19:1 crosslink), eluted in TE (10 mM Tris-HCl, pH 8.0; 1 mM EDTA, pH 8.0) overnight at 37°C and end-labelled with [γ -³²P]-ATP (Mandel) using T4 polynucleotide kinase (Pharmacia Biotech). Unincorporated nucleotides and salts were removed by use of a G-25 Sephadex column (Pharmacia Biotech). The description and sequence of the oligonucleotide probes used in this thesis is presented in Table 4.

7.2 Extract preparation and analysis

7.2.1 Detection of IRF DNA binding

Whole cell extracts for analysis of IRF DNA binding were prepared as described in (35). Essentially, cells were pelleted after the induction period, packed cell volumes of lysis buffer (20 mM Hepes (K⁺) pH 7.9, 0.2 mM EDTA, 0.2 mM ethylene-glycol bis (β -aminoethyl ether)-N,N,N',N'-tetraacetic acid (EGTA), 0.5 mM spermidine, 0.15 mM spermine, 10% glycerol, 10 mM sodium molybdate, 1 mM DTT containing 0.5 mM PMSF and 1 μ g/ml leupeptin, pepstatin and aprotinin as protease inhibitors. Cells were lysed by the addition of high salt concentration in one packed cell volume of 2 M KCl. After 30 min incubation by rotation, cell debris was removed by 15 min centrifugation at 14 000 rpm.

Twenty micrograms (20 μ g) of whole cell extract or one to twenty-five nanograms (1-25 ng) of recombinant protein was preincubated for 10 min at room temperature in the presence of binding buffer (10 mM Tris-HCl (pH 7.5), 50 mM NaCl, 1 mM EDTA, 1 mM DTT, 5% glycerol, 0.5% Nonidet P-40, and 62.5 μ g/ml of the non-specific DNA competitor poly (dI-dC) (Pharmacia

Table 4 Description and Sequence of EMSA Oligonucleotide Probes

<u>Probe</u>	<u>Description and Sequence</u>
PRDI (P1) probe	<i>nt -79 to -64 of the IFN-β promoter; IRF binding site</i> 5'-GGGAGAAGTGAAAGTG-3'
Th probe	<i>synthetic tetrahexamer of minimal IRF binding site</i> 5'-(AAGTGA) ₄ -3'
iNOS probe	<i>IRF-1 binding site in the iNOS promoter</i> 5'-GTCAATATTTCACTTTCATAATGGAAAATTCCAT-3'
ISRE probe	<i>ISRE element in the ISG-15 promoter</i> 5'-GATCGGGAAAGGGAAACCGAAACTGAAGCC-3'
GAS probe	<i>GAS element in the IFP-53 promoter</i> 5'-GATCCAGATTCTCAGAAA-3'
BS1 probe	<i>nt -89 to -61 of the SLPI promoter</i> 5'-AGCTGGGAGAGGCCCGAAAGAATTCTGGT-3'
BS2 probe	<i>nt -79 to -45 of the SLPI promoter</i> 5'-GCCCCGAAAGAATTCTGGTGGGGCCACACCCACTG-3'
BS12 probe	<i>nt -89 to -45 of the SLPI promoter (BS1 and BS2 combined)</i> 5'-AGCTGGGAGAGGCCCGAAAGAATTCTGGTGGGGC- CACACCCACTG-3'

Biotech) in a total volume of 20 ul. Reaction mixtures involving the recombinant proteins also contained 10 mg/ml bovine serum albumin. After 30 minutes of incubation with 1 ul of 75 000 cpm/ul labelled probe at room temperature, the mixtures were loaded on a 5% polyacrylamide gel (60:1 cross-link) prepared in 0.2X TBE. After running at 200 V for 2.5 h, the gel was dried and exposed to Kodak film at -70°C overnight. To test the specificity of DNA binding, whole cell extract or recombinant protein was pre-incubated with 1 ul of antiserum or 1 ug of commercial antibody specific to IRF-1, IRF-2, RelA or STAT1(p91), with or without 1 ug of competitor peptide for 10 min at room temperature in binding buffer, prior to the addition of radiolabelled probe.

7.2.2 Detection of STAT1 and ISGF3 DNA binding

Whole cell extracts for analysis of STAT1 and ISGF3 DNA binding (IRF binding is also detectable with whole cell extracts prepared by this method) were prepared by washing cells in phosphate-buffered saline and lysing the resulting cell pellet in lysis buffer (50 mM Tris-Cl pH 8.0, 0.1 mM EDTA, 10% glycerol, 0.5 % NP-40) with 0.5 mM PMSF and 2 ug/ml leupeptin, pepstatin and aprotinin as protease inhibitors and 0.5 ng/ul chymostatin and 0.25 uM microcystin as phosphatase inhibitors.

The DNA binding reaction mixture (10 ul) contained 20 mM HEPES pH 7.9, 40 mM KCl, 1 mM MgCl₂, 0.1 mM EGTA, 0.5 mM DTT, 10% glycerol, 250 ng/ul poly (dI-dC), 0.5 mM PMSF, 2 ug/ml of leupeptin, pepstatin and aprotinin, and 1 ul of 75 000 cpm/ul radiolabelled probe. The reactions were loaded on a 6% nondenaturing polyacrylamide gel (50:1 crosslink) prepared in 0.2X TBE buffer.

8 RNA detection

8.1 RNA isolation

Total cellular RNA was isolated by the guanidium thiocyanate method as described in (31). Poly A+ enhanced RNA was isolated from the resulting total RNA by the Oligotex mRNA Kit (Qiagen Inc).

8.2 Reverse transcriptase-PCR assay.

To detect IRF-2 transgene expression, 2 ug of total RNA was analyzed by a quantitative reverse transcriptase (RT)-PCR assay previously described (38,39) using a 5' primer specific for the CMV plasmid (5'-ATATCGAATTCCTGC-3', encompassing the HindIII, EcoRV and EcoRI sites in the multiple cloning region) and a 3' primer specific for IRF-2 (5'-GATGCTTTCCTGTATG-3', representing nucleotides 334 to 350 of the IRF-2 cDNA). IFN- β mRNA levels were measured using IFN- β and SV₂CAT primers previously described in (38,39).

8.3 Northern blot analysis

Total RNA (20 ug) or poly A+ enhanced RNA (2 ug) was denatured, electrophoresed in a denaturing formaldehyde/1.2% agarose gel, and transferred to nylon membrane. IRF-1/RelA, STAT1 and SLPI mRNA were visualized by Northern blot hybridization using the first 300 bp of the IRF-1 cDNA, the complete STAT1 (p91) cDNA and a 400 bp fragment of SLPI cDNA (nucleotides 786 to 1089), respectively, labelled with [α -³²P]dCTP by nick translation using the Oligolabelling Kit (Pharmacia Biotech).

8.4 RNA fingerprinting

The RNA fingerprinting reactions were performed using the Delta™ RNA Fingerprinting Kit (CLONTECH Laboratories, Inc.). The reactions were resolved on a 5% Long Ranger™ gel (50% Concentrate; J. T. Baker, Inc.) in 0.6X TBE. After running at 65 W for 1.5 h, the gel was dried and exposed to Kodak film at -70°C overnight. Bands of interest were removed and reamplified as described in Current Protocols (2), and then subcloned into a Bluescript KS vector containing overhang thymidine (T) bases inserted at the *EcoRV* site in the multiple cloning region (constructed by Dr. Rongtuan Lin).

9 DNase I footprinting

9.1 Preparation of DNA

Two differentially end-labelled SLPI promoter fragments were used for the footprinting reactions. For DNase I footprinting of the sense (+) strand, a *HindIII/AccI* fragment encompassing the complete known promoter region (nucleotides -276 to +1 of the SLPI gene) was end-labelled at the *HindIII* site as described in section 7.1 of this chapter. For DNase I footprinting of the antisense (-) strand, a *HindIII/EcoRI* fragment encompassing nucleotides -276 to -69 of the SLPI promoter was end-labelled at the *EcoRI* site. 10 000 to 20 000 cpm of probe was used for DNA ladder formation and for each footprint reaction.

9.2 Ladder formation and footprinting reactions

An adenine-guanine (A+G) DNA ladder was formed with each probe using the chemical (Maxam-Gilbert) sequencing method described in Molecular Cloning (1). Essentially, end-labelled DNA in the presence of 40 ug of

sonicated salmon sperm DNA was treated with 1 M piperidine formate, pH 2.0 (4% formic acid adjusted to pH 2.0 with piperidine) for 15 min at 37°C. The reaction was then completed by the addition of hydrazine stop solution (0.3 M sodium acetate, pH 7.0; 0.1 mM EDTA, pH 8.0; and 100 ug/ml yeast tRNA) and three volumes of 95% ethanol, left in dry ice for 5 min, and the DNA was collected by centrifugation at 14 000 rpm for 5 min. The resulting DNA was then reprecipitated and then resuspended in 6 ul of formamide loading buffer (90% formamide, 10% bromophenol blue and 10% xylene cyanol).

The footprinting reactions were performed as described in (116). Essentially, end-labelled DNA was incubated in the presence of DNA binding buffer (described in section 7.2.1 of this chapter) containing 10 mg/ml BSA but no poly (dI-dC) and 0 to 150 ng of polyhistidine-tagged recombinant IRF-1 protein in a final volume of 20 ul. After 10 min at room temperature, 10 ul of a mixture containing 0.8 units of DNase I per reaction and DNase buffer (40 mM Tris, pH 7.9; 10 mM NaCl, and 60 mM MgCl₂) was added and the reaction was incubated for 2 min at 30°C. The reaction was then terminated by the addition of stop solution (0.6 M sodium acetate, pH 5.2, 50 mM EDTA and 1.5 mg/ml salmon sperm DNA). Protein was removed by two phenol-chloroform extractions and the resulting DNA was precipitated and resuspended in 6 ul of formamide loading buffer. The DNA ladder and footprinting reactions were then electrophoresed on a 5% (antisense (+) strand) or 8% (sense (-) strand) polyacrylamide (19:1 crosslink)-8M urea sequencing gel. After running at 65 W for 1.5 h, the gel was dried and exposed to Kodak film at -70°C overnight.

CHAPTER III

MUTATIONAL ANALYSIS OF INTERFERON REGULATORY FACTORS -1 AND -2: EFFECTS ON THE INDUCTION OF INTERFERON- β GENE EXPRESSION

IRF-1 and IRF-2 are structurally similar but functionally distinct transcription factors that bind to the positive regulatory domains I and III (PRDI/III) within the human IFN- β promoter. To begin structure-function analysis of the IRF proteins, the regulatory potential of C-terminal deletion mutants was analyzed by co-transfection studies in human cells and was correlated with DNA binding capacity.

Construction of IRF-1 and IRF-2 deletion mutants. One common N-terminal primer and different C-terminal primers were used to create IRF-1 and IRF-2 deletion mutants by PCR amplification (summarized in Figures 9 and 12, respectively). After PCR amplification from an IRF-1 or IRF-2 cDNA template, deletion fragments were separated on an agarose gel and subcloned into a high efficiency eukaryotic expression vector, CMV-BL (see Materials and Methods). The ability of each deletion mutant to transactivate or repress reporter gene activity was measured by CAT gene expression using the synthetic tetrahexamer (AAGTGA)₄ sequence (Th-CAT) and the entire IFN- β gene promoter (-281 to +19; SV₀ β -CAT). In addition, electrophoretic mobility shift assays (EMSAs) were performed to correlate transactivation and transrepression potential with DNA binding capacity.

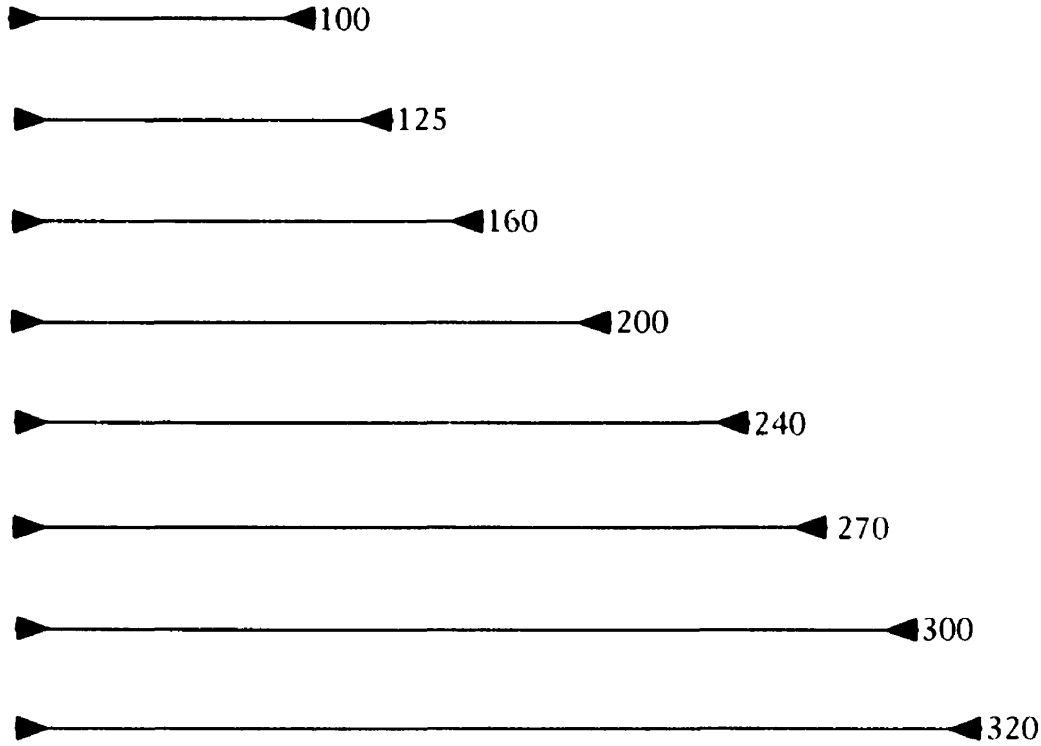
Repression by IRF-2 deletions. Co-transfection assays were performed with the full length IRF-2 construct and with the IRF-2 deletion mutants to determine which regions of IRF-2 were responsible for transcriptional repression. Each IRF-2 deletion mutant was co-transfected with the SV₀ β -CAT construct and the cells were subsequently induced by Sendai virus (summarized in Figure 9). Sendai virus induction stimulated SV₀ β -CAT gene expression about 60-fold; co-transfection with wild-type IRF-2 decreased

Sendai virus induced CAT activity to only four-fold. The level of repression by the IRF-2 deletion mutants IRF-2(160), (200), (240), (270), (300) and (320) were all comparable to that of wild-type IRF-2 (Figure 9). In contrast, the IRF-2(125) deletion mutant displayed a reduced repression capability in this co-transfection assay. In this case, Sendai-induced CAT activity was 13-fold, i.e. expression was reduced about 5-fold compared to the effect produced by co-expression of wild-type IRF-2 or the other IRF-2 deletion mutants (Figure 9, SV_oβ-CAT values), suggesting that this deletion may be very close to the boundary of the IRF-2 domain required for repression. Interestingly, the next deletion protein - IRF-2(100) - failed to repress Sendai virus induced expression of the reporter gene. Essentially similar results were obtained in a repression assay using the Th-CAT gene as reporter (Figure 9, Th-CAT values); in this assay, wild-type IRF-1 was co-transfected with the various IRF-2 deletions to assess the repressive activity of IRF-2. Again, IRF-2(100) failed to repress IRF-1 mediated transactivation. Trans-repression by IRF-2 deletion mutants was also examined using the SV_oβ-CAT construct in combination with the p50, RelA and IRF-1 expression plasmids (see Figure 13); in this assay, transcriptional repression by IRF-2 resides within the first 125 N-terminal amino acids of the protein (data not shown).

DNA binding activity of IRF-2 deletion mutants. The ability of the IRF-2 deletion mutants to bind DNA was examined to correlate trans-repression with DNA binding capacity. Whole cell extracts from 293 cells transiently transfected with the various deletion mutations were tested for their ability to bind to an IFN-β PRDI specific probe. Extracts from CMV-BL transfected cells produced two weak complexes (Figure 10, lane 1) which based on competition studies appear to be endogenous IRF-2 forms (34,153). Extracts from cells

Figure 9. Analysis of IRF-2 deletion mutants in repression assays. The hatched bar represents the primary structure of the human IRF-2 protein and is divided into the DNA binding domain (darker shaded area) and the carboxy terminal domain (lighter shaded area). Lines below the full length protein represent the various IRF-2 deletion mutants, and numbers on the right signify the size in amino acids of each deletion mutant. Primers used in PCR amplification are depicted by the arrowheads. *SV₀β-CAT repression assay.* 293 cells were transfected with SV₀β-CAT either alone or together with various CMV-IRF-2 deletion mutants (5 μg each) and were induced with Sendai virus (500 HAU/mL) 20-24h post-transfection. Cells were harvested 42-48 h post-transfection and soluble protein extracts were analyzed for CAT activity using 100 μg of total protein for 2-4h at 37°C. Relative CAT activity (compared to basal level transfection with the reporter gene and CMV-BL vector alone) was measured. The value 60.0 is the fold increase in CAT activity observed in Sendai virus induced versus uninduced samples; the ability of IRF-2 deletions to decrease the relative inducibility was determined in three separate experiments. *Th-CAT repression assay.* Th-CAT and CMV-IRF-1 were transfected into 293 cells together with the various CMV-IRF-2 deletion mutants (5 μg each). The ability of the IRF-2 deletions to interfere with IRF-1 mediated transactivation of Th-CAT was measured at 48 h as described above. *DNA binding.* Whole cell extracts from CMV-IRF-2 transfected 293 cells were examined for binding to the PRDI and Th probes as described in the Materials and Methods. "-", no DNA binding; "++", DNA binding detected in EMSA.

IRF-2 349 aa



Relative CAT Activity

SV β -CAT Th-CAT

DNA binding

	4.0	0.2	++
100	48.0	4.2	-
125	13.0	0.6	++
160	4.2	0.4	++
200	4.0	0.3	++
240	4.4	0.3	++
270	4.7	0.3	++
300	4.5	0.3	++
320	3.9	0.3	++
CMV-BL (vector alone)	60.0*	4.3*	-

transfected with different IRF-2 deletion mutants generated protein-DNA complexes migrating to different positions in the EMSA corresponding to the size of the IRF-2 protein (Figure 10, lanes 2 to 9). Wild-type IRF-2 and IRF-2(320) (Figure 10, lanes 2 and 3) generated multiple complexes with the P1 probe, probably reflecting IRF-2 proteolytic products that maintain DNA binding (34,153). In multiple experiments using either human 293 extracts transfected with the various deletions, no IRF-2(100) DNA binding activity was observed (Figure 10, lane 10, summarized in Figure 9). The fact that IRF-2(125) possesses DNA binding activity indicates that most of the DNA binding region in IRF-2 is contained within the N-terminal one third of the protein. Thus, IRF-2 mediated repression of IFN- β gene expression correlates directly with DNA binding capacity; based on these experiments, the C-terminal end of the IRF-2 DNA binding region is located between aa 100 and aa 125.

Transcriptional activation by IRF-1 deletion mutants. Using a similar strategy, the effects of full length IRF-1 and the IRF-1 deletion mutants on IFN gene activity were examined. Initially, an immunoblot analysis was performed to determine if the IRF-1 deletion mutants were expressed to similar levels in 293 cells (Figure 11). Polyclonal IRF-1 antibody (a kind gift from Dr. R. Pine) was able to detect the wild-type IRF-1 and the IRF-1(300), (250), and (200) proteins (Figure 11A, lanes 1, 2, 3 and 7 respectively), but did not detect the IRF-1(170), (150) and (120) deletion mutants (Figure 11A, lanes 4, 5 and 6 respectively). This result suggests that the major epitope recognized by the IRF-1 antibody is located between amino acids 200 and 170. Mobility shift analysis confirmed that the IRF-1 deletions including IRF-1(150) retained DNA binding capacity (Figure 11B, lanes 2 to 7), with the exception of IRF-1(120) which displayed no DNA binding activity in multiple assays (Figure

Figure 10. DNA binding activity of the IRF-2 deletion mutants. EMSA was performed on whole cell extracts (20 μ g) derived from cells transfected with the various CMV-IRF-2 deletion mutants. The 32 P-labeled probe corresponds to the PRDI site. Each lane is marked with the appropriate expression plasmid used in the 293 cell transfection. As a negative control, lane 1 contains extracts from cells transfected with the CMV-BL vector. Protein-DNA complexes representing endogenous IRF-2 forms are shown by the arrows (34).

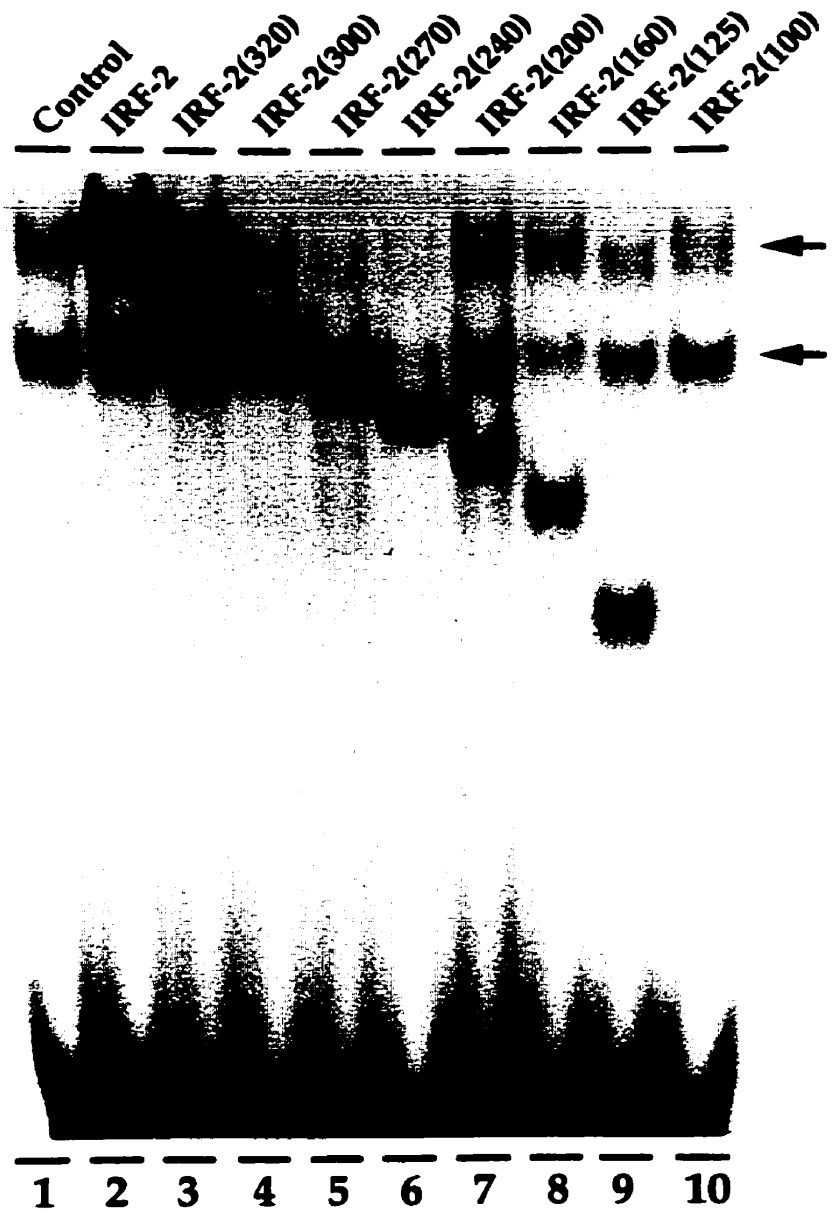
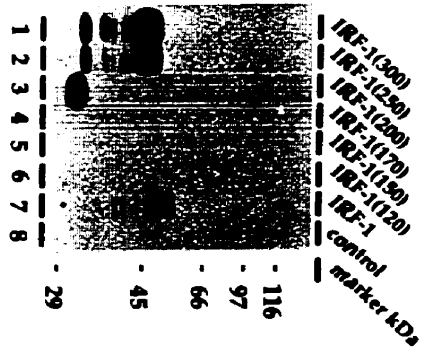
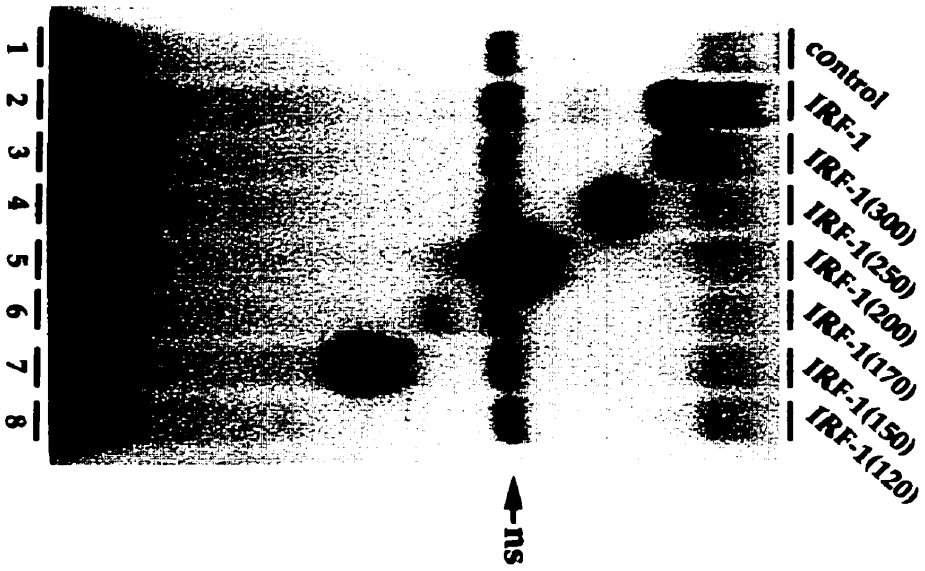


Figure 11. Analysis of IRF-1 deletion mutants. **A.** Western blot analysis of IRF-1 proteins. Whole cell extracts were prepared from 293 cells transfected with 5 μ g of CMV-IRF-1 or the various CMV-IRF-1 deletion mutants, separated on SDS-PAGE, transferred to nitrocellulose membrane, and immunoblotted with an IRF-1 polyclonal antibody. Full length IRF-1 protein (lane 7) as well as the IRF-1(300), (250) and (200) deletion mutants (lanes 1-3) were detected in transfected cell extracts (20 μ g). IRF-1(170), IRF-1(150) and IRF-1(120) are not detected by the IRF-1 antibody (lanes 4-6). Extracts from cells transfected with the CMV-BL vector were analyzed as negative control (lane 8). Protein molecular weight markers are shown on the right side of the diagram in kilodaltons (kDa). **B.** DNA binding activity of IRF-1 deletion mutants. EMSA was performed on whole cell extracts (25 μ g) derived from cells transfected with the various CMV-IRF-1 deletion mutants using the 32 P-labeled Th oligonucleotide as a probe. Each lane is marked with the appropriate expression plasmid used in the 293 cell transfection. Lane 1 represents the control lane and contains extracts from cells transfected with the CMV-BL vector. The arrow corresponds to a low molecular weight non-specific protein-DNA complex.

A.



B.



11B, lane 8). In several experiments, IRF-1(170) was expressed to a lower level than either IRF-1(200) or IRF-1(150) (Figure 11B, lanes 5 to 7).

Full length human IRF-1 and the 6 deletion mutants were examined for their ability to transactivate the Th-CAT reporter gene. Full length IRF-1 induced reporter gene activity four-fold (Figure 12, Th-CAT activation assays) whereas with the shortest IRF-1 proteins - IRF-1(120) and IRF-1(150) - no increase in CAT activity was observed. As the length of IRF-1 was increased with the IRF-1(170) and (200) proteins, the level of activity actually dropped below the basal level to 0.6 and 0.4 respectively. The activity of IRF-1(250) and IRF-1(300) were 1.5 and 2.4 respectively, indicating that only the IRF-1(300) protein retained significant transactivating potential (Figure 12).

The activation of the intact IFN- β promoter (SV₀ β -CAT) by full-length IRF-1 and the various deletion mutants was also examined (Figures 12 and 13). Unlike the Th-CAT reporter gene, IRF-1 alone only weakly activates the IFN- β promoter in the SV₀ β -CAT construct; efficient induction minimally requires the synergistic effects of IRF-1 and the PRDII binding NF- κ B proteins ((60,81,109), and Figure 13). Therefore, combinations of the various IRF-1 deletion mutants were examined together with NF- κ B subunits p50 and RelA in a transactivation assay (summarized in Figure 12, SV₀ β -CAT activation assays and Figure 13). With p50 and RelA expression plasmids alone, CAT gene expression was about 3 times higher than basal levels (Figure 12, comparing lanes 1 and 2). A triple transfection of p50, RelA, and IRF-1 expression plasmids resulted in about 18-fold stimulation of CAT activity (Figure 13, lane 3). Co-transfections of IRF-1(120), (150), (170), and (200) with the NF- κ B p50 and RelA subunits resulted in basal levels of activity similar to

Figure 12. Analysis of IRF-1 deletion mutants in activation and repression assays. The upper schematic bar represents the primary structure of the human IRF-1 protein and is divided into the DNA binding domain (dark hatched area) and transactivating potential (progressively darker shading). IRF-1 deletion mutants are represented by the lines below the full length protein with their amino acid size. Primers used in PCR amplification are illustrated by the arrowheads.

Th-CAT activation assay. Cells were transfected with Th-CAT and CMV-IRF-1 or the various CMV-IRF-1 deletions (5 μ g each). 42-48h post-transfection, cells were harvested and soluble protein extracts were analyzed for CAT activity using 100 μ g of total protein for 2h at 37°C. Relative CAT activity (compared to basal level transfection with the reporter gene and CMV-BL vector alone) was measured; the data represents the average of three experiments.

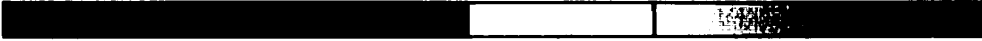
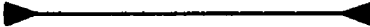
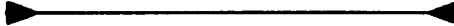
SV₀ β -CAT activation assay. Cells were transfected with SV₀ β -CAT and CMV-based NF- κ B subunits p50 and RelA or different IRF-1 deletion mutants (5 μ g each). Cells were harvested 42-48h post-transfection and extracts were assayed for CAT activity as described above.

Th-CAT repression assay. Th-CAT and CMV-IRF-1 (5 μ g each) were transfected into 293 cells together with the various CMV-IRF-1 deletion mutants. The ability of the IRF-1 deletions to interfere with IRF-1-mediated transactivation of Th-CAT was measured at 48h as described above.

SV₀ β -CAT repression assay. SV₀ β -CAT and the various CMV-IRF-1 deletion constructs (5 μ g each) were transfected into 293 cells and induced with Sendai virus 24h later; the ability of the IRF-1 deletions to interfere with Sendai virus induced SV₀ β -CAT activity was measured at 48h as described above.

DNA binding. Whole cell extracts from CMV-IRF-1 transfected 293 cells were examined for binding to the PRDI and Th probes. "-", no DNA binding; "++", DNA binding detected in EMSA.

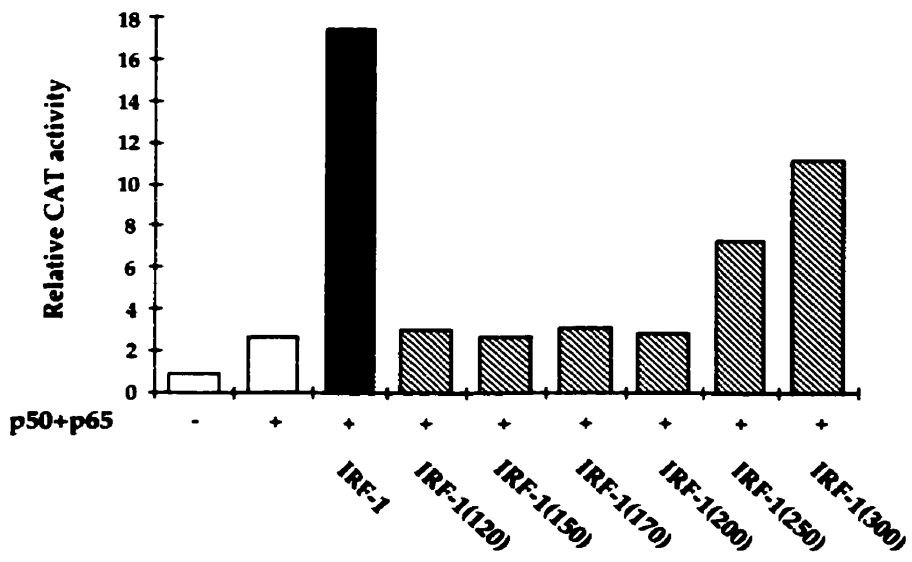
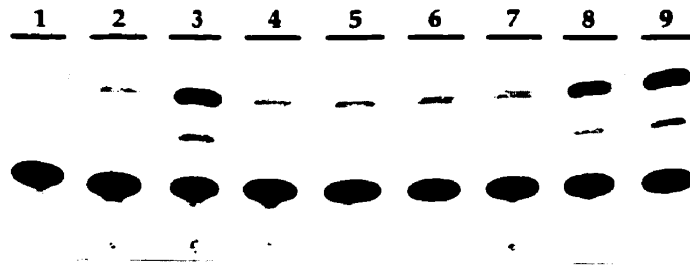
IRF-1 325 aa**Relative CAT Activity Levels****DNA Binding**

	50	100	150	200	250	300	Activation Assays		Repression Assays		
							Th-CAT	SVo β -CAT	Th-CAT	SVo β -CAT	
							4.2	17.5	4.2	56.0	++
							1.2	3.1	4.1	59.0	-
							1.1	2.7	2.9	17.7	++
							0.6	3.2	2.2	11.8	++
							0.4	2.9	1.5	5.8	++
							1.5	7.4	3.1	29.0	++
							2.4	11.2	3.8	48.0	++
CMV-BL (vector alone)							1.0	3.0	4.2	60.0	-

those seen with p50 and RelA alone (Figure 13, lanes 4, 5, 6 and 7). IRF-1(250) and IRF-1(300), together with p50 and RelA, induced CAT expression 7- and 11-fold respectively (Figure 13, lanes 8 and 9). Based on these results, it appears that C-terminal sequences of IRF-1, particularly beyond aa 250, play a crucial role in IRF-1 transcriptional activation.

Repression by IRF-1 deletion mutants. In co-transfection assays involving the Th-CAT construct and the IRF-1(170) and IRF-1(200) deletion mutants, relative CAT activity was observed to be lower than basal levels (Figure 12, Th-CAT and SV β -CAT activation assays), suggesting that certain IRF-1 deletion mutants may possess a repressive capability. To examine the repressive effect of the IRF-1 deletion mutants, co-transfection assays were performed using the IFN- β promoter (SV β -CAT) construct together with various IRF-1 deletion mutants. At 24h after transfection, cultures were infected with Sendai virus and the relative levels of CAT activity were determined. Infection with Sendai virus induced the IFN- β promoter of SV β -CAT over 50-fold, as demonstrated previously (Figure 12, SV β -CAT repression assays). Co-transfection with the full length IRF-1 did not alter the level of inducibility; similarly, co-transfection with IRF-1(120) did not change the inducibility of the IFN- β promoter (Figure 12, SV β -CAT repression assays), presumably due to the lack of DNA binding activity. C-terminal truncation of IRF-1 to a protein of between 150 and 200 aa resulted in IRF-1 proteins that effectively interfered with Sendai virus inducibility of the IFN- β promoter; for example, the IFN- β promoter was induced only 5-fold in the presence of IRF-1(200). With IRF-1(250), the inducibility of the IFN- β promoter was nearly 30-fold higher than the basal level and with IRF-1(300) virus inducibility was intact (Figure 12). Similar results were obtained in an

Figure 13. Activation of the IFN- β promoter by NF- κ B and IRF-1 deletion mutants. Cells were transfected with SV₀ β -CAT and CMV-based NF- κ B subunits p50 and RelA (5 μ g each; RelA is written as "p65") where indicated ("+" or "-"). The different CMV-IRF-1 deletion mutants (5 μ g each) are indicated at the bottom of each lane. Cells were harvested 42-48h post-transfection and soluble protein extracts were assayed for CAT activity using 100 μ g of total protein for 2 hours at 37°C. Relative CAT activity (compared to basal level transfection with the reporter gene alone) is measured on the y-axis. A representative CAT assay is shown above the graph.

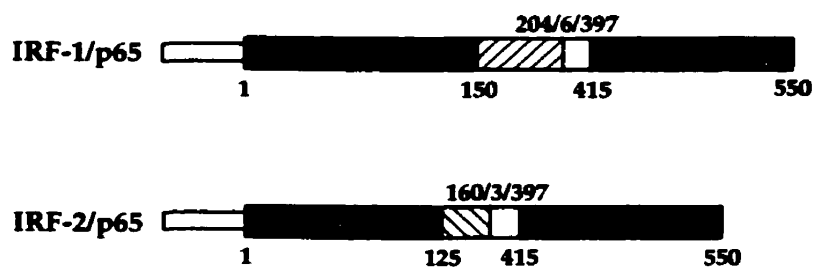


experiment using the Th-CAT construct induced by wild-type IRF-1 and the various IRF-1 deletion mutants (Figure 12, Th-CAT repression assays). Together, these results indicate that deletion of IRF-1 to a protein of less than 200 aa converts the activator IRF-1 into a repressor activity, and repression activity correlates with DNA binding ability.

Activity of IRF/NF- κ B RelA fusion proteins. Fusion proteins were generated that link the IRF-1 and IRF-2 DNA binding domains to the C-terminal transactivation domain of NF- κ B RelA(p65) (Figure 14A). These proteins were efficiently expressed in 293 cells (Figure 14B, lanes 2 and 3) and were detected in Western blot analysis using an antibody directed against a C-terminal peptide of RelA. The prominent band at 66kDa represents endogenous NF- κ B RelA (Figure 14B, lane 1). These fusion proteins were used in co-expression assays using the Th-CAT (Figure 14C) or 3xPRDI-CAT (data not shown) to examine the ability of the fusion proteins to stimulate or repress gene activity. Interestingly, both IRF-1/RelA and IRF-2/RelA fusion proteins were stronger transcriptional activators than wild type IRF-1. Wild-type IRF-2 was capable of full repression of IRF-1/RelA or IRF-2/RelA mediated induction (Figure 14C). The IRF-2(125) was able to completely repress the activation mediated by IRF-1/RelA but only partially repressed IRF-2/RelA mediated activation, while IRF-2(100) failed to repress reporter gene activation. This experiment further supports the idea that IRF-2 repressor activity is an intrinsic function of the N-terminal 125 aa domain of IRF-2. To examine the activation of the intact IFN- β promoter by IRF/RelA fusion proteins, the IFN- β promoter (SV β -CAT) construct was co-transfected with p50, RelA and/or IRF/RelA expression plasmids (Figure 14D). Like IRF-1, IRF-1/RelA alone only weakly activated the IFN- β promoter; efficient

Figure 14. Activity of IRF-1/RelA and IRF-2/RelA fusion proteins. A. Protein structure of IRF-1/RelA and IRF-2/RelA. IRF-1/RelA and IRF-2/RelA are written here as IRF-1/p65 and IRF-2/p65, respectively. IRF-1/RelA contains 364 aa: 204 aa from IRF-1 (aa 1-204), 154 aa from RelA (aa 397-550), and a 6 aa spacer (KLAALD). IRF-2/RelA consists of 317 aa: 160 aa from IRF-2 (aa 1-160), 3 aa for spacing (VLD), and 154 aa from RelA (aa 397-550). **B.** Analysis of IRF-1/RelA and IRF-2/RelA protein by Western blot . 20 ug of whole cell extract from 293 cells transfected with IRF-1/RelA and IRF-2/RelA were separated on SDS-PAGE, transferred to nitrocellulose membrane, and immunoblotted with a C-terminal anti-RelA antibody. Arrowheads indicate the positions of IRF-1/RelA (1) and IRF-2/RelA (2), respectively.

A.



B.

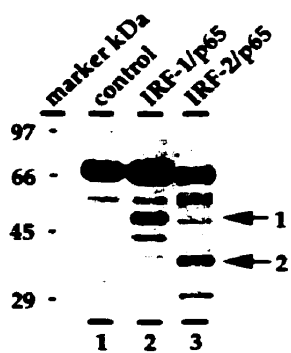
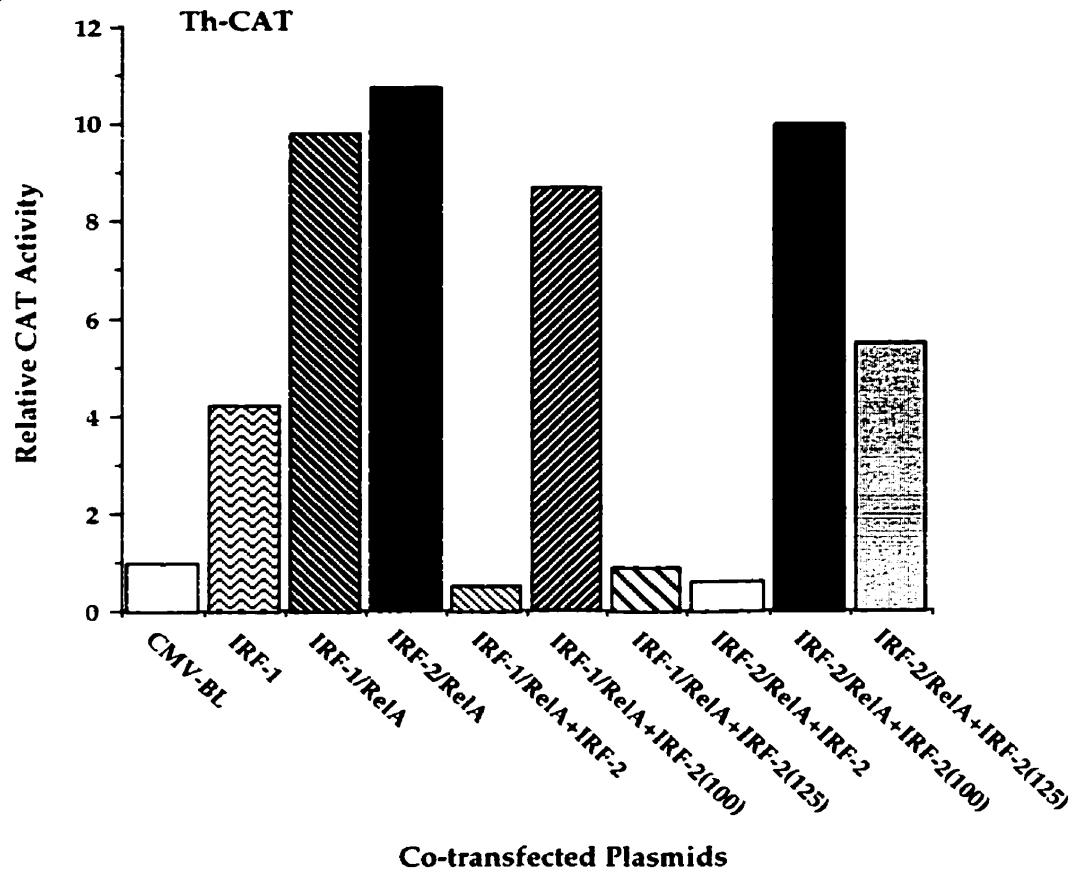
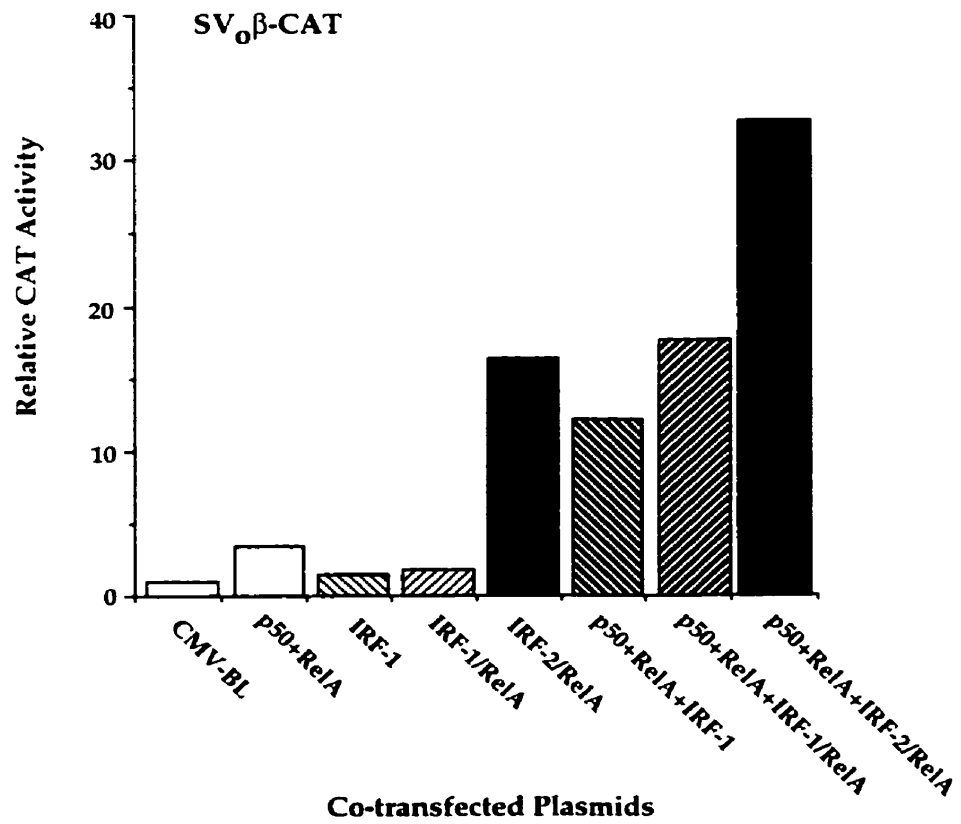


Figure 14 (continued). **C.** Activation of Th-CAT by IRF/RelA fusion proteins. 293 cells were transfected with Th-CAT and the various expression plasmids indicated below the bar graph (5 μ g each). CAT activity was analyzed 48h post-transfection; the values represent the average of three experiments with less than 20% variability. **D.** Activation of the IFN- β promoter by IRF/RelA fusion proteins. 293 cells were transfected with SV $_0$ β -CAT and expression plasmids indicated below the bar graph (5 μ g each). CAT activity was analyzed 48h post-transfection; the values represent the average of three experiments with less than 20% variability.

C.



D.



activation required both IRF-1/RelA and NF- κ B proteins. Interestingly, IRF-2/RelA alone resulted in high level of stimulation of CAT activity (about 17-fold), a level of stimulation similar to that observed with p50, RelA and IRF-1 expression plasmids.

CHAPTER IV

**TRANSCRIPTION FACTOR IRF-2 EXERTS ITS ONCOGENIC PHENOTYPE
THROUGH THE DNA BINDING/TRANSCRIPTION REPRESSION
DOMAIN**

In the previous chapter the relationship between DNA binding activity and transcriptional activation/repression by IRF-1 and IRF-2 was analyzed, and it was found that transcriptional repression by IRF-2 correlated directly with IRF-2 DNA binding. Studies on the oncogenic and tumor suppressor activities of IRF-1 and IRF-2 suggest that relative amounts of these functionally antagonistic proteins appear to play a role in cell growth regulation (73), implicating a potential link between their transcriptional properties (DNA binding and transactivation/repression) and their respective antioncogenic and oncogenic potentials. To analyze the relationship between DNA binding/transcriptional repression activity and oncogenic transformation phenotype exerted by the IRF-2 protein, NIH3T3 cells expressing C-terminal deletions of IRF-2 were established and assayed for transformation and tumorigenic properties.

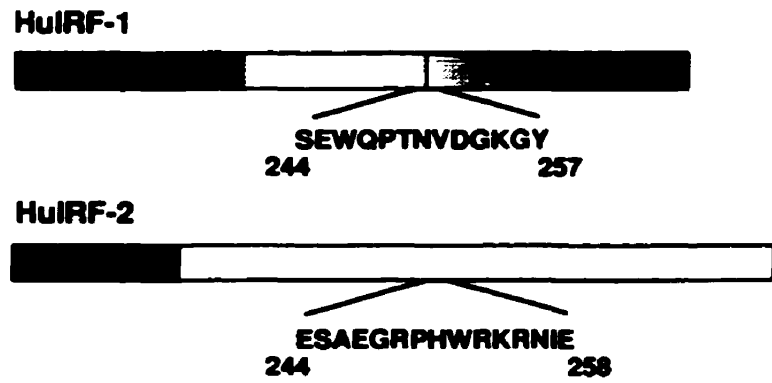
IRF-1 and IRF-2 specific antisera. Polyclonal antisera specific for unique hydrophilic and antigenic peptide sequences in the C-terminal domains of human IRF-1 and IRF-2 proteins were prepared by repeated inoculation into rabbits (Figure 15A). After three to five boosts with peptide, sera were tested for antibody reactivity and specificity in Western blot analyses and shifted shift assays using polyhistidine-tagged recombinant human IRF-1 and IRF-2 proteins. The antibodies recognized their respective recombinant proteins in Western blot analyses (Figure 15B, lanes 2 and 5) and this recognition was specific, as incubation of antiserum in the presence of corresponding peptide eliminated reactivity against the appropriate IRF protein (Figure 15B, lanes 3 and 10). As expected, the IRF-1 and IRF-2 antibodies did not cross-react (Figure 15B, lanes 1 and 4).

The IRF-2 antibody was tested for reactivity against the human and murine IRF-2 proteins using whole cell extracts from untreated and Sendai virus-infected NIH3T3 and 293 cells. The IRF-2 antibody specifically recognized IRF-2 from both murine and human untreated cells. In NIH3T3 cells, two specific IRF-2 species of about 45 to 48kd were consistently observed, whereas a slightly larger, 49 to 52 kd single IRF-2 species was detected in 293 cells (Figure 15B, lanes 6 and 11; 8 and 12). The two murine IRF-2 species may represent full-length IRF-2 and its degradation product or its phosphorylated form. Since IRF-2 is proteolytically cleaved to a 25 kd species following Sendai virus infection (34,153), due to the location of the peptide chosen for antibody preparation, it is not surprising that full-length IRF-2 was not detectable in Sendai virus-infected murine and human cells (Figure 15B, lanes 7 and 9). Sera were also tested for antibody reactivity and specificity in shifted shift assays using the recombinant human IRF proteins. While there was no recognition by preimmune sera (Figure 15C, lanes 1 and 2; 7 and 8), the IRF-1 and IRF-2 antibodies were able to specifically shift their respective protein-DNA complexes (Figure 15C, lanes 3 and 4; 9 and 10). Addition of IRF-1 resulted in the formation of slowly migrating complexes (Figure 15C, lanes 1 and 2) which likely represent IRF-1 dimers. Furthermore, as seen in Western blot analyses, the antibodies did not cross-react (Figure 15C, lanes 5 and 6; 11 and 12).

Establishment of NIH3T3 cells expressing full-length and deletion mutant IRF-2 proteins. CMV-based plasmids expressing full length (FL; 349 aa) and C-terminally truncated (320, 300, 270, 240, 200, 160, 125, and 100 aa) IRF-2 proteins as well as the CMV driven expression plasmid as control were cotransfected with an RSV-neo plasmid into NIH3T3 cells by the calcium-phosphate

Figure 15. IRF-1 and IRF-2 peptide specific antisera. **A.** The primary structures of the human IRF-1 and IRF-2 proteins, including important functional domains, are schematically represented. The letters and numbers represent the amino acid sequence and location, respectively, of the peptides chosen for antibody production. The shaded boxes represent different functional domains:  , IRF-1 DNA binding domain;  , IRF-2 DNA binding and repression domain;  , IRF-1 transactivation domain. **B.** Specific reactivity of antisera in Western blot analyses. 10 ng of recombinant IRF-1 (lanes 2 and 4), 2.5 ng of recombinant IRF-2 (lanes 1 and 5) and 20 ug of whole cell extract prepared from untreated and Sendai virus-infected (500 hemagglutinating units/ml) NIH3T3 (lanes 6 and 7, respectively) and 293 (lanes 8 and 9, respectively) cells were separated on SDS-PAGE, transferred to nitrocellulose membrane, and immunoblotted with the indicated antisera. The competitor peptide against which the antiserum was raised was added to the incubations at a concentration of 5 ug/ml as indicated by a "+" to test the specificity of the antiserum to IRF-1 (lane 3), IRF-2 (lane 10) and IRF-2 in NIH3T3 (lane 11) and 293 (lane 12) cells.

A



B

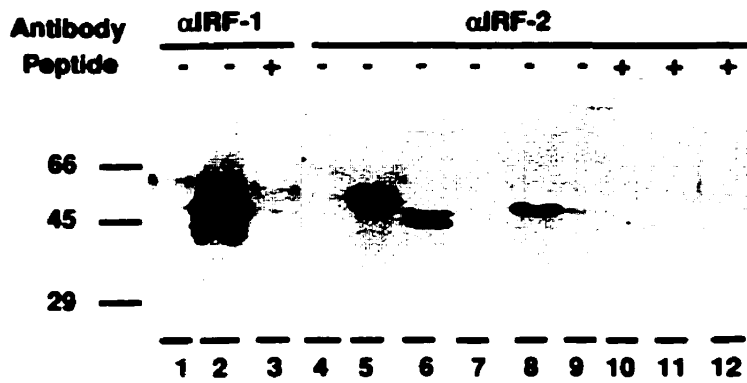


Figure 15 (continued). C. Specific reactivity of antisera in shifted shift assays. 1 ng of IRF-1 (lanes 1 to 6) and 0.5 ng of IRF-2 (lanes 7 to 12) were pre-incubated with 1 ul of either preimmune (P), anti-IRF-1 (αF_1) or anti-IRF-2 (αF_2) antiserum, in the presence (+) or absence (-) of 1 ug of IRF-1 (lanes 1 to 6) or IRF-2 (lanes 7 to 12) competitor peptide, prior to the addition of ^{32}P -labeled Th probe and then analyzed by EMSA. The arrows correspond to the IRF protein-DNA and supershift (S) complexes.

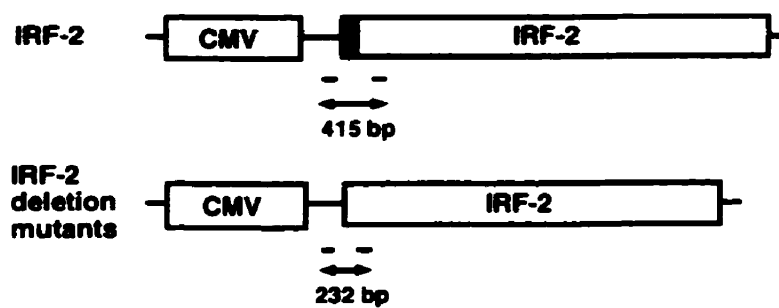
method. Cells were selected in G418 and drug-resistant colonies were isolated and characterized for IRF-2 expression at the RNA and protein levels.

Clones expressing various IRF-2 proteins were initially screened by RT-PCR analysis using primers specific to the CMV-IRF-2 plasmid (Figure 16A). This method distinguishes between expression of endogenous and transfected FL IRF-2 protein and allows for the detection of expression of the 100 aa IRF-2 protein, which does not bind DNA and which is too small to be detected by Western blot analysis. In FL IRF-2 clones, an expected RT-PCR product of approximately 415 base pairs (bp) was detected (Figure 16B, lanes 5 and 6). In clones expressing the deletion mutant proteins (whose N-terminal ends lack the flanking sequences present in the FL protein), a predicted RT-PCR product of approximately 230 bp was observed (Figure 16B, lanes 7 to 13). As expected, RT-PCR products were not seen in NIH3T3 cells nor control clones transfected with the CMV plasmid (Figure 16B, lanes 1 to 4). Of the 10 to 20 clones isolated per cell line, approximately 70% expressed the transfected protein.

The clones were then analyzed for IRF-2 expression patterns at the protein level, using EMSA and Western blot analyses. A representative EMSA is depicted in Figure 17. Whole cell extracts from each cell line (with the exception of IRF-2 (100)) contained PRDI complexes having relative sizes corresponding to the size of the transfected IRF-2 protein. As expected, a PRDI complex corresponding to IRF-2 (100) was not observed in the IRF-2 (100) clones, even on longer running gels. As measured by densitometry, the IRF-2 DNA binding activities in the IRF-2 (FL) cells was approximately three- to four-fold higher than endogenous levels. Levels of DNA binding activity among the clones isolated for each cell line were similar (data not shown).

Figure 16. Expression of IRF-2 RNA in full-length and deletion mutant IRF-2 clones. **A.** Schematic representation of the CMV-IRF expression fragment in the full-length and deletion mutant expression plasmids, respectively. Primers used in RT-PCR analyses for the detection of transfected IRF-2 are represented by the short dark lines. Expected PCR product sizes are indicated. The shaded region depicts flanking sequences in full-length IRF-2 which are not present in the deletion mutant IRF-2 sequences. **B.** Detection of transfected IRF-2 RNA in full-length and deletion mutant IRF-2 clones. Total RNA was isolated from G418-resistant clones isolated from NIH3T3 cells transfected with full-length and deletion mutant IRF-2 proteins. RT-PCR amplification was performed with 2 ug of RNA, using primers specific for the CMV-IRF plasmid, as described in Materials and Methods. The marker lane is the pAT153 plasmid cut with HaeIII, located left of lane 1. Among the clones expressing transfected IRF-2 RNA were full-length (FL) clones 2 and 6 (lanes 5 and 6); IRF-2 (300) clones 9 (lane 7); IRF-2 (160) clones 2 and 7 (lanes 8 and 9); IRF-2 (125) clone 1 (lane 10) and IRF-2 (100) clones 1,6 and 7 (lanes 11 to 13). No transfected IRF-2 RNA was detected in parental NIH3T3 cells (lane 1) or control CMV clones 1, 6 and 7 (lanes 2 to 4).

A



B

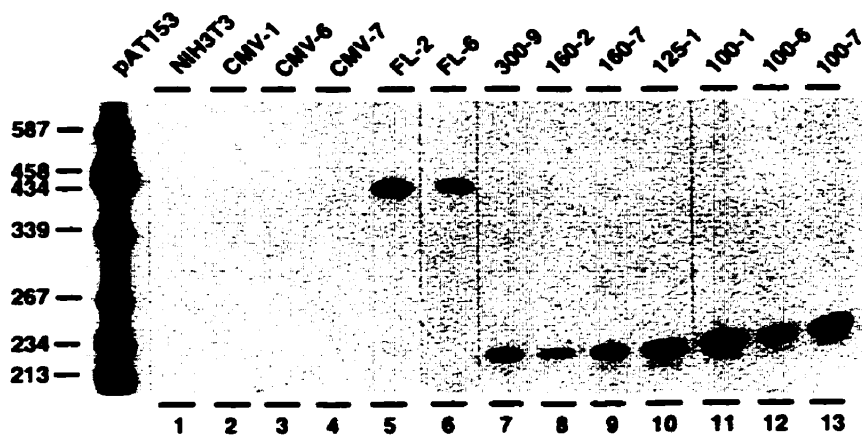
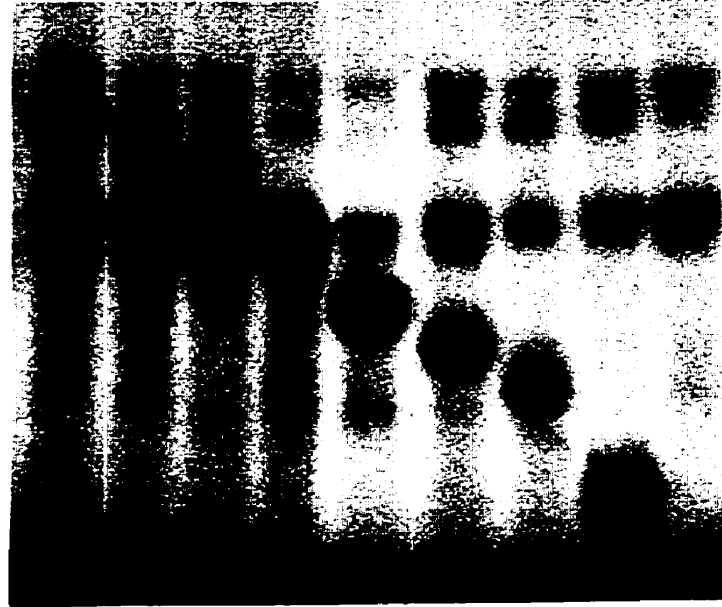


Figure 17. DNA binding activities of full-length and deletion mutant IRF-2 clones. EMSA was performed on whole cell extracts (25 ug) derived from G418-resistant clones isolated from NIH3T3 cells transfected with the full-length and deletion mutant IRF-2 proteins. The ³²P-labeled probe corresponds to the PRDI site. Each lane is marked with the appropriate expression plasmid transfected. The arrows correspond to protein-DNA complexes that represent endogenous IRF-2 forms. "ns" corresponds to a nonspecific protein-DNA complex.

· IRF-2 (FL)
· IRF-2 (320)
· IRF-2 (300)
· IRF-2 (270)
· IRF-2 (240)
· IRF-2 (200)
· IRF-2 (160)
· IRF-2 (125)
· IRF-2 (100)



1 2 3 4 5 6 7 8 9

ns
↑
↑

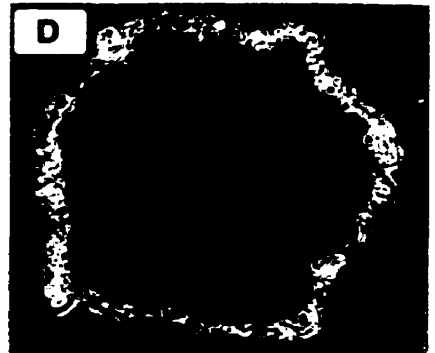
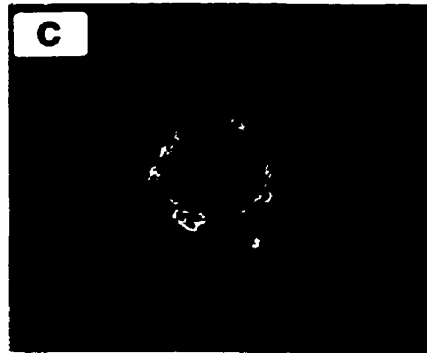
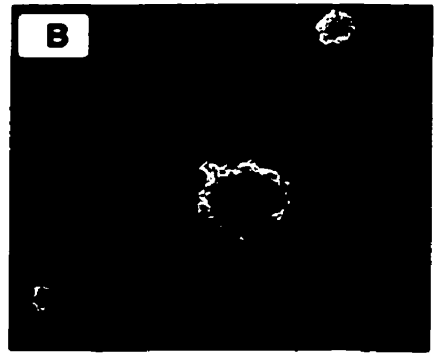
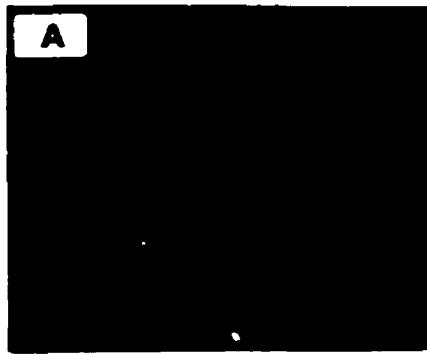
The specificity of the PRDI complexes observed in the IRF-2(FL), (320), (300), and (270) aa expressing cells were confirmed by shifted shift assays using the IRF-2 antibodies described above (data not shown). Based on these analyses, all IRF-2 deletions were stably expressed in NIH3T3 cells.

Growth and tumorigenic properties of the full length and deletion mutant IRF-2 expressing clones. IRF-2 was previously described as an oncogene, capable of inducing malignant transformation when overexpressed in NIH3T3 cells (73). To determine the region of IRF-2 responsible for this phenotype, the effects of overexpression of various IRF-2 deletion proteins on the oncogenic transformation of NIH3T3 cells were analyzed. Cell lines used to test for oncogenic transformation were: CMV cells (negative control), NIH3T3 cells overexpressing the *ras* oncogene (positive control), IRF-2(FL), IRF-2(300) (which lacks 49 aa from the C-terminal end), IRF-2(160) (which lacks the entire C-terminal end), IRF-2 (125) (which possesses the minimum DNA binding/repression domain) and IRF-2(100) (which lacks a functional DNA binding/repression domain). Although the cell lines did not exhibit obvious cellular morphological changes, they displayed strikingly distinct growth characteristics compared to the control CMV cells (summarized in Table 5). Cells expressing the IRF-2 FL, 300, and 160 aa proteins had a rapid doubling time, similar to the *ras* transformants; in contrast, the IRF-2 (125) and (100) expressing cell lines displayed doubling times identical to the control CMV cells. Also, cells overexpressing the FL, 300 and 160 aa IRF-2 proteins grew to high saturation density under reduced serum conditions as indicated by the 5.5 to 8.3 fold increase in saturation densities over control CMV cells (Table 5). In contrast, the IRF-2(125) and (100) expressing clones displayed saturation densities which were indistinguishable from the control

Table 5. Growth and tumorigenic properties of full-length and deletion mutant IRF-2 clones. *Numbers represent the mean value for 2 to 3 clones analyzed \pm the standard deviation. Saturation density is the number of cells four days postconfluence. The doubling time is the growth rate of exponentially growing cells. Cells grown in soft agar were counted 20 days after plating, and cloning efficiency was determined as the number of colonies \times 100 divided by the number of cells plated (mean value of two experiments, 2 to 3 clones per cell line). Assay for tumorigenicity was performed using two independently isolated clones per cell line tested; three mice per clone were injected. The time required to produce tumors of at least 5 mm diameter was considered the latency period. ND: not determined. NA: not applicable. >60: mice did not show sign of tumor development 60 days after injection and were sacrificed.

Cell lines	*Saturation Density (2% serum) (x 10 ⁶)	*Doubling Time (10% serum) (hours)	Colony Formation in Soft Agar (%)	Tumorigenicity	
				Tumors / Injection	Latency (days)
CMV	0.4 ± 0.2	21.8 ± 0.5	0	0/6	> 60
Ras	4.0 ± 0.2	16.4 ± 0.2	35	2/2	9-11
IRF-2 (FL)	2.5 ± 0.2	17.5 ± 0.2	13	6/6	17-24
IRF-2 (300)	3.3 ± 0.4	17.9 ± 0.2	22	ND	NA
IRF-2 (160)	2.2 ± 0.2	16.8 ± 0.4	38	6/6	16-18
IRF-2 (125)	0.4 ± 0.2	21.9 ± 0.6	18	0/6	> 60
IRF-2 (100)	0.4 ± 0.4	22.1 ± 0.8	0	0/6	> 60

Figure 18. Soft agar colonies of FL and deletion mutant IRF-2 clones. Photographs were taken after 3 weeks of culture. Panels **A** and **B** were taken at 40x magnification, while panels **C** to **F** were taken at 100X magnification. Control CMV clones (panel **A**) and IRF-2 (100) clones (not shown) displayed similar phenotypes. Anchorage independent growth was observed in positive control Ras clones (panel **C**), IRF-2 (FL) clones (panel **F**), IRF-2 (160) clones (panels **B** and **D**), and IRF-2 (125) clones (panel **E**).



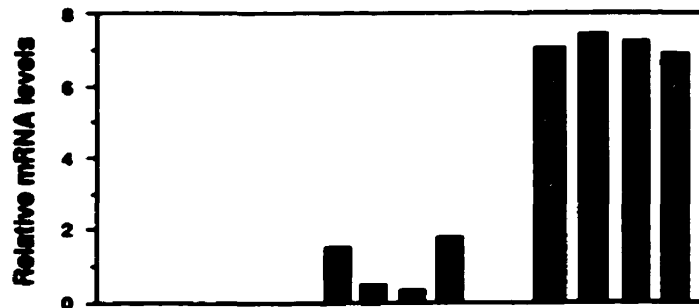
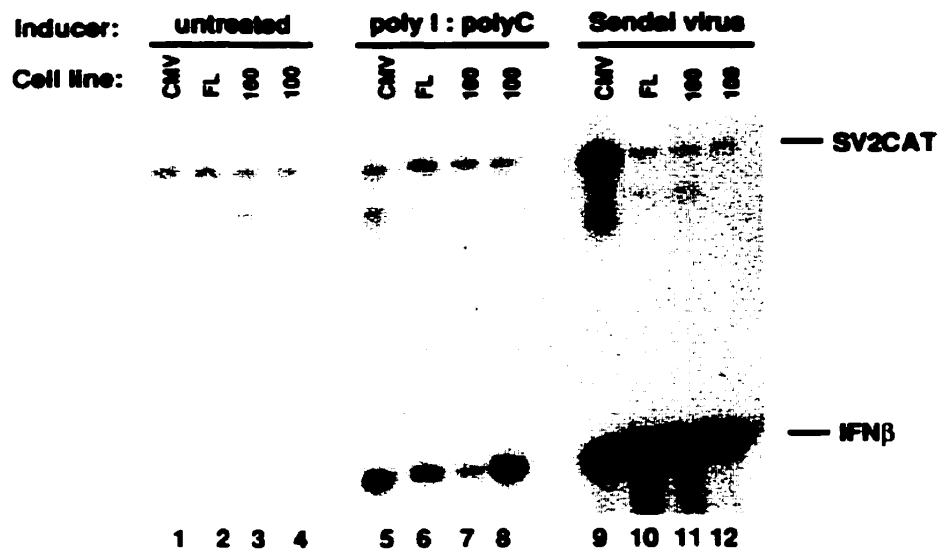
CMV cells. The cell lines which grew under reduced growth factor conditions - FL, IRF-2 (300) and IRF-2 (160) - also displayed a loss in anchorage-dependent growth and formed colonies in soft agar with efficiencies of 13% to 38%. Surprisingly, the IRF-2 (125) cells, despite having control saturation density levels, also formed colonies in soft agar. On the other hand, cells expressing the IRF-2 (100) protein, like the control CMV cells, did not exhibit anchorage-independent growth. Strikingly, subcutaneous injection of two clones of each of the IRF-2(FL) and (160) cell lines into 3 nude mice each resulted in tumor formation 16 to 24 days following injection. Control CMV, IRF-2(125) and IRF-2(100) cell lines did not generate tumors in nude mice.

Transformation by IRF-2 was unique in several ways. Cells expressing the 160 aa IRF-2 deletion protein formed much larger soft agar colonies than those formed by the other IRF-2 expressing cells (Figure 18, panels B and D). Furthermore, the 160 aa IRF-2 expressing cells grew tumors in nude mice at a slightly faster rate than the wild-type (FL) IRF-2 expressing cells (Table 5). This observation is reflected in the more rapid doubling time of the IRF-2 (160) cells compared to IRF-2(FL) cells (Table 5). Taken together, these results directly correlate tumorigenic potential with DNA binding and transcriptional repression ability of IRF-2.

Virus and dsRNA inducibility of IFN- β mRNA in IRF-2 expressing cells. To investigate whether IRF-2 could exert its oncogenic phenotype through the regulation of IFN- β gene expression (60,129,197), the effects of the FL, 160 and 100 aa IRF-2 proteins on IFN- β mRNA production when stably expressed in NIH3T3 cells were analyzed. Cell lines were assayed 4 hours following induction by double-stranded RNA (dsRNA; poly (I):poly (C)) and

Figure 19. IFN- β RNA levels in the IRF-2 (FL), (160), and (100) cell lines.

Total RNA was isolated from the cell lines four hours following induction by dsRNA (25 ug/ml)/cycloheximide (50 ug/ml) or by Sendai virus (50 hemagglutinating units/ml). Quantitative RT-PCR amplification was performed with 2 ug of RNA, using primers specific for SV2CAT or IFN- β as described in Materials and Methods. Relative intensities of the PCR products and the protein-DNA complexes were scanned by laser densitometry and plotted.



cycloheximide or by Sendai virus, using a quantitative RT-PCR assay. As expected, untreated control and IRF-2(FL), (160) and (100) cells had undetectable levels of IFN- β mRNA (Figure 19, lanes 1 to 4). Following induction by dsRNA, control CMV and IRF-2(100) cells exhibited relatively similar levels of IFN- β mRNA (Figure 19, lanes 5 and 8). In contrast, cell lines expressing the FL and 160 aa IRF-2 proteins displayed 3-fold and 5-fold lower levels of IFN- β mRNA, respectively (Figure 19, lanes 6 and 7). Inducibility by Sendai virus infection was much stronger than that of dsRNA; IFN- β mRNA levels were 3- to 4-fold higher in Sendai virus-induced over dsRNA-induced control CMV cells (Figure 19, lanes 5 and 9). Interestingly, levels of IFN- β mRNA in the IRF-2(FL), (160), and (100) cells were indistinguishable from that of the control cells (Figure 19, lanes 9 to 12). These results were quantified as previously described (38,39,60). These findings indicate that although overexpression of the functional (FL) and (160) IRF-2 proteins results in reduced IFN- β levels when induced with dsRNA, there is no direct effect of the IRF-2 proteins on IFN- β inducibility by Sendai virus infection.

Displacement of IRF-1 by IRF-2 in DNA binding assays. One of the molecular mechanisms by which IRF-2 overexpression induces transformation may involve competition between IRF-2 and IRF-1 proteins for various transcriptional target sites. To measure the relative DNA binding affinity of the IRF proteins for the IFN- β -PRDI site, IRF-1, IRF-2 and IRF-2(160) polyhistidine-tagged recombinant proteins were analyzed by EMSA with increasing amounts of IRF-2 or IRF-2(160) combined with a constant amount of IRF-1. In the absence of IRF-2 protein, IRF-1 bound stably to PRDI (Figure 20, lanes 1 and 6). However, addition of an equal amount of IRF-2 or IRF-1(160) to the reaction sharply reduced IRF-1 DNA binding levels, concomitant

with the appearance of an IRF-2-PRDI complex (Figure 20, lanes 2 and 7). Detectable IRF-1 DNA binding activity was eliminated by addition of increasing IRF-2 protein (Figure 20, lanes 3 to 5 and 8 to 10, respectively), demonstrating that IRF-2 competes efficiently with IRF-1 for the same PRDI site. The strong binding of IRF-2(160) to the PRDI probe also complements previous studies demonstrating a higher affinity of IRF-2 for the PRDI site compared to IRF-1 (72,222). Similar results were obtained using the iNOS IRF-1 site (92) as a probe (data not shown). In these experiments, no indirect evidence for the formation of an IRF-1/IRF-2 heterodimer was obtained.

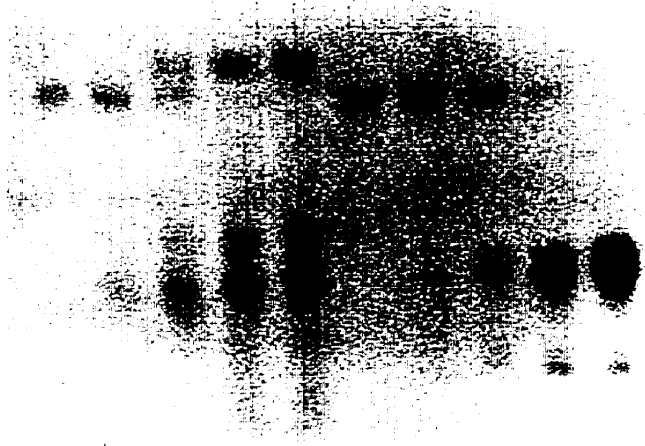
Figure 20. Displacement of IRF-1 by IRF-2 and IRF-2 (160) in DNA binding assays. Recombinant IRF-1 (0.4 ng; lanes 1 to 10) and fourfold increasing amounts of recombinant IRF-2 (2, 8, 32, and 128 ng in lanes 2 to 5, respectively) or IRF-2 (160) (0.6, 2.4, 9.6, and 38.4 ng in lanes 7 to 10, respectively) were incubated with ³²P-labeled PRDI probe and analyzed by EMSA. 0.4 ng, 2 ng, and 0.6 ng of IRF-1, IRF-2 and IRF-2 (160), respectively, were previously shown to exhibit minimal and equivalent DNA binding affinities for the PRDI probe (data not shown).

IRF-2

IRF-2 (160)



IRF-2 →
IRF-1 →



← **IRF-2 (160)**

1 2 3 4 5 6 7 8 9 10

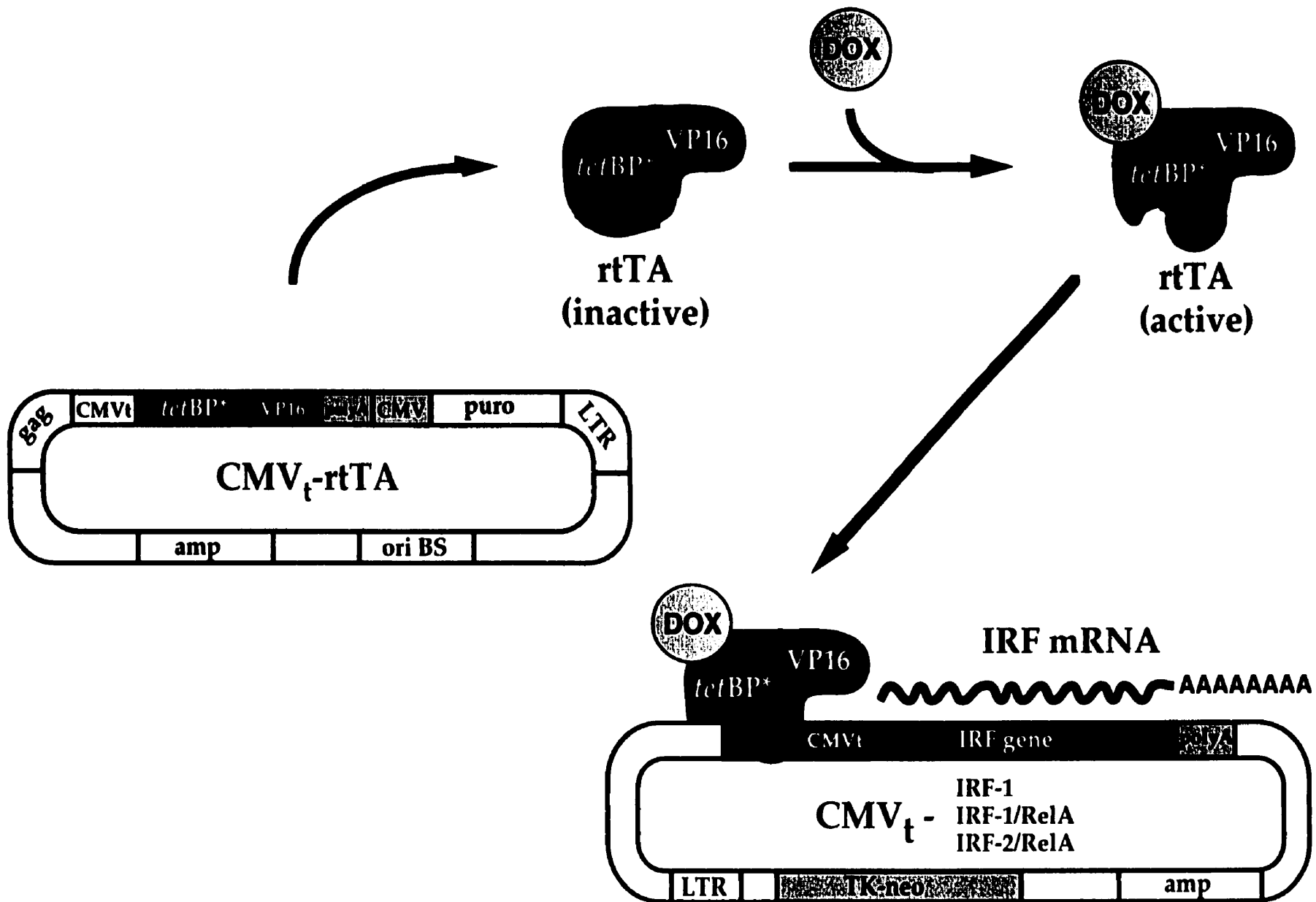
CHAPTER V

**ACTIVATION OF MULTIPLE GROWTH REGULATORY GENES
FOLLOWING INDUCIBLE EXPRESSION OF IRF-1 OR IRF/RELA FUSION
PROTEINS**

The role of IRF-1 as a tumor suppressor has been substantiated by several recent studies (73,74,152,189,192,224). However, the mechanisms by which IRF-1 exerts its antioncogenic effects remain to be elucidated. The previous chapter established a relationship between the DNA binding/transcriptional repression and oncogenic activity of IRF-2. Similarly, experiments in the present chapter provide an analysis between IRF-1 transactivation function and tumor suppression. To further characterize the potential targets of IRF-1 cell growth regulation, IRF-1 was expressed under the control of the tetracycline-inducible system in murine NIH3T3 cells. Due to their ability to mimic IRF-1 transactivator function, the regulatory potential of IRF-1/RelA and IRF-2/RelA fusion proteins was also examined.

Establishment of NIH 3T3 cells inducibly expressing IRF-1 and the IRF/RelA fusion proteins. Cell lines constitutively expressing IRF-1 have been difficult to establish because of the growth-suppressive effects of IRF-1 (103,111). Consequently, IRF-1, IRF-1/RelA and IRF-2/RelA (the latter two will be collectively referred to as IRF/RelA) were introduced into the tetracycline-inducible system utilizing the reverse tTA activator (rtTA) (63,64,179), which permits doxycycline (Dox) inducible expression of IRF-1 and IRF/RelA (Figure 21). Eighteen to fifty potential clones from each of the rtTA-IRF-1 and rtTA-IRF/RelA cell lines were expanded individually and screened for protein expression by immunoblot analysis, following growth in medium lacking or containing Dox for a period of 48h. IRF-1 expression was detected using an IRF-1 antibody, whereas IRF/RelA expression was detected using a C-terminal RelA antibody; use of the RelA antibody permitted the direct comparison of IRF/RelA expression level with that of endogenous RelA. For each of the cell lines (referred to as rtTA-IRF-1 and rtTA-IRF/RelA cells), two to three

Figure 21. Tetracycline regulated expression of IRF-1 and IRF/RelA. This system consists of two plasmid components; one encodes a tetracycline-responsive, VP16-based transactivator protein (rtTA) and the other contains the gene of interest - IRF-1, IRF-1/RelA or IRF-2/RelA - downstream of the CMV_t promoter. In the absence of doxycycline (a derivative of tetracycline), the rtTA protein is inactive. However, Dox-induced changes in protein conformation enables rtTA to bind regulatory tetracycline operon sequences present in the CMV_t promoter and activate gene transcription. Active rtTA protein also binds to the CMV_t promoter driving expression of itself, resulting in positive autoregulation of the rtTA gene. Using this system, expression of IRF-1 or IRF/RelA could be tightly regulated.



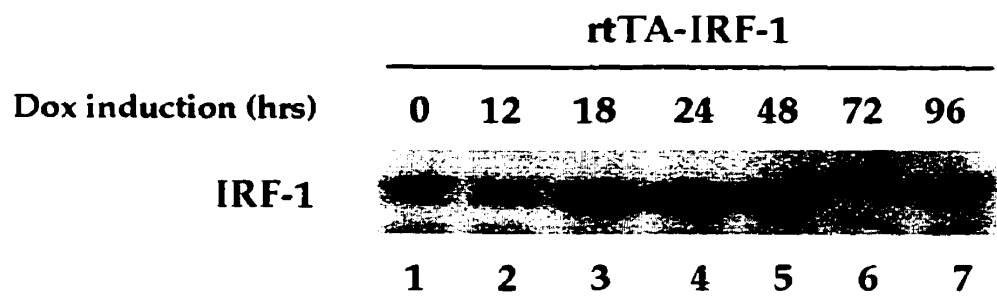
positive clones possessing minimal uninduced protein levels and high inducible expression were chosen for further study.

The kinetics of transgene induction were characterized at various times following Dox induction, using Western and Northern blot analyses. Figure 22 illustrates the kinetics of expression of a representative clone from each of the rtTA-IRF-1 and rtTA-IRF/RelA cell lines. Each cell line possessed unique expression patterns. In the IRF-1 cell line, IRF-1 protein was detectable at peak levels within 18h following addition of Dox (Figure 22A, lane 3) and levels remained relatively constant thereafter. As measured by densitometry, peak IRF-1 levels were approximately 16-fold greater than uninduced levels. IRF-1/RelA protein was detectable within 12h, reaching maximal levels at 48h following Dox induction in the IRF-1/RelA cell line (Figure 22B, lanes 3 and 4). Peak IRF-1/RelA expression was high - approximately 53-fold greater than basal levels and 3-fold higher than the steady state level of endogenous RelA(p65) (Figure 22B, lanes 3 to 7). Within 18h of Dox induction, IRF-2/RelA protein was detectable in the rtTA-IRF-2/RelA cell line; peak expression was attained within 24h with levels approximately 25-fold higher than basal levels (Figure 22C, lanes 3 and 4). As represented by rtTA-IRF-1/RelA in Figure 2D, kinetics of mRNA induction correlated closely with protein expression (Figure 22B). The relative Tet inducibility of the cell lines is depicted graphically in Figure 22E.

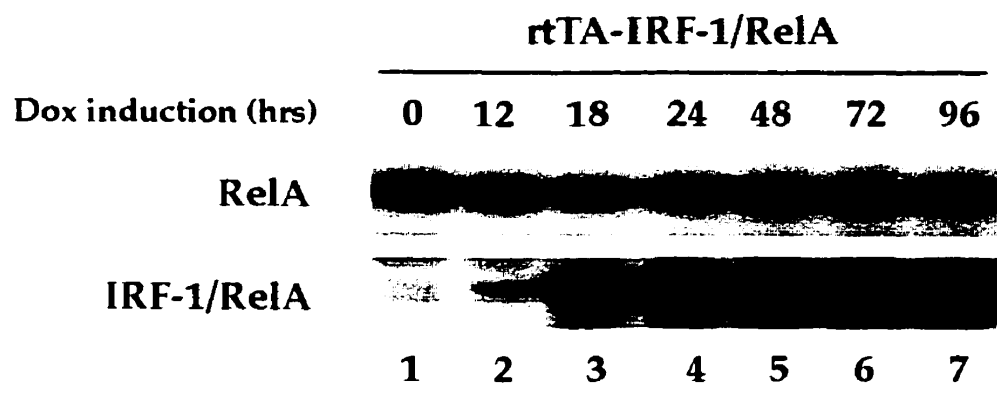
To test the functionality of the induced IRF-1 and IRF/RelA proteins, rtTA-IRF-1 and rtTA-IRF/RelA cells were analyzed for DNA binding activity using EMSA; a representative EMSA is depicted in Figure 23. At 48h following Dox induction, whole cell extracts from each cell line contained ISRE binding

Figure 22. Inducible expression of IRF-1 and IRF/RelA in NIH3T3 cells. **A.** IRF-1 expression. **B.** IRF-1/RelA expression. **C.** IRF-2/RelA expression. Whole cell extracts (20 ug) prepared from rtTA-IRF-1, rtTA-IRF-1/RelA or rtTA-IRF-2/RelA cells induced with Dox for 0-96h were subjected to SDS-PAGE and transferred to nitrocellulose membrane. IRF-1 levels were detected using an IRF-1 antibody and IRF/RelA levels were detected using a C-terminal NF- κ B RelA(p65) antibody. **D.** Inducible expression of IRF-1/RelA mRNA. 0-72h following Dox induction, total RNA was prepared from rtTA-IRF-1/RelA cells. Total RNA (20 ug) was used for Northern blot analysis, with a 5' 300 bp IRF-1 DNA fragment as a probe.

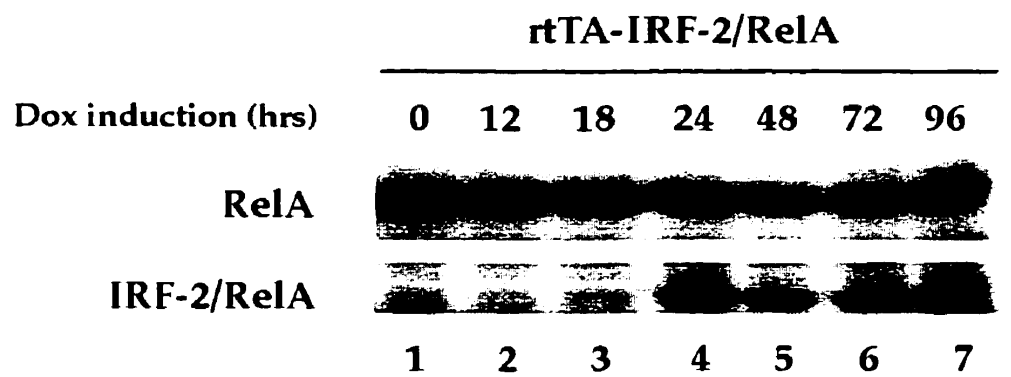
A



B



C



D

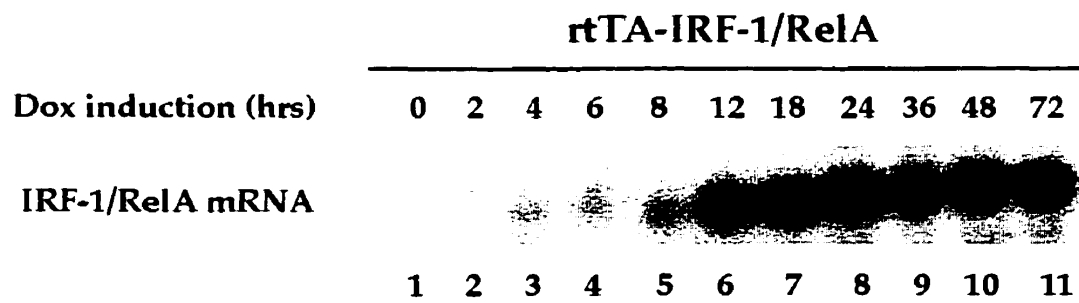
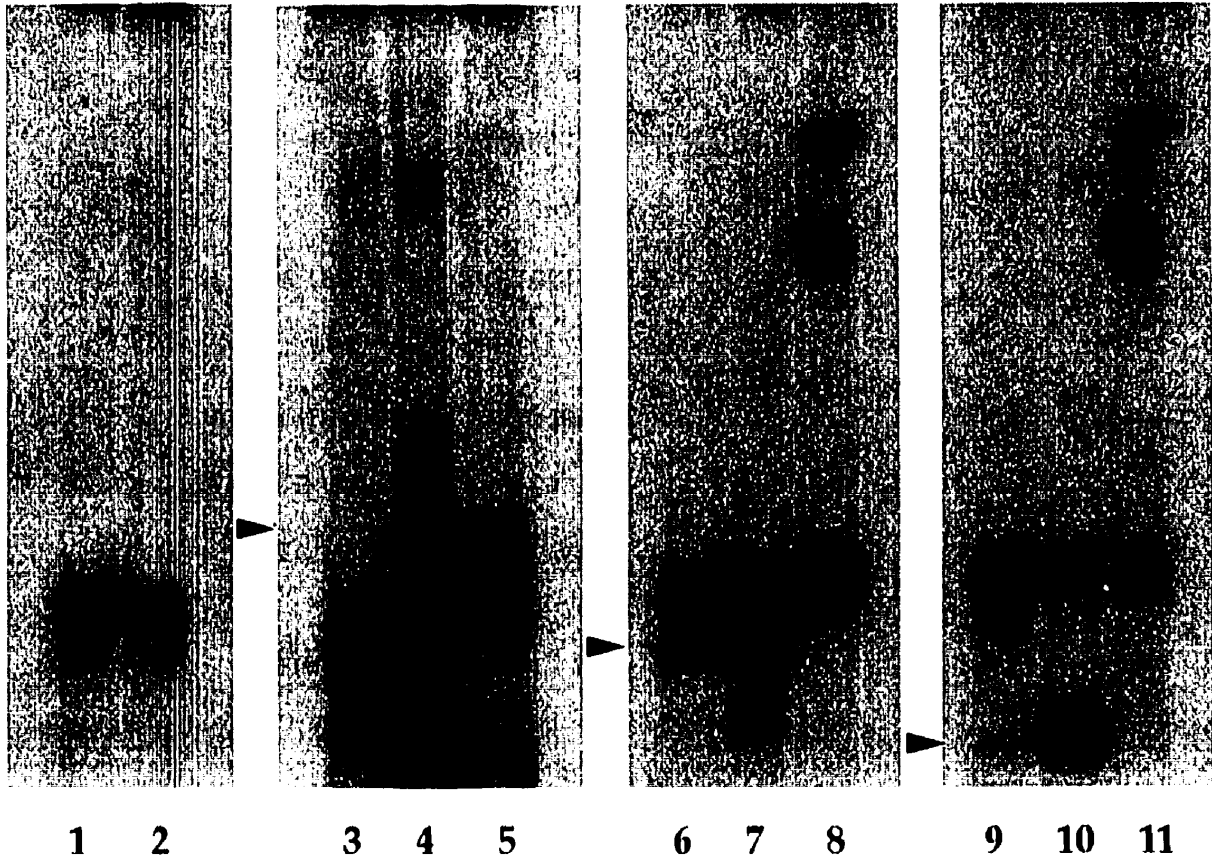


Figure 23. DNA binding activities in rtTA-IRF-1 and rtTA-IRF/RelA expressing cells. EMSA was performed on whole cell extracts (10 ug) derived from control rtTA, rtTA-IRF-1, and rtTA-IRF/RelA cells which were uninduced (lanes 1, 3, 6 and 9) or Dox induced for 48h (lanes 2, 4, 7 and 10). To test the specificity of complex formation, Dox-induced extracts were preincubated with IRF-1 (α F1; lane 5), or RelA(p65) (α RelA; lanes 8 and 11) antibody prior to probe addition. The 32 P-labelled probe corresponds to the ISRE of the IFN- α/β -inducible ISG-15 gene. The arrows correspond to the specific IRF-1 or IRF/RelA protein-DNA complex. 'SS' corresponds to IRF/RelA supershift complexes.

	rtTA		rtTA-IRF-1			rtTA-IRF-1/RelA			rtTA-IRF-2/RelA		
Dox	-	+	-	+	+	-	+	+	-	+	+
Antibody	-	-	-	-	α F1	-	-	α RelA	-	-	α RelA



SS

complexes with relative sizes corresponding to the size of the transfected IRF-1 (Figure 23, lane 4), IRF-1/RelA (Figure 23, lane 7) or IRF-2/RelA (Figure 23, lane 10) protein. As with the kinetics of protein expression (Figure 22, A to D), these complexes were inducible, since they were not present in the control rtTA (Figure 23, lanes 1 and 2) or uninduced cells (Figure 23, lanes 3, 6 and 9). The specificity of the complexes was confirmed by supershift analysis with the appropriate antibody directed against IRF-1 or a C-terminal peptide of RelA (Fig. 23, lanes 5, 8 and 11). Based on these analyses, IRF-1 and IRF/RelA proteins were highly inducible and functionally expressed in NIH 3T3 cells.

Growth-suppressive and apoptotic properties of the inducible IRF-1 and IRF/RelA cell lines. Since the IRF/RelA proteins were able to mimic IRF-1 in its role as an activator of IFN- β gene transcription (120), their potential to mimic IRF-1 in its role as a tumor suppressor was also assessed. Growth kinetics of the rtTA-IRF-1 and rtTA-IRF/RelA cell lines were analyzed over a 5 day period following Dox induction (Figure 24A). In contrast to control rtTA cells, growth of IRF-1 and IRF/RelA expressing cells was significantly reduced upon Dox induction, indicating that IRF/RelA proteins mimicked IRF-1 in cell growth inhibition. Growth rate correlated with the level of transgene expression, and the highly-expressing rtTA-IRF-1/RelA cells displayed a dramatic decrease in growth rate. Interestingly, peak expression of the cell lines at 24 to 72h after Dox induction also caused a low level of apoptosis in the cell population (approximately 10%), as assayed by microscopic analyses using the DNA intercalating dye acridine orange (Figure 24B). At high concentrations, IRF/RelA appears to induce apoptosis, rather than cell growth arrest of NIH 3T3 cells.

Figure 24. Growth-suppressive and apoptotic properties of IRF-1 and IRF/RelA. A. Growth rate of IRF-1 and IRF/RelA expressing cell lines. Control rtTA, rtTA-IRF-1 and rtTA-IRF/RelA cell lines were cultured in the presence of 1 ug/ml Dox in complete medium for a period of 5 days. Cells were initially plated at a density of 5×10^4 cells per 35 mm dish and then counted using the Coulter counter every 24h. Values obtained are the average of three experiments performed on two independent isolated clones per cell line.

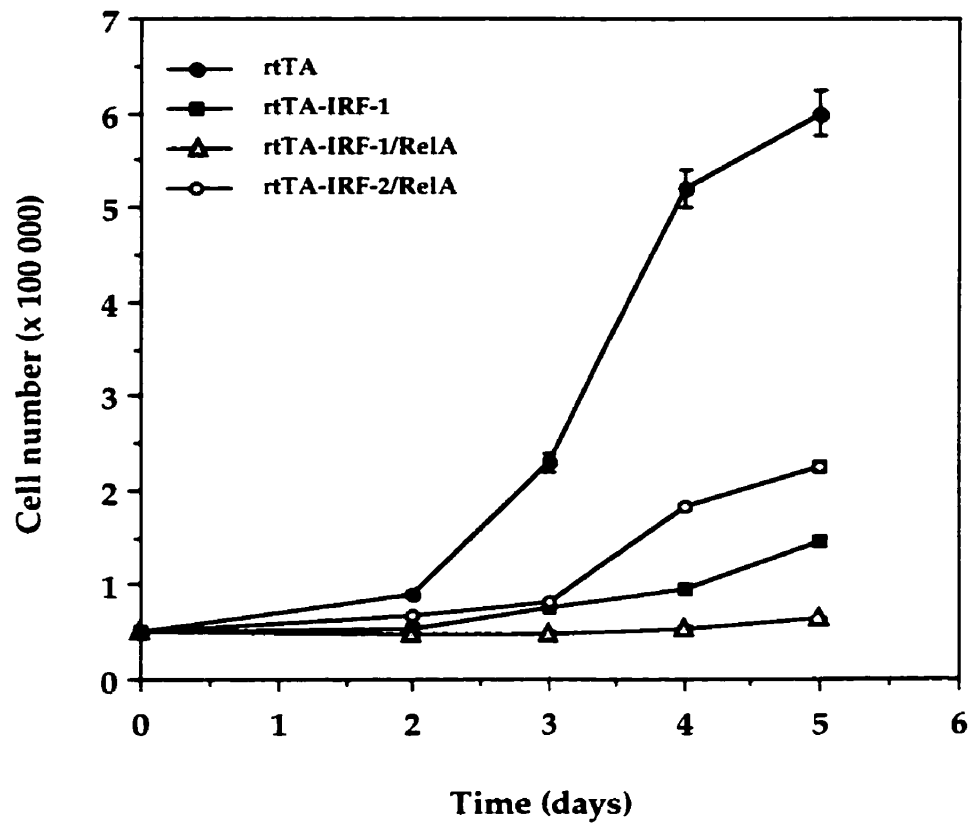
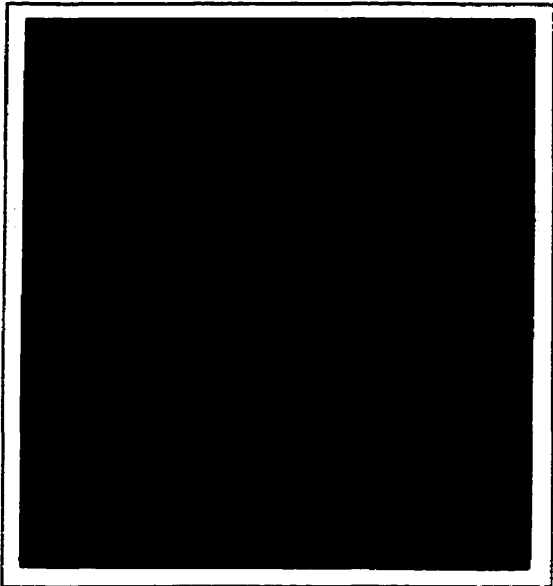


Figure 24 (continued). B. Apoptotic rtTA-IRF-1/RelA cells. At 24-72h following 1 ug/ml Dox addition, control rtTA and rtTA-IRF-1/RelA NIH 3T3 cells were stained with the DNA-intercalating dye acridine orange and then viewed under UV illumination.

Control rTA cells + DOX



IRF-1/RelA cells + DOX

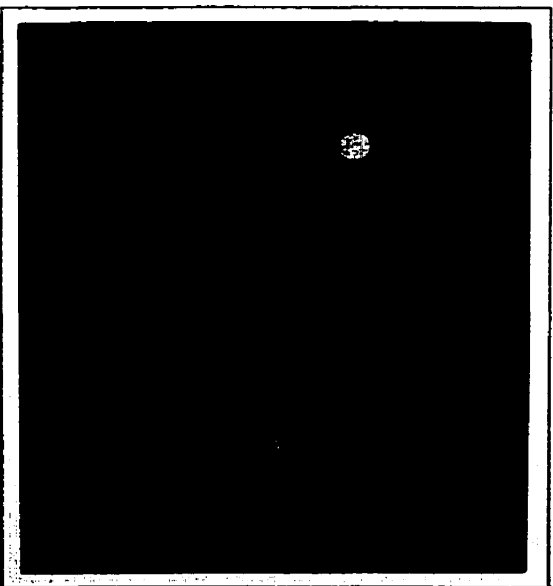
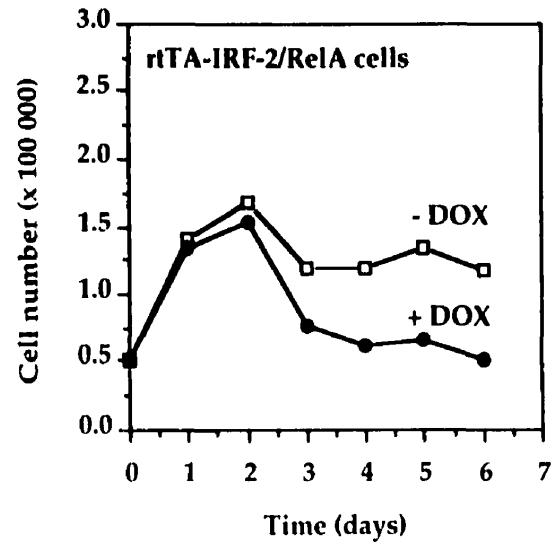
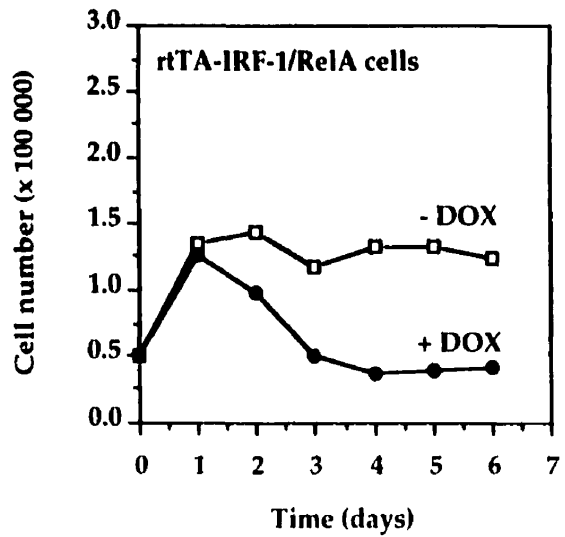
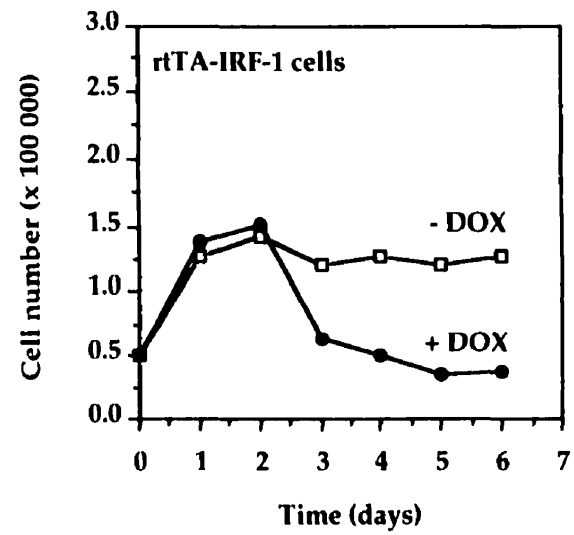
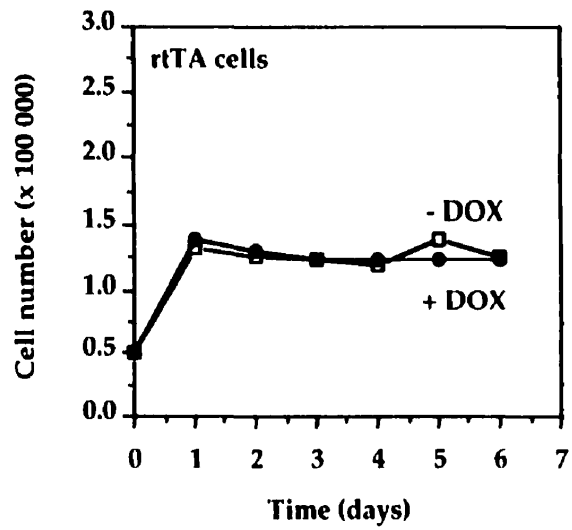


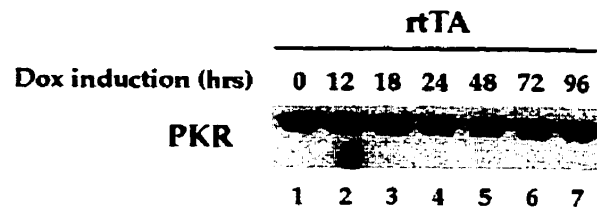
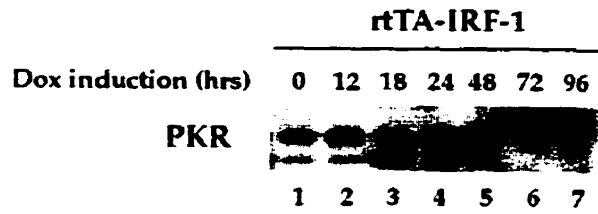
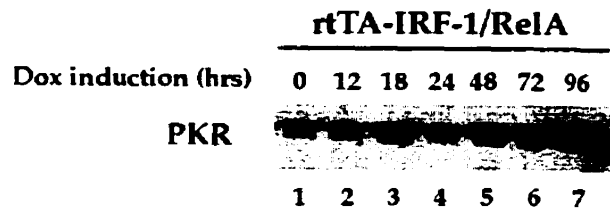
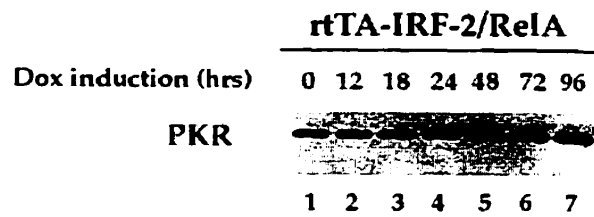
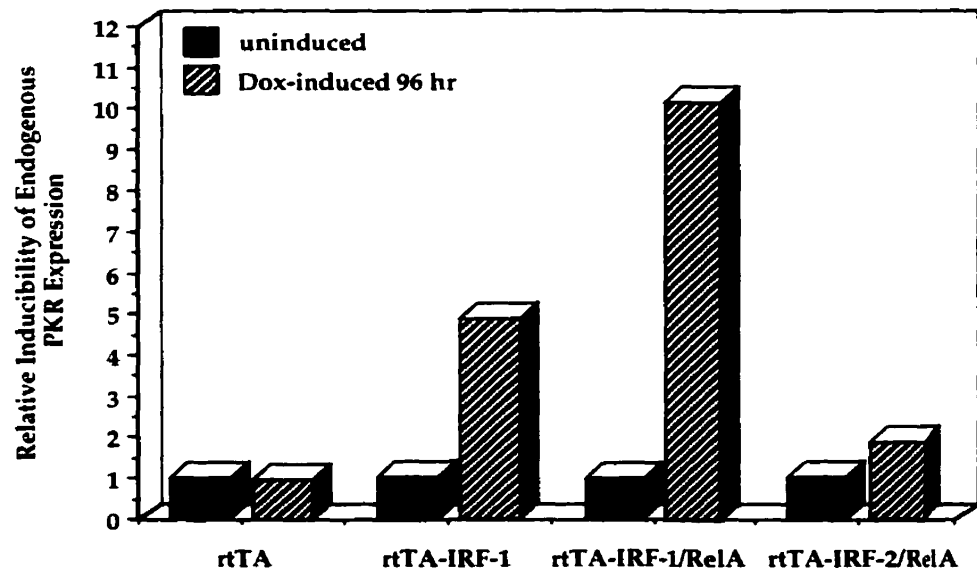
Figure 24 (continued). C. Growth rate of rtTA-IRF-1 and rtTA-IRF/RelA cells under conditions of serum starvation. Control rtTA, rtTA-IRF-1, and rtTA-IRF/RelA cells were cultured in the presence of 1 ug/ml Dox in medium containing 0.5% heat-inactivated calf serum for a period of 6 days. Cells were initially plated at a density of 5×10^4 cells per 35 mm dish and then counted every 24h. Values obtained are the average of three experiments.



Recent evidence implicates IRF-1 in apoptotic cell death in response to DNA damage (152,189). To investigate whether IRF-1 modulated cell growth in response to serum starvation, growth kinetics of rtTA-IRF-1 and rtTA-IRF/RelA cells were analyzed over a 6 day period in the absence or presence of Dox (Figure 24C). Control rtTA cells in the absence or presence of Dox were growth arrested within 24 to 48h after serum starvation; similarly, IRF-1 and IRF/RelA expressing cells in the absence of Dox were growth arrested. However, within 48 to 72h after Dox induction under the same conditions, cell number decreased in the rtTA-IRF-1 and rtTA-IRF/RelA cell lines, indicating that IRF-1 and IRF/RelA expression caused cell death in serum starved cells. This result implicates IRF-1 as a cell growth regulator which can respond to cell stress in the form of serum starvation. Also, these studies further confirm the ability of the IRF/RelA proteins to physiologically mimic IRF-1 in its role as a growth regulatory transcription factor.

Expression of PKR in the IRF-1 and IRF/RelA inducible cell lines. The double-stranded RNA activated serine-threonine kinase p68 kinase (PKR), is an IFN-inducible gene which plays an important role in the regulation of cell proliferation and leukemogenesis (14,71,105,183). To test whether IRF-1 expression affects PKR, the kinetics of expression of endogenous PKR was analyzed in the rtTA-IRF-1 and rtTA-IRF/RelA cell lines following Dox induction. As shown in Figure 25, endogenous PKR expression was induced by IRF-1 and IRF/RelA expression in the IRF-1 (Figure 25B) and IRF/RelA cell lines (Figure 25, C and D) but was unaffected by Dox addition to the control rtTA cell line (Figure 5A). These results support the observation that IRF-1 tumor suppressor activity may involve the IFN-responsive protein

Figure 25. Expression of PKR in IRF-1 and IRF/RelA expressing cells. **A.** PKR expression in control rtTA cells. **B.** Inducible PKR expression in IRF-1 cells. **C.** Inducible PKR expression in rtTA-IRF-1/RelA cells. **D.** Inducible PKR expression in IRF-2/RelA cells. Whole cell extract (20 ug) prepared from control rtTA, rtTA-IRF-1 and rtTA-IRF/RelA cells induced with Dox for 0-96h was subjected to SDS-PAGE, transferred to nitrocellulose membrane, and immunoblotted with PKR antibody. **E.** The relative intensities of PKR protein were scanned by laser densitometry and plotted.

A**B****C****D****E**

PKR (102), and confirms the ability of the IRF/RelA fusion proteins to mimic IRF-1 transactivator function (120).

Expression of STAT1 (p91) in the IRF-1 and IRF/RelA inducible cell lines.

The JAK-STAT pathway regulates signalling in response to many cytokines including IFN. To test the idea that IRF-1 may exert its growth regulatory activities via the JAK-STAT pathway, the kinetics of expression of endogenous STAT1 (p91) was analyzed in the IRF-1 and IRF/RelA cell lines following Dox induction (Figure 26). Although endogenous STAT1 expression was unaffected by Dox addition in the control rtTA cell line (Figure 26A), expression of STAT1 protein was increased following induction of expression of IRF-1 (Figure 26B) and IRF/RelA (Figure 26, C and D). As represented by the rtTA-IRF-1/RelA cell line in Figure 26E, IRF-1 and IRF/RelA appear to regulate STAT1 expression at the transcriptional level, since STAT1 mRNA also increased in response to Dox-induced IRF-1 and IRF/RelA expression.

To test the functionality of the induced STAT1 protein, rtTA, rtTA-IRF-1 and rtTA-IRF/RelA cells were analyzed for STAT1 DNA binding activity by EMSA, using the ISRE from the IFN- α/β inducible ISG-15 gene as a probe and whole cell extracts prepared from 96h Dox-induced cells (Figure 27). In uninduced (Figure 27, lane 1) and Dox-induced (Figure 27, lane 2) control rtTA cells, no ISRE protein-DNA complexes were found. As expected, when Dox-induced rtTA cells were stimulated for 20 minutes with 500 units/ml IFN- α/β (Figure 27, lane 4), an ISRE complex corresponding to ISGF3 was detected. The presence of STAT1 in Dox-induced and IFN and Dox-induced rtTA cells was tested by supershift analysis (Figure 27, lanes 3 and 5).

Figure 26. Expression of STAT1 (p91) in IRF-1 and IRF/RelA expressing cells.

A. STAT1 expression in control rtTA cells. **B.** Inducible STAT1 expression in rtTA-IRF-1 cells. **C.** Inducible STAT1 expression in rtTA-IRF-1/RelA cells. **D.** Inducible STAT1 expression in rtTA-IRF-2/RelA cells. Whole cell extract (20 ug) prepared from control rtTA, rtTA-IRF-1 and rtTA-IRF/RelA cells induced with Dox for 0-96h was subjected to SDS-PAGE, transferred to nitrocellulose membrane, and immunoblotted with STAT1 antibody. **E.** mRNA levels of STAT1 following induction of IRF-1/RelA expression. Total RNA (20 ug) prepared from rtTA-IRF-1/RelA cells 0-48h following Dox induction was used for Northern blot analysis, with STAT1 cDNA as a probe. **F.** The relative intensities of STAT1 protein were scanned by laser densitometry and plotted.

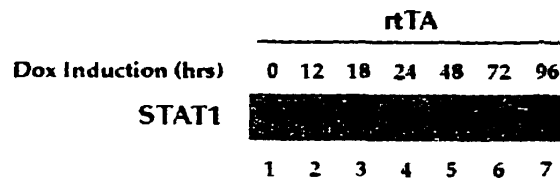
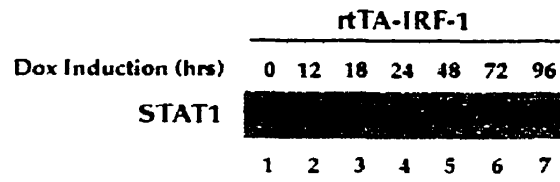
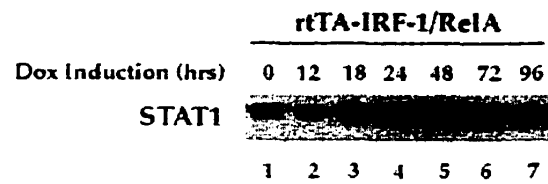
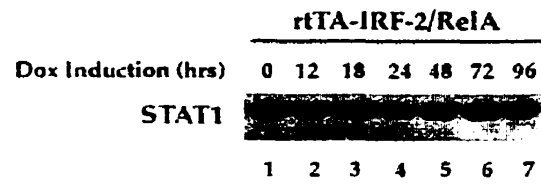
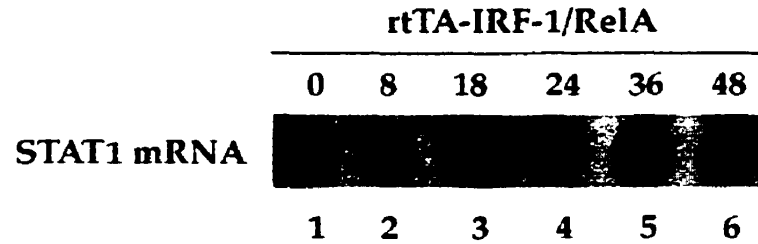
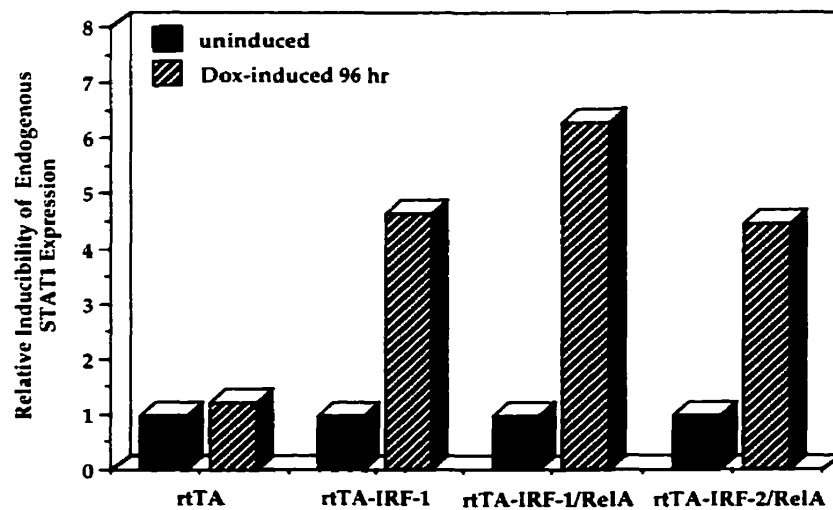
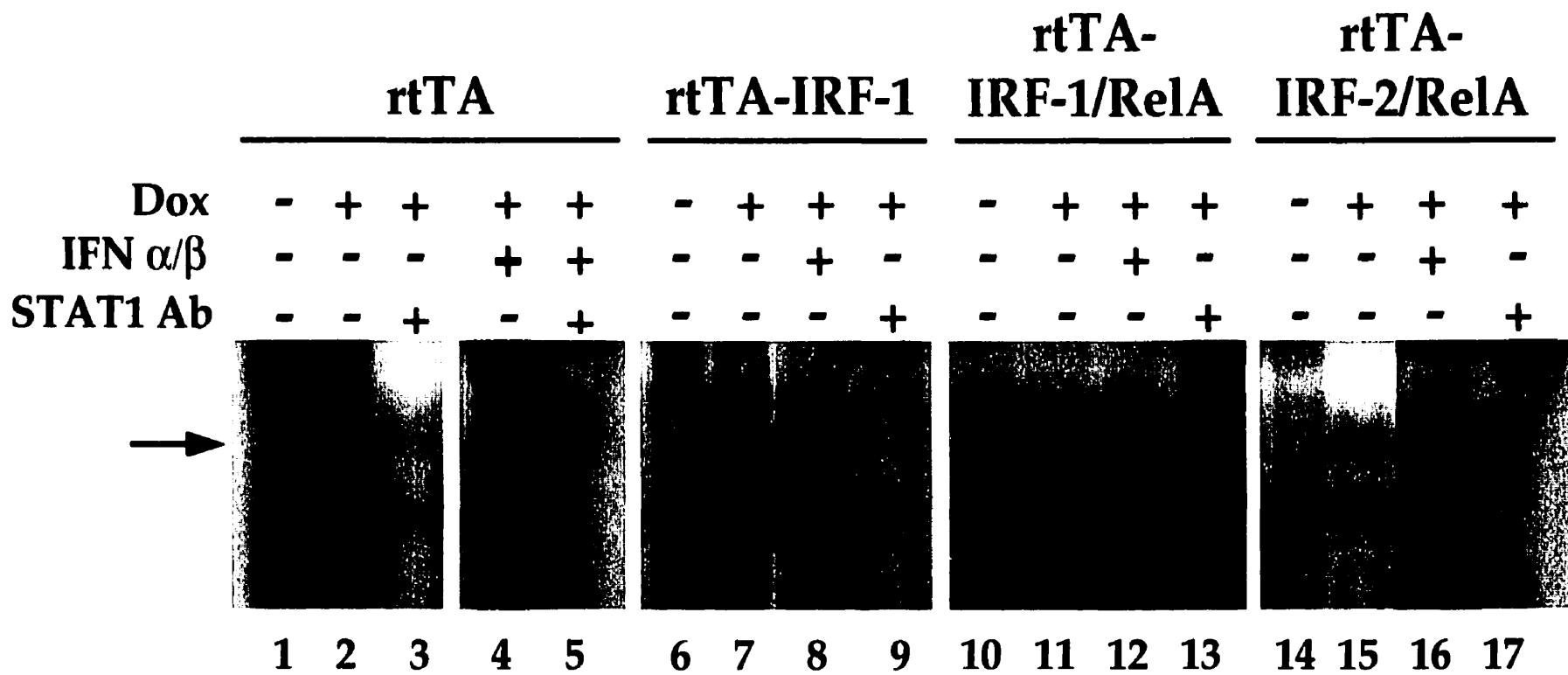
A**B****C****D****E****F**

Figure 27. STAT1 binding activity in IRF-1 and IRF/RelA expressing cells.

EMSA was performed on whole cell extracts (10 ug) derived from control rtTA, rtTA-IRF-1, and rtTA-IRF/RelA cells which were uninduced (lanes 1, 6, 10 and 14), Dox-induced for 96h (lanes 2, 7, 11 and 15), or stimulated for 20 min with 500 units/ml IFN- α/β (Sigma) following 96h Dox induction (lanes 4, 8, 12 and 16). The ISGF3 complex is indicated by the arrow. The ^{32}P -labeled probe corresponds to the ISRE of the IFN- α/β -inducible ISG-15 gene. To test for specific STAT1 activity in the protein-DNA complexes, Dox-induced (lanes 3, 9, 13 and 17) or Dox and IFN-induced extracts (lane 5) were preincubated with STAT1 antibody prior to addition of probe.

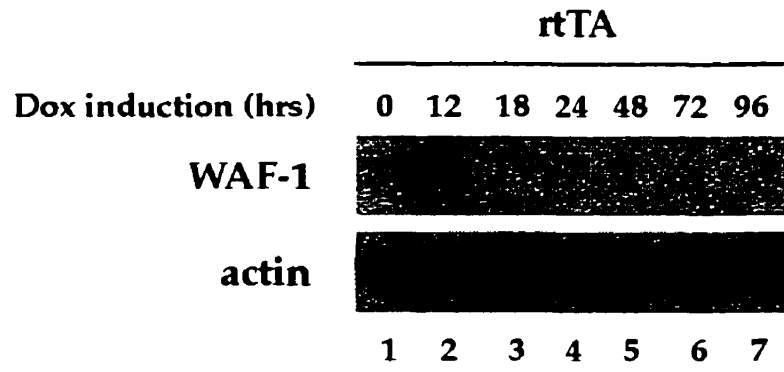


Interestingly, Dox-induced rtTA-IRF-1 (Figure 27, lane 7) and rtTA-IRF/RelA cells (Figure 27, lanes 11 and 15) also exhibited an ISRE complex with a similar migration pattern as ISGF3 and which contained STAT1, as confirmed by supershift analysis (Figure 27, lanes 9, 13 and 17). This complex was also inducible, as it was not present in uninduced rtTA-IRF-1 (Figure 27, lane 6) and rtTA-IRF/RelA cells (Figure 27, lanes 10 and 14). Following a 20 min treatment with IFN- α/β , ISRE binding was enhanced in Dox-induced rtTA-IRF-1 (Figure 27, lane 8) and rtTA-IRF/RelA cells (Figure 27, lanes 12 and 16), to levels similar to that seen in IFN-treated control cells (Figure 27, lane 4). Taken together, these results implicate the JAK-STAT pathway as a novel target by which IRF-1 may exert its growth regulatory activities.

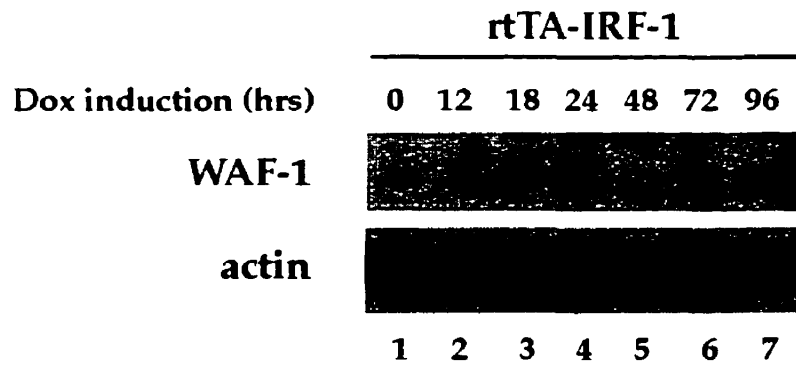
Expression of WAF1 in the IRF-1 and IRF/RelA inducible cell lines. STAT1 has been shown to activate transcription of the p21 (WAF1, CIP1) CDK inhibitor in response to induction by IFN γ or EGF (epidermal growth factor), resulting in cell growth inhibition (30). Tumor suppressor activity associated with IRF-1 in the inducible cell lines may be due to WAF1 activation by IRF-1-induced STAT1. To test this hypothesis, the kinetics of expression of endogenous WAF1 was analyzed in the IRF-1 and IRF/RelA cell lines following Dox induction (Figure 28). Our findings were surprising in two ways. First, elevated levels of WAF1 were detected in the IRF-1 (Figure 28B) and IRF-1/RelA (Figure 28C) cell lines, but not in the IRF-2/RelA or rtTA cells (Figure 28A and D). The absence of WAF1 in the rtTA and rtTA-IRF-2/RelA cell lines was not due to the quality of whole cell extract, as actin levels were normal (Figure 28, A and D, bottom) and IRF-2/RelA expression levels were as anticipated (data not shown). Second, WAF1 expression in the rtTA-IRF-1 and rtTA-IRF-1/RelA cell lines did not correlate with the inducibility of IRF-1

Figure 28. Expression of WAF1 in IRF-1 and IRF/RelA expressing cells. A. WAF1 expression in control rtTA cells. **B.** WAF1 expression in rtTA-IRF-1 cells. **C.** WAF1 expression in rtTA-IRF-1/RelA cells. **D.** WAF1 expression in rtTA-IRF-2/RelA cells. Whole cell extract (20 ug) prepared from control rtTA, rtTA-IRF-1 and rtTA-IRF/RelA cells induced with Dox for 0-96h was subjected to SDS-PAGE, transferred to nitrocellulose membrane, and immunoblotted with WAF1 antibody. The same blots were then stripped and immunoblotted with actin antibody.

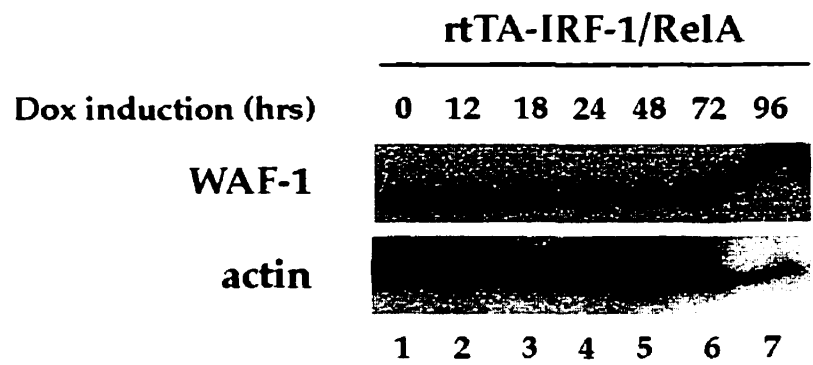
A



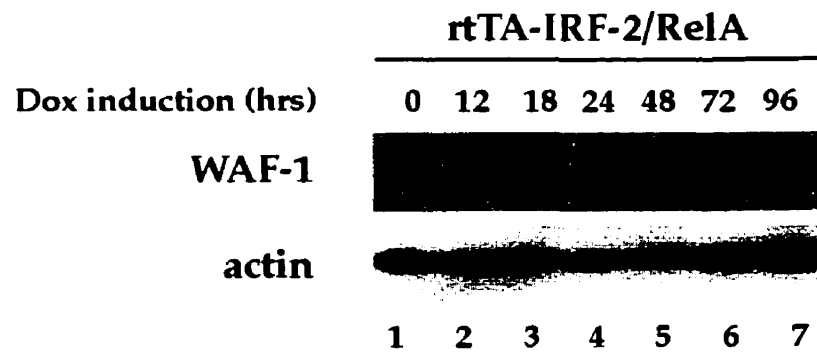
B



C



D



and IRF-1/RelA; rather, WAF1 levels were constitutively activated even in the absence of Dox. It is possible that low level IRF-1 or IRF/RelA expression in the rtTA-IRF-1 and rtTA-IRF/RelA in the absence of Dox may be sufficient to activate WAF1 expression. Together, the results implicate the involvement of the cell cycle in IRF-1 tumor suppressor activity through WAF1. However, due to distinct kinetics of endogenous STAT1 and WAF1 expression in the IRF-1 and IRF-1/RelA cell lines, the observed increase in WAF1 expression is probably not caused by IRF-1-induced STAT1.

CHAPTER VI

**IDENTIFICATION OF THE SECRETORY LEUKOCYTE PROTEASE
INHIBITOR (SLPI) AS A TARGET OF IRF-1 REGULATION**

In the last chapter, it was demonstrated that IRF-1 and IRF/RelA transactivation activity and tumorigenic phenotype correlate with the upregulation of the PKR, STAT1(p91) and WAF1(p21) growth regulatory genes. To identify novel targets of IRF-1-mediated tumor suppressor or immunomodulatory activities, the IRF-1 and IRF-1/RelA inducible cell lines characterized previously were analyzed using the method of RNA fingerprinting.

RNA fingerprinting of cell lines inducibly expressing IRF-1/RelA. RNA fingerprinting is a method comparable to differential display, as both strategies seek to compare RNA samples of two different cell populations (reviewed in (215)). A schematic representation of the RNA fingerprinting method is depicted in Figure 29. Essentially, cDNA resulting from reverse transcribed RNA of the two cell populations to be compared is amplified using numerous pairwise combinations of 5' (P) and 3' (T) primers. The primers selected, when used in their totality, should give rise to a series of amplified cDNA products which is representative of the total mRNA population. Using this technique, genes which are preferentially upregulated or downregulated in a specific cell sample could be identified.

To identify genes regulated by IRF-1, RNA fingerprinting was performed on tetracycline-inducible control rtTA and rtTA-IRF-1/RelA expressing NIH3T3 cells. rtTA-IRF-1/RelA cells were used in preference to the physiologically relevant rtTA-IRF-1 cells due to low uninduced transgene levels and high inducibility of expression. An RNA fingerprint resulting from cDNA amplification using three different primer sets is presented in Figure 30. A prominent 400 base pair (bp) band amplified from primer set 1 in undiluted

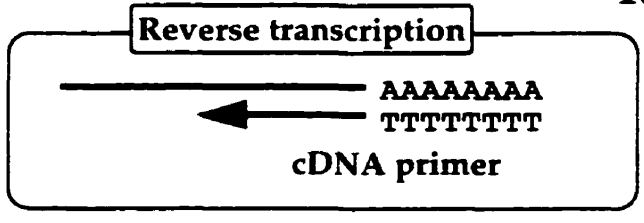
Figure 29. The RNA fingerprinting method. This schematic is adapted from the Delta™ RNA Fingerprinting Kit Manual (CLONTECH Laboratories, Inc.). Control cells and cells expressing a gene of interest "X" are the two different cell populations compared. RNA extracted from cells is reverse transcribed using an oligo(dT) primer. The cDNA product is PCR-amplified using various pairwise combinations of P and T primers. Specifically, three low stringency cycles are executed with an annealing temperature of 40°C, allowing imprecise anchoring of the P and T primers to various cDNA strands. These initial reactions are followed by 22 to 28 high stringency cycles with an annealing temperature of 60°C, resulting in the amplification of specific cDNAs representative of the RNA population in the cell sample. An example of an RNA fingerprint is shown on the lower half of the figure. Using hypothetical P1/T1 primers, a differentially expressed band is detected in cells expressing gene "X". In contrast, a band amplified from cDNA derived from control cells with the P2/T2 primers is found to be absent in cells expressing gene "X". Using this method, novel gene targets regulated by gene "X" could be identified.

Control cells

Cells + gene X

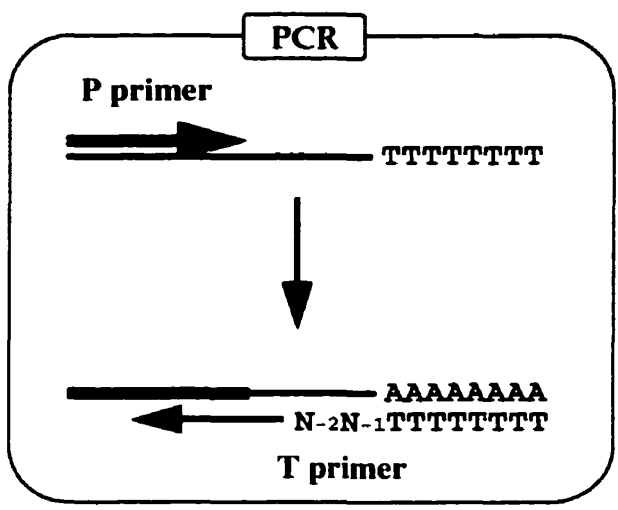
RNA #1

RNA #2



cDNA #1

cDNA #2



P1/T1		P2/T2	
1	2	1	2

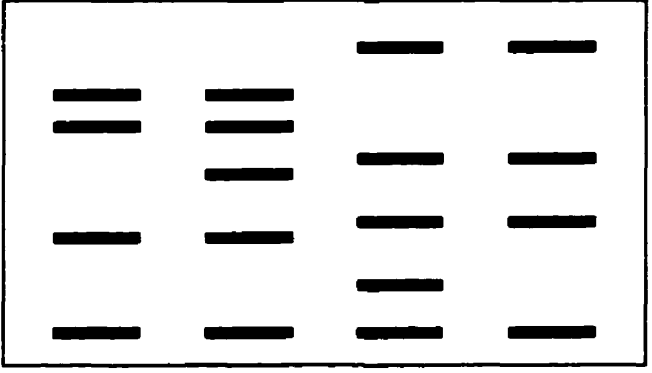


Figure 30. RNA fingerprint of rtTA and rtTA-IRF-1/RelA cells. 72 hours following Dox induction, total RNA was prepared from rtTA and rtTA-IRF-1/RelA cells. Total RNA (2 ug) was used for RNA fingerprinting reactions using the Delta™ RNA Fingerprinting Kit (CLONTECH Laboratories, Inc.). RNA fingerprints of rtTA (lanes 1, 2, 5, 6, 9, and 10) and rtTA-IRF-1/RelA cells (lanes 3, 4, 7, 8, 11 and 12) were performed using three different primer sets. To ensure reproducibility, PCR reactions were also performed on 1:100 dilutions of the cDNA product from each cell sample. Reactions were resolved on a 5% Long Ranger™ gel. The 400 bp band found to be differentially expressed in rtTA cells following amplification with Primer set #1 and which corresponds to SLPI is identified.

and 100-fold diluted cDNA from 72h Dox-induced control rtTA cells (Figure 30A, lanes 1 and 2) was absent in cDNA from 72h Dox-induced IRF-1/RelA cells (Figure 30A, lanes 3 and 4). The band was isolated, subcloned and sequenced, and the resulting sequence was 100% homologous to a fragment of the murine secretory leukocyte protease inhibitor (SLPI) gene.

The 400 bp fragment was used as a probe for Northern blot to analyze SLPI expression following induction of IRF-1 and IRF/RelA at varying times following Dox induction. Figure 31B illustrates the kinetics of expression of SLPI mRNA following induction of IRF-1/RelA. Uninduced cells exhibited detectable endogenous levels of SLPI. Interestingly, following Dox induction of IRF-1/RelA, there were two distinct patterns of SLPI mRNA expression. Two hours after Dox treatment (Figure 31B, lane 2), SLPI levels increased, attaining peak levels 4 hours following Dox induction, when IRF-1/RelA mRNA levels were detected (Figure 31B, lane 3). However, 12 to 24 hours following Dox induction of IRF-1/RelA expression, SLPI mRNA levels decreased to undetectable levels, soon after peak IRF-1/RelA levels were acquired (Figure 31B, lanes 4 to 10). Several experiments, including that described in Figure 32 confirm that the increase in SLPI expression observed early in induction is not due to the effects of doxycycline itself. From these results, SLPI is a gene which is dually regulated by IRF-1; its expression is both activated and later suppressed following induction of IRF-1 or IRF-1/RelA.

dsRNA activation of SLPI mRNA in the IRF-1 and IRF-1/RelA inducible cell lines. dsRNA is a strong activator of IFN- β , an IRF-1 regulated gene. To investigate whether dsRNA could induce SLPI expression, control rtTA, rtTA-IRF-1 and rtTA-IRF-1/RelA cells were either uninduced or Dox-induced

Figure 31. Expression of SLPI mRNA in rtTA-IRF-1/RelA cells. 20 ug of total RNA prepared from rtTA-IRF-1/RelA cells 0 to 96 hours following Dox induction was used for Northern blot analysis with a 400 bp SLPI DNA fragment (isolated from the RNA fingerprint in Figure 30) or a 5' 300 bp IRF-1 DNA fragment as a probe. As a control of RNA loading, 28S RNA obtained from migration of total RNA on the agarose gel used for Northern blot analysis is presented.

Dox Induction (hrs)

0 2 4 6 8 12 48 72 96

SLPI mRNA



IRF-1/RelA mRNA



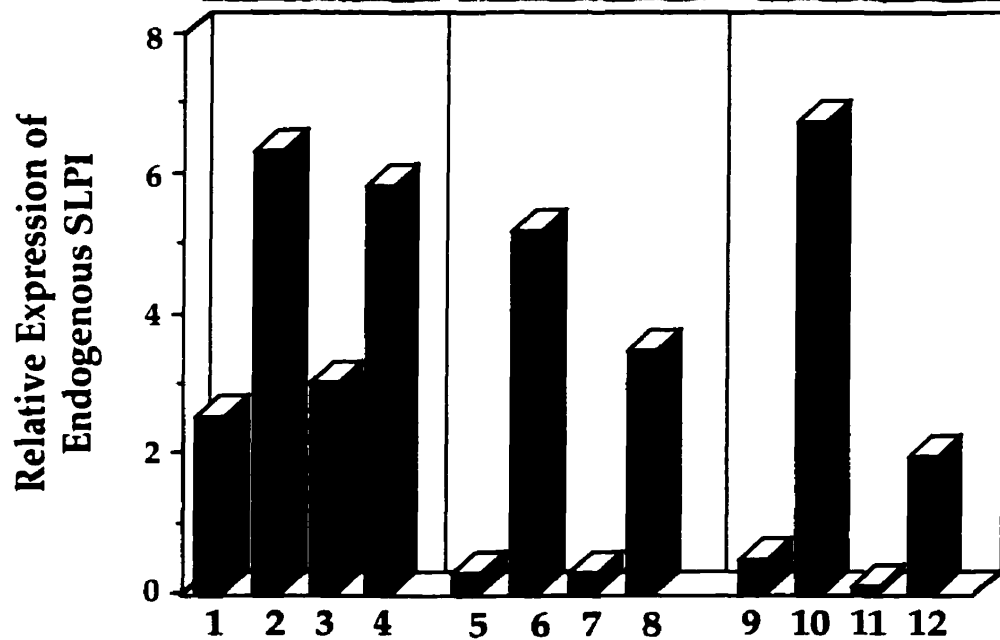
28S RNA



1 2 3 4 5 6 7 8 9

Figure 32. SLPI mRNA in dsRNA treated IRF-1 and IRF-1/RelA cells. 0 or 40 hours following Dox induction, rtTA, IRF-1 and IRF-1/RelA cells were left untreated or were treated for 5 hours with dsRNA (25 ug/ml)/cycloheximide (50 ug/ml). Total RNA was prepared and 20 ug was used for Northern blot analysis with a 400 bp SLPI DNA fragment as a probe. As a control of RNA loading, 28S RNA obtained from migration of total RNA on the agarose gel used for Northern blot analysis is presented.

	rtTA				rtTA-IRF-1				rtTA-IRF-1/RelA			
Dox Induction	-	-	+	+	-	-	+	+	-	-	+	+
poly (I:C)/CHX	-	+	-	+	-	+	-	+	-	+	-	+
SLPI mRNA												
28S RNA												



and untreated or treated with dsRNA in the presence of cycloheximide (CHX) and analyzed for SLPI expression by Northern blot analysis (Figure 32). Uninduced or Dox-induced control cells exhibited basal levels of SLPI (Figure 32, lanes 1 and 3) which were significantly increased upon treatment with dsRNA/CHX (Figure 32, lanes 2 and 4). In IRF-1 and IRF-1/RelA cells, basal SLPI levels in the absence (Figure 32, lanes 5 and 9) and particularly in the presence of Dox (Figure 32, lanes 7 and 11) were relatively lower or absent compared to control cells. The minimal basal levels of SLPI in uninduced IRF-1 and IRF-1/RelA cells may be due to very low basal transgene levels normally not detectable by Northern blot. When treated with dsRNA, SLPI levels were elevated in uninduced IRF-1 (Figure 32, lane 6) and IRF-1/RelA cells (Figure 32, lane 10). However, in the presence of Dox, the increase in SLPI mRNA levels following dsRNA treatment of IRF-1 (Figure 32, lane 8) and particularly IRF-1/RelA cells (Figure 32, lane 12) was less dramatic. Taken together, these findings suggest that dsRNA is a strong activator of SLPI expression, and dsRNA-mediated induction of SLPI expression is suppressed by induced IRF-1 or IRF-1/RelA expression.

IFN γ -inducible DNA binding to potential ISRE and NF- κ B sites in the human SLPI promoter. To characterize the role of IRF-1 in the transcriptional regulation of SLPI gene expression, the available sequence of the human SLPI promoter was analyzed for transcription factor consensus sequences (Figure 33A). One ISRE-like site and two NF- κ B-like sites were identified approximately 90 nt upstream of the transcription start site, and two oligonucleotides (BS1 and BS2) were synthesized to be tested for the presence of DNA-binding proteins by EMSA. BS1 (nt -89 to -61) encompasses

the upstream NF- κ B site and the ISRE site and BS2 (nt -78 to -45) encompasses the ISRE and the downstream NF- κ B site.

No binding of recombinant IRF-1 nor IRF-2 was detected on both BS1 and BS2. To examine whether these sites play a role in the regulation of SLPI in response to previously characterized mediators of SLPI expression, NIH3T3 cells were treated with IFN γ and LPS at various times within an 18 hour period and analyzed for DNA binding activity by EMSA. No changes in BS1 and BS2 DNA binding activity were observed in whole cell extracts from LPS-induced cells. Similarly, IFN γ did not induce any changes in BS2 DNA binding (data not shown). However, as shown in Figure 33B, whole cell extracts from IFN γ -induced cells demonstrated interesting BS1 DNA binding kinetics. In uninduced extracts, five DNA binding complexes (I, II, III, IV and V) were detected (Figure 33B, lane 1). IFN γ treatment resulted in increased binding of complexes IV and V and correlative decreased binding of complex III (Figure 33B, lanes 2 to 5). The DNA binding activities of complexes I and II were not affected by IFN γ treatment.

In attempt to characterize the IFN γ -induced BS1 DNA binding activities, supershift and cold DNA competition EMSAs were performed (data not shown). The DNA binding complexes exhibited three characteristics. First, they did not contain IRF-1 or IRF-2, although expected IRF-1 and IRF-2 DNA binding activities to the IRF-specific TH probe were observed. Second, complexes III and IV were competed away in the presence of cold ISRE but not by cold GAS DNA. Third, complexes I and II were competed away in the presence of the NF κ B-specific PRDII DNA. Surprisingly, these complexes were not shifted in the presence of antibodies specific to RelA, p50, or c-Rel.

Figure 33. IFN γ -inducible DNA binding activity to the SLPI promoter. A. Sequence of the human SLPI promoter. Potential NF- κ B and ISRE-like sites as well as the CAAT and TATA boxes are highlighted. The sequence of the BS1 and BS2 oligonucleotides used in EMSA are delineated in black and gray, respectively. Exon 1 of the SLPI gene is shown in italics.

Figure 33 (continued). B. IFN γ -inducible DNA binding activity to BS1. EMSA was performed on whole cell extracts (20 ug) obtained from NIH3T3 cells treated with 200 units/ml of IFN γ (Sigma) for 0 to 18 hours. The ³²P-labeled probe corresponds to the BS1 oligonucleotide derived from the SLPI promoter depicted in (A). Five protein-DNA binding complexes are detected and labelled as I, II, III, IV and V.

IFN γ treatment (hrs) 0 3 5 10 18

V —

IV —

III —

II —

I —



1 2 3 4 5

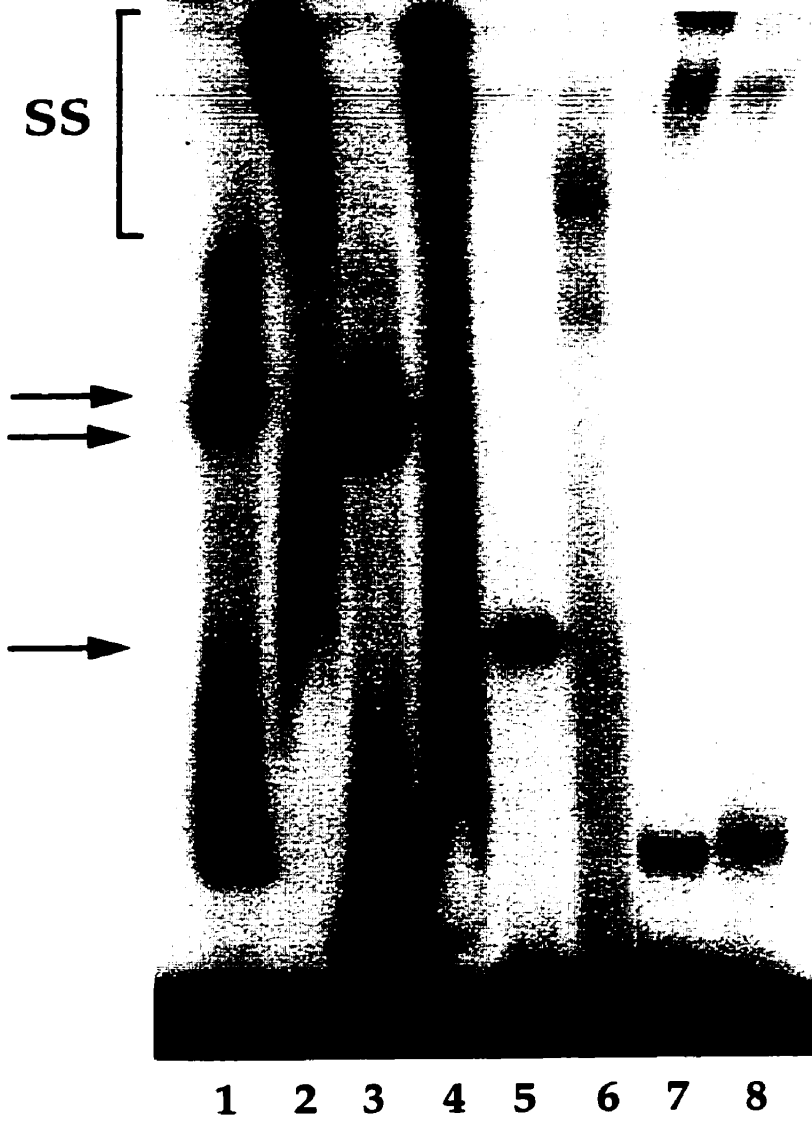
These findings implicate that potential NF- κ B and ISRE sites are present in the SLPI promoter to which IFN γ -inducible complexes bind, and these complexes have yet to be characterized.

Detection of IRF-1 binding activity at two regions of the SLPI promoter, distinct from BS1 and BS2. To further search the SLPI promoter sequence for IRF-1 binding sites, EMSAs were performed with recombinant IRF-1 protein using the entire promoter sequence as a probe (Figure 34). Interestingly, IRF-1 bound to the promoter sequence (Figure 34, lane 1). To isolate the region to which IRF-1 may bind, the promoter was digested with the EcoRI restriction enzyme into two fragments: the 5' 207 nt region (-276 to -69 nt) and the remaining 3' 69 nt region (-69 to +1 nt), which includes 9 nt of the BS1 and the entire BS2 sequence. Strikingly, IRF-1 bound to both fragments of the promoter (Figure 34, lanes 3 and 5). The specificity of the IRF-1 DNA binding complex was confirmed by supershift analysis using an IRF-1 specific antibody (Figure 34, lanes 2, 4 and 6). Expectedly, no IRF-1 DNA binding activity was detected on BS12, a probe consisting of the BS1 and BS2 sites together (-89 to -45 nt); the weak band observed was not shifted in the presence of IRF-1 antibody (Figure 34, lanes 7 and 8). These results demonstrate the presence of at least two IRF-1 binding sites in the SLPI promoter: one site is located within the 5' 207 nt region, and the other site is located within the 3' 45 nt in proximity to the transcriptional start site.

Detection of IRF-1 binding to a -200 region in the SLPI promoter by DNase I footprinting. To further delineate the region(s) in the SLPI promoter where IRF-1 could bind, in vitro footprinting was performed using polyhistidine-tagged recombinant IRF-1 protein and a 5'-radiolabelled SLPI promoter

Figure 34. Detection of IRF-1 DNA binding to the SLPI promoter by mobility shift assays. 25 ng of recombinant IRF-1 protein was incubated with ³²P-labeled probes corresponding to either the entire SLPI promoter (-276 to +1; lanes 1 and 2), the 5' 207 bp of the SLPI promoter (-276 to -69; lanes 3 and 4), the 3' 69 bp of the SLPI promoter (-68 to +1; lanes 5 and 6) or BS12, a combination of the BS1 and BS2 sites (depicted in Figure 33A; -89 to -45; lanes 7 and 8). To confirm specificity of binding, IRF-1 protein was preincubated with 1 ul of anti-IRF-1 antibody #51 (lanes 2, 4, 6 and 8) prior to addition of radiolabelled probe.

SLPI Promoter Region	<u>-276 to +1</u>		<u>-276 to -69</u>		<u>-68 to +1</u>		<u>-89 to -45</u>	
IRF-1 Antibody	-	+	-	+	-	+	-	+



sequence as a probe. A preliminary DNase I footprint is presented in Figure 35. As a DNA ladder, a chemically-synthesized (Maxam-Gilbert) guanine (G)-cytosine (C) sequence of the SLPI probe was used (Figure 35, lane 1). SLPI promoter DNA in the absence of IRF-1 protein displayed a particular DNase I pattern (Figure 35, lane 2). Addition of 10 and 25 ng of IRF-1 (Figure 35, lanes 3 and 4) resulted in DNase I patterns which were indistinguishable from that of naked DNA (Figure 35, lane 2). Interestingly, in the presence of higher amounts of IRF-1 protein, particularly at 100 ng, a region between -200 and -221 nt appears to be protected from DNase I treatment (Figure 35, lanes 5 and 6). Expectedly, the protected sequence is rich in cytosine (C) and thymidine (T) bases, consistent with the affinity of IRF-1 for guanine (G)- and adenine (A)-rich sequences, specifically as stretches of the 5'-GAAA-3' sequence. This finding demonstrates the existence of a potential IRF-1 binding site at a region between -200 and -220 of the SLPI promoter.

Figure 35. Localization of IRF-1 binding to the SLPI promoter by DNase I footprinting. As a DNA ladder (lane 1), an adenine-guanine (A+G) sequence of (+)-sense ^{32}P -end-labeled SLPI promoter DNA was synthesized by the chemical (Maxam-Gilbert) method. In the footprint reactions, (+)-sense ^{32}P -end-labeled SLPI promoter DNA was incubated in the presence of DNA binding buffer and 0 to 100 ng of recombinant IRF-1 protein (lanes 2 to 6), followed by the addition of DNase I. The sequence of the SLPI promoter between -200 and -221 is shown. A DNase I-protected region representing potential IRF-1 binding is depicted on the right.

CHAPTER VII

DISCUSSION

Structure-function analysis of IRF-1. Mutational studies of the IRF-1 protein demonstrate that 1) the transactivation potential of IRF-1 lies primarily C-terminal to aa 200 and, as the length of the protein increases, so does the transactivating function; 2) deletion of IRF-1 to IRF-1(200), IRF-1(170) or IRF-1(150) respectively transforms IRF-1 from an activator into a repressor; and 3) the IRF-1(120) deletion mutant does not bind DNA and has no repressive effect on gene activity. Two regions may contribute to transactivation. A stretch of five consecutive acidic amino acids (Asp-Glu-Asp-Glu-Glu) from aa 226 to 230 is present only in the full length IRF-1 protein as well as in the IRF-1 (250) and IRF-1 (300) deletion mutants, and is not found in the transcriptional repressor IRF-2. Furthermore, this amino acid sequence is also found in the transactivation domains of the NF- κ B RelA(p65) and GAL4 proteins (124,140). Another potentially important acidic region in IRF-1 (Glu-Glu-Pro-Glu-Ile-Asp) is represented by aa 276 to 281 and is also present only in the full length IRF-1 and IRF-1 (300) proteins. These acidic residues may play an important role in IRF-1 transactivation.

In addition to an intact C-terminus, virus- or stimulator-induced IRF-1 activation requires posttranslational modification in addition to increased IRF-1 protein synthesis (217). Phosphorylation is required for IRF-1 activity, since DNA binding is inhibited by treatment with calf intestinal phosphatase (CIP) (159). The posttranslational events affecting IRF-1 may be due in part to phosphorylation by casein kinase II (CKII), a serine/threonine protein kinase involved in the phosphorylation of over 50 proteins including transcription factors and cell growth regulators (160). Recombinant CKII phosphorylates IRF-1 *in vitro* and is shown by far western analysis of protein-protein interactions to physically interact with

IRF-1 (119). Deletion mutation analyses reveal that IRF-1 is phosphorylated on multiple sites by CKII, including a cluster in the DBD (aa 138 to 150) and the transactivation domain (aa 219 to 231). Cotransfection studies comparing wild-type and point-mutated forms of IRF-1 demonstrate that mutations of the four phosphoacceptor residues in the C-terminal transactivation domain, but not the N-terminal cluster, significantly decreases transcription by IRF-1 (119).

Interestingly, IRF-1 proteins lacking the transactivation domain but maintaining an intact DBD convert the IRF-1 activator into a repressor; IRF-1(150), (170) and (200) display a stepwise reduction in CAT gene expression, with the IRF-1(200) deletion mutant having maximum repression capability. This phenomenon is also observed for some IRF repressors, namely IRF-2 (Chapter III), ICSBP (201) and IRF-4 (49). Repression by these DBD mutants probably occurs by a dominant negative mechanism by which the protein binds target IRF sites and prevents formation of an active transcription complex with full length IRF-1 protein. Harada *et al.* also demonstrated a repressive effect with a truncated form of IRF-1 containing 188 N-terminal amino acids (72).

While IRF-1 (150) binds strongly to DNA, the IRF-2 (120) protein is a nonfunctional protein which does not bind DNA. This result localizes the DBD within the first 100-150 aa. Interestingly, the amino acids between 120 and 150 in IRF-1 are rich in basic residues present in the DNA binding region of other proteins (138). The lack of these basic amino acid residues in the IRF-1 (120) deletion mutant may contribute to its inability to bind DNA.

Structure-function analysis of IRF-2. Similar mutational studies on IRF-2 reveal that the repressive capacity of IRF-2 is maintained with an IRF-2 protein containing the N-terminal 125 amino acids but is lost with an IRF-2 100 amino acid polypeptide; similarly, repression correlates with DNA binding capacity. IRF-2(125) is notable in its compromised ability to repress IFN gene activity while retaining DNA binding. These findings indicate that the C-terminal region is not required for the repressive function of IRF-2, and repressor activity appears to be an intrinsic property of the IRF-2 N-terminal region. Uegaki *et al.* produced a truncated version of IRF-2 by α -chymotrypsin digestion that contains 113 N-terminal amino acids and has a molecular weight of about 14 kDa. This IRF-2 protein binds DNA although its biological activity with regard to transcriptional repression was not assessed (204).

An independent deletion analysis mapping functional domains of IRF-2 present contradictory findings (228). In this study, IRF-2 repression is localized to the protein's C-terminal 59 aa; fusion of this region to the C-terminal end of IRF-1 inhibits transactivation. Furthermore, a latent activation domain is found in the central region of IRF-2, between aa 160 to 220, which is considered to be "silenced" by the C-terminal repression domain. These results implicate IRF-2 as a "mosaic" transcription factor possessing both activator and repressor activities (228). Surprisingly, our studies produce contrasting findings. IRF-2 deletion mutants containing either the N-terminal 200 or 240 aa do not exhibit transactivation; furthermore, the C-terminal end of IRF-2 is not required for transcriptional repression.

IRF-2 repression dominates IRF-1 activation. Full length IRF-2 or different C-terminal deletions down to IRF-2 (160) are able to repress expression induced by Sendai virus, IRF-1 or the strong IRF/RelA fusion proteins. Therefore, the transcriptional repression phenotype appears to be dominant over the transcriptional activation phenotype. Previous studies have demonstrated that the half-life of IRF-2 is approximately 8 hours as compared to 30 minutes for IRF-1 (217). Also, as judged from scatchard plot analysis, IRF-2 appears to have a 5-fold higher affinity for the Th sequence than IRF-1 (72). These properties may also contribute to the dominant repressive nature of IRF-2 over IRF-1. Together, these findings suggest that in uninduced cells, IRF-2 masks the PRDI/PRDIII DNA binding domains. The transient increase in the amount of IRF-1 or IRF-1-related proteins after virus induction may compete for the binding to PRDI/PRDIII; other IFN- β domains, such as PRDII and PRDIV also contribute to the synergistic activation of the IFN- β promoter (46,54,62,72,109,126).

IRF-1/RelA and IRF-2/RelA mimic IRF-1 transactivation function. As mentioned previously, the NF- κ B subunit RelA(p65) and the yeast GAL4 transcriptional proteins, like IRF-1, contain consecutive acidic residues in their transcriptionally active domains (124,140). As demonstrated in this study, the activation domain of RelA can contribute to transactivation in IRF-1/RelA and IRF-2/RelA fusion proteins. IRF-1/RelA and IRF-2/RelA fusion proteins act as strong transcriptional activators which can nonetheless be inhibited by IRF-2 mediated repression. Interestingly, the IRF-2/RelA fusion protein appears to bypass the requirement for the synergistic activation of the IFN- β promoter (60) and is able to strongly stimulate promoter activity, probably due to the stronger IRF-2 DNA binding affinity (72).

Localization of IRF-2 oncogenic activity. NIH3T3 cells overexpressing IRF-2 proteins of at least 160 aa induce malignant transformation as measured by increased saturation density, growth in soft agar and tumorigenicity in nude mice. Interestingly, the IRF-2 160 aa protein displays more potent oncogenic properties than the wild-type protein, as indicated by a faster growth rate, larger soft agar colonies and a rapid induction of tumor formation. Furthermore, cells expressing the 125 aa IRF-2 protein behave as control cells with regard to tumor formation and saturation density but display anchorage-independent growth. These results directly correlate transforming phenotype with DNA binding and transcriptional repression ability of IRF-2, since 1) the 160 aa protein binds DNA more efficiently (222) and represses transcription at least as strongly than the wild-type proteins ((222) and Chapters III and IV); and 2) as demonstrated in Chapter III, the 125 aa protein possesses the minimal DNA binding domain and represses transcription weakly compared to wild-type IRF-2. The 125 aa IRF-2 protein, although able to bind DNA, appears to exert its repressive function only to a limited extent, resulting in minimal changes in growth phenotype but not in tumorigenesis.

It is striking that IRF-2 may exert its transforming activities by binding to DNA. Such a phenomenon suggests that IRF-2 could exert its transforming phenotype by a dominant negative mechanism as characterized for several other oncogenic transcription factors. This model is consistent with the idea that in uninduced cells, IRF-2 exerts its repressive effects by engaging the IRF-E recognition site and occluding DNA binding by IRF-1 protein or other regulatory proteins. It was shown in Chapter IV that IRF-2 is able to efficiently compete with IRF-1 for the PRDI site *in vitro*. This observation is supported by the higher affinity of IRF-2 for the Th sequence than IRF-1 (72),

the longer half-life of IRF-2 compared to IRF-1 (217), and the dominance of IRF-2 transcriptional repression phenotype over IRF-1 transcriptional activation phenotype discussed earlier. Therefore, IRF-2 overexpression may give rise to constitutive occlusion of the IRF target site and prevention of IRF-1 DNA binding. As a result, IRF-1 may be unable to exert activities related to its antioncogenic potential. These findings support the proposed notion that changes in the relative balance between IRF-1 and IRF-2 proteins may predispose to cellular transformation (73).

IRF-2 regulation of dsRNA and Sendai virus mediated IFN gene activation. IRF-2 expression represses IFN- β inducibility by dsRNA in the NIH3T3 cells, whereas induction of IFN- β by Sendai virus is unaffected by IRF-2. Levels of Type I IFN mRNA are decreased after dsRNA induction but not after virus infection in IRF-1^{-/-} mice and are increased following dsRNA induction in IRF-2^{-/-} mice (129). These results support the concept that multiple pathways are involved in virus-mediated induction of IFN- β transcription and a dsRNA dependent mechanism represents one of these pathways.

In response to dsRNA or viral induction, the 50 kD IRF-2 protein which is identical to the DNA binding activity PRDI-BFc (153) is proteolytically processed into a smaller, 24-27 kDa protein comprising the 160 aa DBD of IRF-2, independently termed PRDI-BFi (153), TH3 (34) or In4 (222). The ability of PRDI-BFi to function as a repressor in co-transfection experiments is significantly less than that of full length IRF-2 protein (153). However, in two other independent studies, TH3 and In4 bind DNA and repress transcription more efficiently than full length IRF-2 protein (120,222). The physiological role for this inducer-mediated IRF-2 posttranslational modification is not

clear. Since the induction kinetics of TH3 are slower than that of IFN- β in response to dsRNA or viral infection (34,222), the IRF-2 cleavage product may be a post-induction repressor of IFN- β gene expression (222).

What is the nature of the IRF-1/IRF-2 regulated genes critical for 3T3 cell transformation? The differential inducibility of IFN- β by dsRNA in IRF-2 expressing cells suggests that one potential target for IRF-2 is the double stranded RNA dependent protein kinase (PKR). It was demonstrated in Chapter V that IRF-1 plays a role in the regulation of PKR; this potential IRF target will be discussed in the following section.

Control of cell growth and expression of growth regulatory genes by IRF-1 and IRF/RelA. To characterize IRF-1 tumor suppressor activity, IRF-1 expressing cell lines were generated with the tetracycline-inducible expression system to minimize basal expression and maximize transgene inducibility following doxycycline addition (63,64,179). Using these cell models, it was demonstrated in Chapter V that inducible IRF-1 expression correlates with: 1) cell growth arrest and apoptosis; 2) inducible expression of PKR protein; 3) increased STAT1(p91) gene expression and enhanced ISGF3 binding; and 4) constitutively increased p21(WAF1) cyclin-dependent kinase (CDK) inhibitor levels. In addition, we showed that the IRF-1/RelA and IRF-2/RelA fusion proteins mimic IRF-1 in terms of cell growth inhibition, induction of apoptosis and gene activation. Since they exhibit similar effects, the use of the IRF/RelA fusion genes strengthens the results of the IRF-1 studies and imply that the phenotypic changes observed may result from affecting transcription of downstream genes which are regulated by IRF-1/IRF-2 sites.

IRF-1 plays a role in apoptosis in response to DNA damage (189,192). From the present study, IRF-1 also induces apoptosis during serum starvation. The pleiotropic nature of IRF-1 correlates with its role in physiological processes which involve apoptosis such as T-cell selection and maturation. Mice deficient in the IRF-1 gene, while having normal numbers of immature CD4⁻CD8⁺ and CD4⁺CD8⁻ thymocytes, are 90% deficient in mature CD4⁻CD8⁺ T-cells in the thymus (129), suggesting impairment of CD8⁺ cell maturation in the IRF-1 knockout mice.

IRF-1 regulation of PKR expression. Like the IRF proteins, p68 kinase (PKR), a double-stranded RNA activated serine-threonine kinase, is an IFN-inducible gene which plays an important role in the regulation of cell proliferation. Expression of wild-type PKR in yeast inhibits cell growth and correlates with phosphorylation of eIF-2 α (32). Expression of catalytically inactive mutants of PKR encoding proteins lacking eIF-2 kinase activity results in malignant transformation and tumor formation in nude mice (105,136). These results serve as the basis of the hypothesis that wild-type PKR is a tumor suppressor gene product whose activity can be inhibited by the presence of catalytically inactive (dominant negative) PKR mutants. Interestingly, by analogy with IRF-1, the human PKR gene is located to chromosome region 2p21-22 (14,71,183), and abnormalities involving this region are observed among patients with acute myelogenous leukemia, raising the possibility of a PKR role in leukemogenesis. Furthermore, the PKR promoter contains potential IRF binding sites (191). As shown previously (102), we demonstrated that inducible IRF-1 expression results in upregulation of PKR protein levels. IRF-1 expression also results in a slight augmentation of PKR kinase activity (data not shown), suggesting that IRF-1 may regulate PKR gene expression rather

than PKR activity. This finding demonstrates that inhibition of cell growth by IFN-inducible proteins such as IRF-1 may be due to regulation of other IFN induced proteins with anti-growth activities such as PKR.

IRF-1 regulation of STAT1(p91) expression. Most interesting was the observation that inducible IRF-1 expression results in a dramatic increase in STAT1(p91) levels. Furthermore, a percentage of the induced STAT1 is functional, since it binds to an ISRE DNA element. The latter result has several implications: 1) at least a portion of the induced STAT1 is phosphorylated, since phosphorylation is necessary for STAT1 DNA binding; 2) some active or phosphorylated STAT2 must also be present, since the ISGF3 complex requires active STAT1 and STAT2 as well as the ISGF3 γ (p48) member of the IRF family. However, STAT1 and STAT2 phosphorylation and DNA binding normally only occurs upon IFN- α/β induction (79,174,181). It would be of relevance to see whether the induced STAT1 is sufficient to initiate activation of itself, as well as STAT2. Also interesting was the observation that although IFN stimulation of Dox-induced rtTA-IRF-1 and rtTA-IRF/RelA cells results in enhanced ISGF3 binding, DNA binding activity was not relatively higher than levels obtained in IFN-stimulated control cells, despite higher STAT1 protein levels. This phenomenon may be due to the constitutive activation/inactivation cycle of the STAT proteins (79,180), such that only a certain percentage of STAT protein is activated and binds DNA at any given time.

STAT1 has been considered a gene acting upstream of IRF-1 and regulating expression of the IRF-1 promoter (158). The present work suggests that IRF-1 itself, or an IRF-1 induced gene, regulates STAT1 expression at the

transcriptional level. It is possible that following IRF-1 upregulation in response to IFN induction through STAT1, the newly synthesized IRF-1 may in turn activate expression of STAT1, resulting in positive feedback regulation of IRF-1 expression. Such a mechanism could positively autoregulate IFN-mediated activities. It will be interesting to examine whether IRF-1 also regulates other members of the JAK-STAT pathway.

Previously, it has been shown that overexpression of IRF-1 by cDNA transfection results in the "forced" induction of IFN- α/β in COS cells (55). Furthermore, in addition to their well-characterized antiproliferative activities, a potential role of IFNs in the transcriptional regulation of STAT1 has been recently demonstrated (113). Therefore, it is conceivable that the cell growth inhibition and upregulation of PKR, STAT1 and ISGF3 observed in the IRF-1 and IRF/RelA inducible cell lines may be mediated indirectly through IRF-1- or IRF/RelA-induced IFN α/β . However, although endogenous IFN- β gene expression is dramatically induced in dsRNA/cycloheximide - treated control rtTA cells, no IFN- β mRNA is detected by Northern and RT-PCR analysis in Dox-induced IRF-1 and IRF/p65 cells (data not shown). This finding suggests that although the potential role of other members of the IFN family cannot be ruled out, IRF-1-mediated STAT1 upregulation is independent of IFN- β .

IRF-1 regulation of WAF1(p21) expression. STAT1 has been shown to activate transcription of the p21 (WAF1, CIP1) CDK inhibitor in response to induction by IFN γ or EGF (epidermal growth factor), resulting in cell growth inhibition (30). We hypothesized that the tumor suppressor activity associated with IRF-1 in our inducible cell lines may be due to WAF1

activation by IRF-1-induced STAT1. If so, IRF-1 would potentially upregulate WAF1 by two mechanisms: (i) indirectly through activation of STAT1 expression; and (ii) either directly or indirectly, perhaps in cooperation with other proteins. The elevated WAF1 levels observed in the IRF-1 and IRF-1/RelA cells are constitutive, not inducible. Distinct STAT1 and WAF1 expression patterns in the rtTA-IRF-1 and rtTA-IRF-1/RelA cells, as well as the absence of WAF-1 despite STAT1 induction in the rtTA-IRF-2/RelA cells, suggest that IRF-1 activation of WAF-1 is independent of STAT1. Interestingly, transient cotransfection assays from an independent group demonstrate that IRF-1 and the tumor suppressor p53 cooperatively upregulate gene expression of WAF1, implicating the involvement of cell cycle proteins in IRF-1-mediated cell growth regulation (152).

Why is WAF-1 not expressed in the rtTA-IRF-2/RelA cells? Since the major difference between the IRF-1, IRF-1/RelA and IRF-2/RelA protein structures is the IRF-2 DNA binding domain in IRF-2/RelA, we hypothesized that the inability of IRF-2/RelA to induce WAF-1 expression is perhaps due to the inability of IRF-2/RelA to recognize potential "IRF-like" recognition sites present in the WAF-1 promoter. Analysis of the WAF-1 promoter do not reveal any IRF DNA recognition sites (IRF-E), although three potential GAS consensus (5'-TTCNNGAA-3') sequences were identified: 1) 5'-CTTCCCGG AAG-3'; 2) 5'-TTTCTGAGAAAT-3'; and 3) 5'-CTTCTTGGAAAAT-3', present at -640, -2540, and -4183 nucleotides, respectively, from the mRNA start site. Induced extracts from the cell lines as well as recombinant IRF-1 and IRF-2 proteins were tested for DNA binding using the GAS element of the IFN γ -inducible IFP-53 gene (5'-GATCCAGATTCTCAGAAA-3'); however no distinct GAS binding is observed in any of the cell lines or with

recombinant IRF-1 and IRF-2 (data not shown). It is therefore probable that WAF1 activation by IRF-1 and IRF/RelA occurs by an indirect mechanism.

Other IRF-1-regulated genes may be involved in mediating IRF-1 tumor suppressor activity. Splenocytes from IRF-1^{-/-} knockout mice are also deficient in the IL-1 β converting enzyme (ICE), a mammalian homologue of the *Caenorhabditis elegans* cell death gene *ced-3*; ectopic overexpression of IRF-1 results in induction of ICE mRNA expression and enhancement of radiation-induced apoptosis (189). Furthermore, using the method of differential display, lysyl oxidase was identified as another IRF-1 target gene which may play a potential role in IRF-1 tumorigenicity (190). Lysyl oxidase is commonly known for its involvement in the integrity of various cytoskeletal components. However, its localization in the mouse *ras* recision gene (*rrg*) and implication in the reversion of *ras*-transformed NIH3T3 cells (36,70) makes this enzyme an interesting IRF-1-regulated gene which may exert IRF-1-mediated antioncogenic activities.

Wong *et al.* demonstrated that PKR physically associates with STAT1, although PKR does not phosphorylate STAT1. Rather, PKR association inhibits STAT DNA binding and transactivation. Interestingly, the PKR-STAT1 interaction is disrupted in response to induction by IFN or dsRNA (225). How does this observation correlate with the present study which demonstrates upregulation of both PKR and STAT1 by IRF-1? It is conceivable that IRF-1-mediated effects may involve STAT1 activity which could be alleviated by PKR association with STAT1. It will be important to investigate the potential role of STAT1/PKR interactions in IRF-1-mediated cell growth regulation.

SLPI, a novel IRF-1-regulated gene. In Chapter VI, the tetracycline inducible system and the method of RNA fingerprinting were exploited, resulting in the identification of the secretory leukocyte protease inhibitor (SLPI) as a novel IRF-1-regulated gene. Although SLPI appears to be repressed in the presence of IRF-1/RelA from the initial RNA fingerprint, detailed kinetics of SLPI mRNA expression reveal an initial induction of SLPI early following Dox treatment of IRF-1/RelA cells which is then suppressed at later time period, when peak IRF-1/RelA levels are attained. These results implicate a dual function to IRF-1, consisting of both the activation and repression of SLPI expression.

The kinetics of SLPI mRNA expression in itself may reveal a possible autoregulatory feedback mechanism of IRF-1/SLPI regulation. It is possible that induced IRF-1 expression activates SLPI production until SLPI levels reaches a maximum threshold, which then serves as a signal to "turn off" the SLPI gene. It would be of interest to see whether overexpression of SLPI results in induction of IRF-1.

SLPI is a secreted protein belonging to the family of α -1 antitrypsin antiproteases. This nonglycosylated 11.7 kDa enzyme is produced by epithelial cells and which resides in various secretory fluids such as parotid secretions, bronchial, nasal and cervical mucus, and seminal fluid (199). SLPI plays a primary role in the regulation of neutrophil-mediated inflammation through proteolysis and subsequent inhibition of the serine leukocyte proteases, which include the neutrophil proteases (cathepsin G and elastase) and the pancreatic proteases (trypsin and chymotrypsin) (199). Because of its potent antiprotease activity, SLPI serves as a potential therapeutic agent for

the treatment of proteolytic tissue damage seen in degenerative and inflammatory diseases such as cystic fibrosis, allergic rhinitis and asthma ((110); reviewed in (213)). Interestingly, several studies have also implicated SLPI as an anti-HIV-1 agent, as it can block HIV-1 infectivity in monocytes (131,132,214). The predominance of SLPI and SLPI-mediated antiviral activity in human saliva has led to the suggestion that SLPI may be the factor responsible for the low frequency of oral HIV-1 transmission (131).

Up until recently, SLPI was analyzed in terms of its structural properties and antiprotease activity. However, a novel function was assigned to SLPI with its characterization by the Nathan group as a macrophage derived, LPS induced, LPS inhibitor (90). SLPI in this context was identified by differential display as a gene overexpressed in a macrophage cell line from C3H/HeJ mice which are hyporesponsive to LPS (*Lps^d* mice). Although activated by LPS in wild-type macrophages and neutrophils, SLPI antagonizes the LPS response when overexpressed in macrophages. Specifically, SLPI expression inhibits LPS-mediated activation of NF- κ B and suppresses production of nitric oxide and TNF α . Interestingly, IFN γ treatment of *LPS^d* cells reverses the LPS hyporesponsive phenotype and this correction correlates with the ability of IFN γ to suppress SLPI expression at the mRNA level (90).

In addition to LPS, TNF and PMA are other inducers of SLPI expression (90). From our studies, SLPI expression was also found to be dramatically induced in response to dsRNA. It would be of interest to see whether this induction is mediated through dsRNA activated PKR. Inducibility of SLPI expression by dsRNA also implicates the possibility of SLPI regulation by virus

infection. Whether SLPI participates in common or divergent pathways activated in response to bacterial (LPS) and viral (dsRNA) infection is a subject to be addressed in future studies.

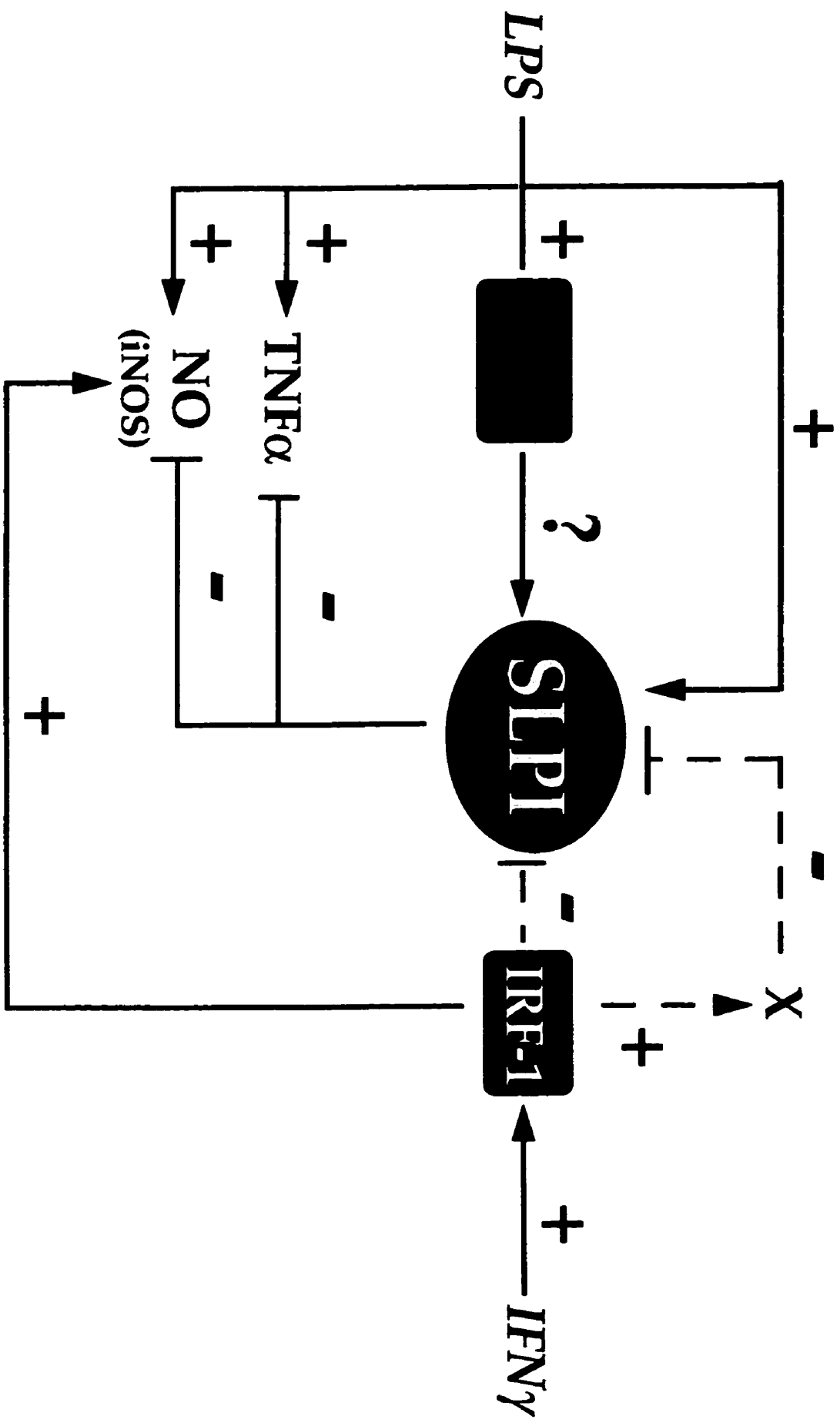
Barber *et al.* performed studies comparing mRNA levels of IRF-1, IRF-2 and ICSBP in LPS responsive (LPS^n) and hyporesponsive (LPS^d) macrophages (15). Basal levels of IRF-1 were 15-fold greater than those of IRF-2 in LPS^n cells; in contrast, IRF-2 was predominantly expressed in LPS hyporesponsive cells. Although there was a dose dependent increase in the three IRF proteins in LPS^n cells upon LPS treatment, no accumulation of IRF transcripts in response to LPS was observed in LPS^d cells. Interestingly, treatment of LPS^n cells with LPS in the presence of cycloheximide resulted in the increase of only IRF-1. Taken together, these studies suggest that IRF-1 is an immediate early, LPS inducible gene which plays a potential role in the regulation of the LPS response (15).

Studies in macrophages from IRF knockout mice reveal an essential role for IRF-1 in the transcriptional induction of the nitric oxide synthase gene (iNOS) in macrophages (92). Macrophages from IRF-1 deficient mice produce little or no nitric oxide and synthesize low levels of iNOS mRNA in response to IFN γ stimulation. The role of IRF-1 in the IFN- γ induced activation of iNOS expression is further supported by the presence of two adjacent IRF-1 response elements in the iNOS promoter (92,127). These findings are consistent with the role of IRF-1 in repressing the expression of SLPI, which inhibits nitric oxide production.

Consistent with the role of IFN γ and IRF-1 in SLPI regulation is the existence of two regions identified in the SLPI promoter to which IFN γ stimulated and IRF-1 DNA binding complexes are detected. A subject of future investigation would be to analyze the effects of these regions in reporter gene assays in response to LPS, IFN γ , IRF-1, dsRNA and viral infection.

Model for regulation of SLPI expression. Based on what is known about SLPI and the data presented in Chapter VI, the following proposed model regarding the regulation of SLPI by IRF-1 is currently being investigated (Figure 36). Response to LPS involves the induction of expression of TNF α and nitric oxide as well as the activation of the NF- κ B family of transcription factors. LPS also activates expression of SLPI (90). It is of interest to find whether NF- κ B mediates LPS-induced activation of SLPI expression, or whether NF- κ B regulates the LPS response by suppressing SLPI expression. In contrast to LPS, IFN γ represses SLPI expression (90). Since IRF-1 is an IFN γ -inducible gene (57), and overexpression of IRF-1 results in repression of SLPI expression (Chapter VI), IRF-1 serves an ideal potential mediator of IFN γ -induced SLPI suppression. IRF-1 could function in a direct manner, as suggested by the results presented in Chapter VI, by binding to SLPI promoter sequences and repressing transcription of the SLPI gene, in which case IRF-1 would be assigned a novel function very different from its common activator role. In contrast, IRF-1 can also function by an indirect mechanism through activation of a factor "X" which then binds directly to the SLPI promoter and repress its transcription.

Figure 36. Model for the regulation of SLPI expression. "-", repression; "+", activation. Response to LPS involves the induction of expression of TNF α and nitric oxide as well as the activation of the NF- κ B transcription factors. LPS also activates expression of SLPI. NF- κ B may mediate LPS-induced activation of SLPI expression or regulate the LPS response by suppressing SLPI expression. In contrast to LPS, IFN γ represses SLPI expression. Since IRF-1 is an IFN γ -inducible gene, and overexpression of IRF-1 results in repression of SLPI expression, IRF-1 serves an ideal potential mediator of IFN γ -induced SLPI suppression. IRF-1 could function in a direct manner by binding to SLPI promoter sequences and repressing transcription of the SLPI gene. In contrast, IRF-1 can also function by an indirect mechanism by activating expression of a factor "X" which would then bind directly to the SLPI promoter and repress its transcription.



CONTRIBUTIONS TO ORIGINAL KNOWLEDGE

The present studies investigating the effects of IRF-1 and IRF-2 on cell growth and gene expression have contributed to a better understanding of the mechanisms of IRF-2 oncogenicity and IRF-1 tumor suppressor activity and have led to the identification of a novel IRF-1 gene target. The candidate's major contributions to original knowledge are listed below:

1. Analysis of C-terminal IRF-2 deletion mutants demonstrate that IRF-2 oncogenic activity maps to its N-terminal DNA binding/transcriptional repression domain. Mutants maintaining functional DNA binding and repressive activity also affect IFN- β gene expression in response to dsRNA, demonstrating a direct correlation between IRF-2 transcriptional repression of gene expression and transformation. Binding studies illustrate that IRF-2 oncogenesis may occur by a dominant negative mechanism, through constitutive engagement of IRF consensus sites and subsequent prevention of IRF-1 tumor suppressor activity.

2. Examination of inducible IRF-1 expression shows a direct correlation between transactivation function and tumor suppressor activity of IRF-1. Specifically, IRF-1 upregulates the expression of STAT1(p91) with kinetics comparable to that of IRF-1 mediated cell growth arrest and apoptosis, implicating the JAK-STAT pathway as a novel target of IRF-1 tumor suppressor activity.

3. For the analysis of IRF-1 tumor suppressor activity, tetracycline-responsive cell lines inducibly expressing IRF-1 and the IRF-1-like IRF/RelA proteins were established. The components of tetracycline-responsive system were modified by the candidate to minimize basal transgene expression and maximize inducibility of expression.

4. Using the method of RNA fingerprinting, the secretory leukocyte protease inhibitor (SLPI) was identified as the first example of an IRF-1-repressed gene. Analysis of the SLPI promoter reveals two regions bound by IRF-1 and IFN γ -induced proteins. These studies open a new avenue of research investigating mechanisms of IRF-1 repression. Furthermore, the function of SLPI as an antiprotease and anti-HIV-1 agent implicates a novel role for IRF-1 in the modulation of inflammatory and antiretroviral responses.

REFERENCES

1. 1989. DNA sequencing. In *Molecular cloning: a laboratory manual*. J. Sambrook, E. F. Fritsch, and T. Maniatis, editors. Cold Spring Harbor Laboratory Press, Plainview, New York. 13.78-13.95.
2. 1994. Differential display of mRNA by PCR. In *Current Protocols in Molecular Biology*. F. M. Ausubel, R. Brent, R. E. Kingston, D. D. Moore, J. G. Seidman, J. A. Smith, and K. Struhl, editors. Greene Publishing Associates, Inc., Brooklyn, New York. 15.8.5-15.8.6.
3. **Abdollahi, A., K. A. Lord, B. Hoffman-Liebermann, and D. A. Liebermann.** 1991. Interferon regulatory factor 1 is a myeloid differentiation primary response gene induced by interleukin-6 and leukemia inhibitory factor: role in growth inhibition. *Cell Growth Differ.* 2:401-407.
4. **Algarté, M., H. Nguyen, R. Lin, and J. Hiscott.** 1998. Differential regulation of interferon- β transcription by I κ B α and I κ B β . *Oncogene* (manuscript in preparation)
5. **Alkalay, I., A. Yaron, A. Hatzubai, S. Jung, A. Avraham, O. Gerlitz, I. Pashut-Lavon, and Y. Ben-Neriah.** 1995. *In vivo* stimulation of I κ B phosphorylation is not sufficient to activate NF- κ B. *Mol. Cell. Biol.* 15:1294-1301.
6. **Alkalay, I., A. Yaron, A. Hatzubai, A. Orian, A. Ciechanover, and Y. Ben-Neriah.** 1995. Stimulation-dependent I κ B α phosphorylation marks the NF- κ B inhibitor for degradation *via* the ubiquitin-proteasome pathway. *Proc. Natl. Acad. Sci. USA* 92:10599-10603.
7. **Allan, G. and K. Fantes.** 1980. A family of structural genes for human lymphoblastoid (leukocyte-type) interferon. *Nature* 287:408-411.
8. **Arenzana-Seisdedos, F., P. Turpin, M. Rodriguez, D. Thomas, R. T. Hay, J-L. Virelizier, and C. Dargemont.** 1997. Nuclear localization of I κ B α promotes active transport of NF- κ B from the nucleus to the cytoplasm. *J. Cell Sci.* 110:369-378.
9. **Au, W. -C., P. A. Moore, W. Lowther, Y. -T. Juang, and P. M. Pitha.** 1995. Identification of a member of the interferon regulatory factor family that binds to the interferon-stimulated response element and activates expression of interferon-induced genes. *Proc. Natl. Acad. Sci. USA* 92:11657-11661.

10. **Au, W. -C., N. B. Raj, R. Pine, and P. M. Pitha.** 1992. Distinct activation of murine interferon α promoter region by IRF-1/ISGF-2 and virus infection. *Nucl. Acid Res.* **20**:2877-2884.
11. **Au, W. C., Y. Su, N. K. B. Raj, and P. M. Pitha.** 1993. Virus-mediated induction of interferon A gene requires cooperation between multiple binding factors in the interferon alpha promoter region. *J. Biol. Chem.* **268**:24032-24040.
12. **Baeuerle, P. A.** 1991. The inducible transcription activator NF- κ B: regulation by distinct protein subunits. *Biochim. Biophys. Acta.* **1072**:63-80.
13. **Baeuerle, P. A. and T. Henkel.** 1994. Function and activation of NF- κ B in the immune system. *Annu. Rev. Immunol.* **12**:141-179.
14. **Barber, G. N., S. Edelhoff, M. G. Katze, and C. M. Disteche.** 1993. Chromosomal assignment of the interferon-inducible double-stranded RNA-dependent protein kinase (PKR) to human chromosome 2p21-2p22 and mouse chromosome 17 E2. *Genomics* **16**:765-767.
15. **Barber, S. A., M. J. Fultz, C. A. Salkowski, and S. N Vogel.** 1995. Differential expression of interferon regulatory factor 1 (IRF-1), IRF-2 and interferon consensus binding protein genes in lipopolysaccharide (LPS)-responsive and LPS-hyporesponsive macrophages. *Infect. Immun.* **63**:601-608.
16. **Beg, A. A. and S. Baldwin, Jr.** 1993. The I κ B proteins: multifunctional regulators of Rel/NF- κ B transcription factors. *Genes Dev.* **7**:2064-2070.
17. **Beg, A. A., T. S. Finco, P. V. Nantermet, and A. S. Baldwin, Jr..** 1993. Tumor necrosis factor and interleukin-1 lead to phosphorylation and loss of I κ B α : a mechanism for NF- κ B activation. *Mol. Cell Biol.* **13**:3301-3310.
18. **Beg, A. A., S. M. Ruben, R. I. Scheinman, S. Haskill, C. A. Rosen, and A. S. Baldwin, Jr.** 1992. I κ B interacts with the nuclear localization sequence of the subunits of NF- κ B: a mechanism for cytoplasmic retention. *Genes Dev.* **6**:1899-1913.
19. **Bluyssen, H. A. R., J. E. Durbin, and D. E. Levy.** 1996. ISGF3 γ p48, a specificity switch for interferon activated transcription factors. *Cyt. Growth Fact. Rev.* **7**:11-17.
20. **Bours, V., P. R. Burd, K. Brown, J. Villalobos, S. Park, R. -P. Ryseck, R. Bravo, K. Kelly, and U. Siebenlist.** 1992. A novel mitogen-inducible

gene product related to p50/p105-NF- κ B participates in transactivation through a κ B site. *Mol. Cell Biol.* **12**:685-695.

21. **Bovolenta, C., P. H. Driggers, M. S. Marks, J. A. Medin, A. D. Politis, S. N. Vogel, D. E. Levy, K. Sakaguchi, E. Appella, J. E. Coligan, and K. Ozato.** 1994. Molecular interactions between interferon consensus sequence binding protein and members of the interferon regulatory factor family. *Proc. Natl. Acad. Sci. USA* **91**:5046-5050.
22. **Bragança, J., P. Génin, M. -T. Bandu, N. Darracq, M. Vignal, C. Cassé, J. Doly, and A. Civas.** 1997. Synergism between multiple virus-induced-factor-binding elements involved in the differential expression of IFN- α genes. *J. Biol. Chem.* **272**:22154-22162.
23. **Brass, A. L., E. Kehrli, C. F. Eisenbeis, U. Storb, and H. Singh.** 1996. Pip, a lymphoid-restricted IRF, contains a regulatory domain that is important for autoinhibition and ternary complex formation with the Ets factor PU.1. *Genes Dev.* **10**:2335-2347.
24. **Brown, K., S. Park, T. Kanno, G. Franzoso, and U. Siebenlist.** 1993. Mutual regulation of the transcriptional activator NF- κ B and its inhibitor, I κ B α . *Proc. Natl. Acad. Sci. USA* **90**:2532-2536.
25. **Brownell, D., N. Mittereder, and N. R. Rice.** 1989. A human *rel* proto-oncogene cDNA can containing an Alu fragment as a potential coding exon. *Oncogene* **4**:935-942.
26. **Bustin, M., D. A. Lehn, and D. Landsman.** 1990. Structural features of the HMG chromosomal proteins and their genes. *Biochim. et Biophys. Acta* **1049**:231-243.
27. **Cha, Y. and A. B. Deisseroth.** 1994. Human interferon regulatory factor 2 gene. *J. Biol. Chem.* **269**:5279-5287.
28. **Chen, Z., J. Hagler, V. J. Palombella, F. Melandri, D. Scherer, D. Ballard, and T. Maniatis.** 1995. Signal-induced site-specific phosphorylation targets I κ B α to the ubiquitin-proteasome pathway. *Genes Dev.* **9**:1586-1597.
29. **Chen, Z. J., L. Parent, and T. Maniatis.** 1996. Site-specific phosphorylation of I κ B α by a novel ubiquitination-dependent protein kinase activity. *Cell* **84**:853-862.

30. **Chin, Y. E., M. Kitagawa, W. -C. S. Su, Z. -H. You, Y. Iwamoto, and X. -Y. Fu.** 1996. Cell growth arrest and induction of cyclin-dependent kinase inhibitor p21^{WAF1/CIP1} mediated by STAT1. *Science* **272**:719-722.
31. **Chomczynski, P. and N. Sacchi.** 1987. Single step method of RNA isolation by acid guanidinium thiocyanate-phenol-chloroform extraction. *Anal. Biochem.* **162**:150-159.
32. **Chong, K. L., L. Feng, K. Schappert, E. Meurs, T. F. Donahue, J. D. Friesen, A. G. Hovanessian, and B. R. G. Williams.** 1992. Human p68 kinase exhibits growth suppression in yeast and homology to the translational regulator GCN2. *EMBO J.* **11**:1553-1562.
33. **Cohen, L. and J. Hiscott.** 1992. Heterodimerization and transcriptional activation *in vitro* by NF- κ B proteins. *J. Cell. Physiol.* **152**:10-18.
34. **Cohen, L. and J. Hiscott.** 1992. Characterization of TH3, an induction specific protein interacting with the interferon- β promoter. *Virology* **191**:589-599.
35. **Cohen, L., J. Lacoste, M. Parniak, L. Daigneault, D. Skup, and J. Hiscott.** 1991. Stimulation of interferon β gene transcription *in vitro* by purified NF- κ B and a novel TH protein. *Cell Growth Differ.* **2**:323-333.
36. **Contente, S., K. Kenyon, D. Rimoldi, and R. M. Friedman.** 1990. Expression of gene *rrg* is associated with reversion of NIH3T3 transformed by LTR-c-H-*ras*. *Science* **249**:796-798.
37. **Crepieux, P., J. Coll, and D. Stehelin.** 1994. The Ets family of proteins: weak modulators of gene expression in quest for transcriptional partners. *Crit Rev Oncogen* **5**:615-638.
38. **D'Addario, M., A. Roulston, M. A. Wainberg, and J. Hiscott.** 1990. Coordinate enhancement of cytokine gene expression in human immunodeficiency virus type 1-infected promonocytic cells. *J. Virol.* **64**:6080-6089.
39. **D'Addario, M., M. A. Wainberg, and J. Hiscott.** 1992. Activation of cytokine genes in HIV-1 infected myelomonoblastic cells by phorbol ester and tumor necrosis factor. *J. Immunol.* **148**:1222-1229.
40. **Daly, C. and N. C. Reich.** 1993. Double-stranded RNA activates novel factors that bind to the interferon stimulated response element. *Mol. Cell. Biol.* **13**:3756-3764.

41. **Darnell Jr., J. E., I. M. Kerr, and G. R. Stark.** 1994. Jak-STAT pathways and transcriptional activation in response to IFNs and other extracellular signaling proteins. *Science* **264**:1415-1421.
42. **DiDonato, J. A., M. Hayakawa, D. M. Rothwarf, E. Zandi, and M. Karin.** 1997. A cytokine-responsive I κ B kinase that activates the transcription factor NF- κ B. *Nature* **388**:548-554.
43. **Driggers, P. H., D. L. Ennist, S. L. Gleason, W. -H. Mak, M. S. Marks, B. -Z. Levi, J. R. Flanagan, E. Appella, and K. Ozato.** 1990. An interferon γ -regulated protein that binds the interferon-inducible enhancer element of major histocompatibility complex class I genes. *Proc. Natl. Acad. Sci. USA* **87**:3743-3747.
44. **Dron, M., M. Lacasa, and M. G. Tovey.** 1990. Priming affects the activity of a specific region of the promoter of the human beta interferon gene. *Mol. Cell Biol.* **10**:854-858.
45. **Du, W. and T. Maniatis.** 1992. An ATF/CREB binding site is required for virus induction of the human interferon- β gene. *Proc. Natl. Acad. Sci. USA* **89**:2150-2154.
46. **Du, W., D. Thanos, and T. Maniatis.** 1993. Mechanisms of transcriptional synergism between distinct virus-inducible enhancer elements. *Cell* **74**:887-898.
47. **Duncan, G. S., H. W. Mittrucker, D. Kagi, T. Matsuyama, and T. W. Mak.** 1996. The transcription factor interferon regulatory factor-1 is essential for natural killer cell function in vivo. *J. Exp. Med.* **184**:2043-2048.
48. **Eckner, R.** 1996. p300 and CBP as transcriptional regulators and targets of oncogenic events. *Biol. Chem.* **377**:685-688.
49. **Eisenbeis, C. F., H. Singh, and U. Storb.** 1995. Pip, a novel IRF family member, is a lymphoid-specific, PU.1-dependent transcriptional activator. *Genes Dev.* **9**:1377-1387.
50. **El Kharroubi, A. and E. Verdin.** 1994. Protein-DNA interactions within DNase I-hypersensitive sites located downstream of the HIV-1 promoter. *J. Biol. Chem.* **269**:19916-19924.
51. **Enoch, T., K. Zinn, and T. Maniatis.** 1986. Activation of the human beta-interferon gene requires an interferon-inducible factor. *Mol. Cell Biol.* **6**:801-810.

52. **Escalante, C. R., J. Yie, D. Thanos, and A. K. Aggarwal.** 1998. Structure of IRF-1 with bound DNA reveals determinants of interferon regulation. *Nature* **391**:103-106.
53. **Falvo, J. V., D. Thanos, and T. Maniatis.** 1995. Reversal of intrinsic DNA bends in the IFN β gene enhancer by transcription factors and the architectural protein HMG I(Y). *Cell* **83**:1101-1111.
54. **Fan, C. -M. and T. Maniatis.** 1989. Two different virus-inducible elements are required for human β -interferon gene regulation. *EMBO J.* **8**:101-110.
55. **Fujita, T., Y. Kimura, M. Miyamoto, E. L. Barsoumian, and T. Taniguchi.** 1989. Induction of endogenous IFN- α and IFN- β genes by a regulatory transcription factor IRF-1. *Nature* **337**:270-272.
56. **Fujita, T., M. Miyamoto, Y. Kimura, J. Hammer, and T. Taniguchi.** 1989. Involvement of a cis-element that binds as H2TF/NF- κ B like factor(s) in the virus-induced interferon- β gene expression. *Nucl. Acid Res.* **17**:3335-3346.
57. **Fujita, T., L. F. L. Reis, N. Watanabe, Y. Kimura, T. Taniguchi, and J. Vilcek.** 1989. Induction of the transcription factor IRF-1 and interferon- β mRNAs by cytokines and activators of second-messenger pathways. *Proc. Natl. Acad. Sci. USA* **86**:9936-9940.
58. **Fujita, T., J. Sakakibara, Y. Sudo, M. Miyamoto, Y. Kimura, and T. Taniguchi.** 1988. Evidence for a nuclear factor(s), IRF-1, mediating induction and silencing properties to human IFN- β gene regulatory elements. *EMBO J.* **7**:3397-3405.
59. **Fujita, T., H. Shibuya, K. Hotta, K. Yamanishi, and T. Taniguchi.** 1987. Interferon- β gene regulation: tandemly repeated sequences of a synthetic 6 bp oligomer function as a virus-inducible enhancer. *Cell* **49**:357-367.
60. **Garoufalidis, E., I. Kwan, R. Lin, A. Mustafa, N. Pepin, A. Roulston, J. Lacoste, and J. Hiscott.** 1994. Viral induction of the human interferon beta promoter: modulation of transcription by NF- κ B/rel proteins and interferon regulatory factors. *J. Virol.* **68**:4707-4715.
61. **Ghosh, S., A. M. Gifford, L. R. Riviere, P. Tempst, G. P. Nolan, and D. Baltimore.** 1990. Cloning of the p50 DNA binding subunit of NF- κ B: homology to rel and dorsal. *Cell* **62**:1019-1029.

62. **Goodbourn, S. and T. Maniatis.** 1988. Overlapping positive and negative regulatory domains of the human β -interferon gene. *Proc. Natl. Acad. Sci. USA* **85**:1447-1451.
63. **Gossen, M. and H. Bujard.** 1992. Tight control of gene expression in mammalian cells by tetracycline-responsive promoters. *Proc. Natl. Acad. Sci. USA* **89**:5547-5551.
64. **Gossen, M., S. Freundlieb, G. Bender, G. Müller, W. Hillen, and H. Bujard.** 1995. Transcriptional activation by tetracyclines in mammalian cells. *Science* **268**:1766-1769.
65. **Grant, C. E., M. Z. Vasa, and R. G. Deeley.** 1995. cIRF-3, a new member of the interferon regulatory factor (IRF) family that is rapidly and transiently induced by dsRNA. *Nuc. Acids Res.* **23**:2137-2146.
66. **Grossman, A., J. Nicholl, L. Antonio, R. Luethy, S. Duggs, G. R. Sutherland, and T. Mak.** 1997. Characterization of IRF-7, a novel interferon regulatory factor. *J. Virol.* (in press)
67. **Gutterman, J. U.** 1994. Cytokine therapeutics: lessons from interferon alpha. *Proc. Natl. Acad. Sci. USA* **91**:1198-1205.
68. **Génin, P., J. Bragança, N. Darracq, J. Doly, and A. Civas.** 1995. A novel PRDI and TG binding activity involved in virus-induced transcription of IFN-A genes. *Nucl. Acid Res.* **23**:5055-5063.
69. **Haggarty, A., R. Camato, G. Paterno, L. Cohen, J. Hiscott, and D. Skup.** 1991. A developmentally regulated octamer binding activity in embryonal carcinoma cells which represses interferon- β expression. *Cell Growth Differ.* **2**:503-510.
70. **Hajnal, A., R. Klemenz, and R. Schafer.** 1993. Up-regulation of lysyl oxidase in spontaneous revertants of *H-ras*-transformed rat fibroblasts. *Cancer Res.* **53**:4670-4675.
71. **Hanash, S. M., L. Beretta, C. L. Barcroft, S. Sheldon, T. W. Glover, D. Ungar, and N. Sonenberg.** 1995. Mapping of the gene for interferon-inducible dsRNA-dependent protein kinase to chromosome region 2p21-22: a site of rearrangements in myeloproliferative disorders. *Genes Chrom. Cancer* **8**:34-37.
72. **Harada, H., T. Fujita, M. Miyamoto, Y. Kimura, M. Maruyama, A. Furia, T. Miyata, and T. Taniguchi.** 1989. Structurally similar but functionally distinct factors, IRF-1 and IRF-2, bind to the same regulatory elements of IFN and IFN-inducible genes. *Cell* **58**:729-739.

73. **Harada, H., M. Kitagawa, N. Tanaka, H. Yamamoto, K. Harada, M. Ishihara, and T. Taniguchi.** 1993. Anti-oncogenic and oncogenic potentials of interferon regulatory factors-1 and -2. *Science* **259**:971-974.
74. **Harada, H., T. Kondo, S. Ogawa, T. Tamura, M. Kitagawa, N. Tanaka, M. S. Lamphier, H. Hisamaru, and T. Taniguchi.** 1994. Accelerated exon skipping of IRF-1 mRNA in human myelodysplasia/leukemia; a possible mechanism of tumor suppressor inactivation. *Oncogene* **9**:3313-3320.
75. **Harada, H., M. Matsumoto, M. Sato, Y. Kashiwazaki, T. Kimura, M. Kitagawa, T. Yokochi, R. S. -P. Tan, T. Takasugi, Y. Kadokawa, C. Schindler, R. D. Schreiber, S. Noguchi, and T. Taniguchi.** 1996. Regulation of IFN- α/β genes: evidence for a dual function of the transcription factor complex ISGF3 in the production and action of IFN- α/β . *Genes to Cells* **1**:995-1005.
76. **Harada, H., E. -I. Takahashi, S. Itoh, K. Harada, T. -A. Hori, and T. Taniguchi.** 1994. Structure and regulation of the human regulatory factor 1 (IRF-1) and IRF-2 genes: implications for a gene network in the interferon system. *Mol. Cell Biol.* **14**:1500-1509.
77. **Harada, H., K. Willison, J. Sakakibara, M. Miyamoto, T. Fujita, and T. Taniguchi.** 1990. Absence of type I IFN system in EC cells: transcriptional activator (IRF-1) and repressor (IRF-2) genes are developmentally regulated. *Cell* **63**:903-913.
78. **Haskill, S., A. A. Beg, S. M. Tompkins, J. S. Morris, A. D. Yurochko, A. Sampson-Johannes, K. Mondal, P. Ralph, and A. S. Baldwin, Jr.** 1991. Characterization of an immediate-early gene induced in adherent monocytes that encodes I κ B-like activity. *Cell* **65**:1281-1289.
79. **Haspel, R. L., M. Salditt-Georgieff, and J. E. Darnell Jr.** 1996. The rapid inactivation of nuclear tyrosine phosphorylated STAT1 depends upon a protein tyrosine phosphatase. *EMBO J.* **15**:6262-6268.
80. **Henco, K., J. Brosius, A. Fujisawa, J.-I. Fujisawa, J. R. Haynes, T. Kovacic, M. Pasek, A. Schambock, J. Schmid, K. Todokoro, M. Walchli, S. Nagata, and C. Weissmann.** 1985. Structural relationship of human interferon- α genes and pseudogenes. *J. Mol. Biol.* **185**:227-260.
81. **Hiscott, J., D. Alper, L. Cohen, J. -F. Leblanc, L. Sportza, A. Wong, and S. Xanthoudakis.** 1989. Induction of human interferon gene expression is associated with a nuclear factor that interacts with the NF- κ B site of the human immunodeficiency virus enhancer. *J. Virol.* **63**:2557-2566.

82. **Hiscott, J., K. Cantell, and C. Weissmann.** 1984. Differential expression of human interferon genes. *Nucl. Acid Res.* **12**:3727-3746.
83. **Hiscott, J., L. Petropoulos, and J. Lacoste.** 1995. Molecular interactions between HTLV-1 Tax protein and the NF- κ B/I κ B transcription complex. *Virology* **214**:3-11.
84. **Holtzschke, T., J. Löhler, Y. Kanno, T. Fehr, N. Giese, F. Rosenbauer, J. Lou, K. -P. Knobloch, L. Gabriele, J. F. Waring, M. F. Bachmann, R. M. Zingernagel, H. C. Morse III, K. Ozato, and I. Horak.** 1996. Immunodeficiency and chronic myelogenous leukemia-like syndrome in mice with a targeted mutation of the ICSBP gene. *Cell* **87**:307-317.
85. **Horvai, A. E., L. Xu, E. Korzus, G. Brard, D. Kalafus, T. M. Mullen, D. W. Rose, M. G. Rosenfeld, and C. K. Glass.** 1997. Nuclear integration of JAK/STAT and RAS/AP-1 signalling by CBP and p300. *Proc. Natl. Acad. Sci. USA* **94**:1074-1079.
86. **Huth, J. R., C. A. Bewley, M. S. Nissen, J. N. S. Evans, R. Reeves, A. M. Gronenborn, and G. M. Clore.** 1997. The solution structure of an HMG-I(Y)-DNA complex defines a new architectural minor groove binding motif. *Nat. Struct. Biol.* **4**:657-665.
87. **Ihle, J. N.** 1996. STATs: signal transducers and activators of transcription. *Cell* **84**:331-334.
88. **Iida, S., P. H. Rao, M. Butler, P. Corradini, M. Boccadoro, B. Klein, R. S. K. Chaganti, and R. Dalla-Favera.** 1997. Deregulation of *MUM1/IRF-4* by chromosomal translocation in multiple myeloma. *Nat. Gen.* **17**:226-230.
89. **Inoue, J. I., L. D. Kerr, A. Kakizuka, and I. Verma.** 1992. I κ B γ , a 70 kd protein identical to the C-terminal half of p110 NF- κ B: a new member of the I κ B family. *Cell* **68**:1109-1120.
90. **Jin, F. -Y., C. Nathan, D. Radzioch, and A. Ding.** 1997. Secretory leukocyte protease inhibitor: A macrophage product induced by and antagonistic to bacterial lipopolysaccharide. *Cell* **88**:417-426.
91. **John, J., R. McKendry, S. Pellegrini, D. Flavell, I. M. Kerr, and G. R. Stark.** 1991. Isolation and characterization of a new mutant human cell line unresponsive to alpha and beta interferons. *Mol. Cell Biol.* **11**:4189-4195.
92. **Kamijo, R., H. Harada, T. Matsuyama, M. Bosland, J. Gerecitano, D. Shapiro, J. Le, S. I. Koh, T. Kimura, S. J. Green, T. W. Mak, T. Taniguchi,**

- and **J. Vilcek**. 1994. Requirement for transcription factor IRF-1 in NO synthase induction in macrophages. *Science* **263**:1612-1615.
93. **Kanno, Y., C. A. Kozak, C. Schindler, P. H. Driggers, D. L. Ennist, S. L. Gleason, Jr. Darnell, J.E., and K. Ozato**. 1993. The genomic structure of the murine ICSBP gene reveals the presence of the gamma interferon-responsive element, to which an ISGF3 α subunit (or similar) molecule binds. *Mol. Cell Biol.* **13**:3951-3963.
94. **Kawakami, T., M. Matsumoto, M. Sato, H. Harada, T. Taniguchi, and M. Kitigawa**. 1995. Possible involvement of the transcription factor ISGF3 γ in virus-induced expression of the IFN- β gene. *FEBS Lett.* **358**:225-229.
95. **Kee, B. L., J. Arias, and M. R. Montminy**. 1996. Adaptor-mediated recruitment of RNA polymerase II to a signal-dependent activator. *J. Biol. Chem.* **271**:2373-2375.
96. **Keller, A. D. and T. Maniatis**. 1991. Identification and characterization of a novel repressor of β -interferon gene expression. *Genes Dev.* **5**:868-879.
97. **Kessler, D. S., S. A. Veals, X. -Y. Fu, and D. E. Levy**. 1990. Interferon- α regulates nuclear translocation and DNA-binding affinity of ISGF3, a multimeric transcriptional activator. *Genes Dev.* **4**:1753-1765.
98. **Kieran, M., V. Blank, F. Logeat, J. Vandekerckhove, F. Lottspeich, O. Le Bail, M. B. Urban, P. Kourilsky, P. A. Baeuerle, and A. Israël**. 1990. The DNA-binding subunit of NF- κ B is identical to factor KBF1 and homologous to the *rel* oncogene product. *Cell* **62**:1007-1018.
99. **Kim, T. K. and T. Maniatis**. 1998. The mechanism of transcriptional synergy of an in vitro assembled interferon- β enhanceosome. *Mol. Cell.* **1**:119-129.
100. **Kimura, T., Y. Kadokawa, H. Harada, M. Matsumoto, M. Sato, Y. Kashiwazaki, M. Tarutani, R. S-P. Tan, T. Takasugi, T. Matsuyama, T. M. Mak, S. Noguchi, and T. Taniguchi**. 1996. Essential and non-redundant roles of p48 (ISGF3 γ) and IRF-1 in both type I and type II interferon responses, as revealed by gene targeting studies. *Genes to Cells* **1**:115-124.
101. **Kimura, T., K. Nakayama, J. Penninger, M. Kitagawa, H. Harada, T. Matsuyama, N. Tanaka, R. Kamijo, J. Vilcek, T. W. Mak, and T. Taniguchi**. 1994. Involvement of the IRF-1 transcription factor in antiviral responses to interferons. *Science* **264**:1921-1924.

102. **Kirchhoff, S., A. E. Koromilas, F. Schaper, M. Grashoff, N. Sonenberg, and H. Hauser.** 1995. IRF-1 induced cell growth inhibition and interferon induction requires the activity of the protein kinase PKR. *Oncogene* **11**:439-445.
103. **Kirchhoff, S., F. Schaper, and H. Hauser.** 1993. Interferon regulatory factor 1 (IRF-1) mediates cell growth inhibition by transactivation of downstream target genes. *Nucl. Acid Res.* **21**:2881-2889.
104. **Kondo, T., N. Minamino, T. Nagamura-Inoue, M. Matsumoto, T. Taniguchi, and N. Tanaka.** 1997. Identification and characterization of nucleophosmin/B23/numatrin which binds the anti-oncogenic transcription factor IRF-1 and manifests oncogenic activity. *Oncogene* **15**:1275-1281.
105. **Koromilas, A. E., S. Roy, G. N. Barber, M. G. Katze, and N. Sonenberg.** 1992. Malignant transformation by a mutant of the IFN-inducible dsRNA-dependent protein kinase. *Science* **257**:1685-1689.
106. **Kumar, A., J. Haque, J. Lacoste, J. Hiscott, and B. R. G. Williams.** 1994. Double-stranded RNA-dependent protein kinase activates transcription factor NF- κ B by phosphorylating I κ B. *Proc. Natl. Acad. Sci. USA* **91**:6288-6292.
107. **Lamphier, M. and T. Taniguchi.** 1994. The transcription factors IRF-1 and IRF-2. *The Immunol* **2**:167-171.
108. **Le Bail, O., R. Schmidt-Ullrich, and A. Israël.** 1993. Promoter analysis of the gene encoding the I κ B α /MAD-3 inhibitor of NF- κ B: positive regulation by members of the rel/NF- κ B family. *EMBO J.* **12**:5043-5049.
109. **Leblanc, J. -F., L. Cohen, M. Rodrigues, and J. Hiscott.** 1990. Synergism between distinct enhancer domains in viral induction of the human beta interferon gene. *Mol. Cell Biol.* **10**:3987-3993.
110. **Lee, C. H., Y. Igarashi, R. J. Hohman, H. Kaulbach, M. V. White, and M. A. Kaliner.** 1993. Distribution of secretory leukoprotease inhibitor in the human nasal airway. *Am. Rev. Resp. Dis.* **147**:710-716.
111. **Lee, F. S., J. Hagler, Z. J. Chen, and T. Maniatis.** 1997. Activation of the I κ B α kinase complex by MEKK1, a kinase of the JNK pathway. *Cell* **88**:213-222.
112. **Lehming, N., D. Thanos, J. M. Brickman, J. Ma, T. Maniatis, and M. Ptashne.** 1994. An HMG-like protein that can switch a transcriptional activator to a repressor. *Nature* **371**:175-179.

113. **Lehtonen A., S. Matikainen, and I. Julkunen.** 1997. Interferons up-regulate STAT1, STAT2, and IRF family transcription factor gene expression in human peripheral blood mononuclear cells and macrophages. *J. Immunol.* **159**:794-803.
114. **Lenardo, M. J., C. -M. Fan, T. Maniatis, and D. Baltimore.** 1989. The involvement of NF- κ B in β -interferon gene regulation reveals its role as widely inducible mediator of signal transduction. *Cell* **57**:287-294.
115. **Liang, C., X. Li, Y. Quan, M. Laughrea, L. Kleiman, J. Hiscott, and M. A. Wainberg.** 1997. Sequence elements downstream of the human immunodeficiency virus type 1 long terminal repeat are required for efficient viral gene transcription. *J. Mol. Biol.* **272**:167-177.
116. **Lin, R., B. Ernsting, I. N. Hirshfield, R. G. Matthews, F. C. Neidhardt, R. L. Clark, and E. B. Newman.** 1992. The *lrp* gene product regulates expression of *lysU* in *E.coli* K-12. *J. Bacteriol.* **174**:2779-2784.
117. **Lin, R., D. Gewert, and J. Hiscott.** 1995. Differential transcriptional activation *in vitro* by NF- κ B/Rel proteins. *J. Biol. Chem.* **270**:3123-3131.
118. **Lin, R., C. Heylbroeck, P. Pitha, and J. Hiscott.** 1998. Virus dependent phosphorylation of the IRF-3 transcription factor regulates nuclear translocation, transactivation potential and proteasome mediated degradation. *Mol. Cell. Biol.* (in press)
119. **Lin, R. and J. Hiscott.** 1998. A role for casein kinase II phosphorylation in the regulation of IRF-1 transcriptional activity. *Mol. Cell. Biochem.* (in press)
120. **Lin, R., A. Mustafa, H. Nguyen, and J. Hiscott.** 1994. Mutational analysis of interferon (IFN) regulatory factors 1 and 2: Effects on the induction of IFN- β gene expression. *J. Biol. Chem.* **269**:17542-17549.
121. **Lin, Y. -C., K. Brown, and U. Siebenlist.** 1995. Activation of NF- κ B requires proteolysis of the inhibitor I κ B- α : signal-induced phosphorylation of I κ B- α alone does not release active NF- κ B. *Proc. Natl. Acad. Sci. USA* **92**:552-556.
122. **Liou, H. -C., G. P. Nolan, S. Ghosh, T. Fujita, and D. Baltimore.** 1992. The NF- κ B p50 precursor, p105, contains an internal I κ B-like inhibitor that preferentially inhibits p50. *EMBO J.* **11**:3003-3009.
123. **Liou, H. C. and D. Baltimore.** 1993. Regulation of the NF- κ B/rel transcription factor and I κ B inhibitor system. *Curr. Opin. Cell Biol.* **5**:477-487.

124. **Ma, J. and M. Ptashne.** 1987. Deletion analysis of GAL4 defines two transcriptional activating segments. *Cell* **48**:847-853.
125. **MacDonald, N. J., D. Kuhl, D. Maguire, D. Naf, P. Gallant, A. Goswamy, H. Hug, H. Buëler, M. Chaturvedi, J. de la Fuente, H. Ruffner, F. Meyer, and C. Weissmann.** 1990. Different pathways mediate virus inducibility of the human IFN- α 1 and IFN- β genes. *Cell* **60**:767-779.
126. **Maniatis, T., L. -A. Whittenmore, W. Du, C. -M. Fan, A. D. Keller, V. J. Palombella, and D. Thanos.** 1992. Positive and negative control of human interferon β gene expression. In *Transcriptional Regulation*. K. R. Yamamoto and S. L. McKnight, editors. Cold Spring Harbor Laboratories, Cold Spring Harbor, N.Y.. 1193-1220.
127. **Martin, E., C. Nathan, and Q. -W. Xie.** 1994. Role of interferon regulatory factor 1 in induction of nitric oxide synthase. *J. Exp. Med.* **180**:977-984.
128. **Matsuyama, T., A. Grossman, H. -W. Mittrücker, D. P. Siderovski, F. Kiefer, T. Kawakami, C. D. Richardson, T. Taniguchi, S. K. Yoshinaga, and T. W. Mak.** 1995. Molecular cloning of LSIRF, a lymphoid-specific member of the interferon regulatory factor family that binds the interferon-stimulated response element (ISRE). *Nucl. Acid Res.* **23**:2127-2136.
129. **Matsuyama, T., T. Kimura, M. Kitagawa, N. Watanabe, T. Kundig, R. Amakawa, K. Kishihara, A. Wakeham, J. Potter, C. Furlonger, A. Narendran, H. Suzuki, P. Ohashi, C. Paige, T. Taniguchi, and T. Mak.** 1993. Targeted disruption of IRF-1 or IRF-2 results in abnormal type I IFN induction and aberrant lymphocyte development. *Cell* **75**:83-97.
130. **McKinsey, T. A., J. A. Brockman, D. C. Scherer, S. W. Al-Murrani, P. L. Green, and D. W. Ballard.** 1996. Inactivation of I κ B β by the Tax protein of human T-cell leukemia virus type 1: a potential mechanism for constitutive induction of NF- κ B. *Mol. Cell. Biol.* **16**:2083-2090.
131. **McNeely, T. B., M. Dealy, D. J. Dripps, J. M. Orenstein, S. P. Eisenberg, and S. M. Wahl.** 1995. Secretory leukocyte protease inhibitor: a human saliva protein exhibiting anti-human immunodeficiency virus 1 activity *in vitro*. *J. Clin. Invest.* **96**:456-464.
132. **McNeely, T. B., D. C. Shugars, M. Rosendahl, C. Tucker, S. P. Eisenberg, and S. M. Wahl.** 1997. Inhibition of human immunodeficiency virus type 1 infectivity by secretory leukocyte protease inhibitor occurs prior to viral reverse transcription. *Blood* **90**:1141-1149.

133. **Meraz, M. A., J. M. White, K. C. Sheehan, E. A. Bach, S. J. Rodig, A. S. Dighe, D. H. Kaplan, J. K. Riley, A. C. Greenlund, D. Campbell, K. Carver-Moore, R. N. DuBois, R. Clark, M. Aguet, and R. D. Schreiber.** 1996. Targeted disruption of the *Stat1* gene in mice reveals unexpected physiologic specificity in the JAK-STAT signalling pathway. *Cell* **84**:431-442.
134. **Mercurio, F., H. Zhu, B. W. Murray, A. Shevchenko, B. L. Bennett, J. W. Li, D. B. Young, M. Barbosa, and M. Mann.** 1997. IKK-1 and IKK-2: cytokine-activated I κ B kinases essential for NF- κ B activation. *Science* **278**:860-866.
135. **Merika, M., A. J. Williams, G. Chen, T. Collins, and D. Thanos.** 1998. Recruitment of CBP/p300 by the IFN β enhanceosome is required for synergistic activation of transcription. *Mol. Cell.* **1**:277-287.
136. **Meurs, E. F., J. Galabru, G. N. Barber, M. G. Katze, and A. G. Hovanessian.** 1993. Tumor suppressor function of the interferon-induced double-stranded RNA-activated protein kinase. *Proc. Natl. Acad. Sci. USA* **90**:232-236.
137. **Mittrücker, H. -W., T. Matsuyama, A. Grossman, T. M. Kündig, J. Potter, A. Shahinian, A. Wakeham, B. Patterson, P. S. Ohashi, and T. W. Mak.** 1997. Requirement for the transcription factor LSIRF/IRF4 for mature B and T lymphocyte function. *Science* **275**:540-543.
138. **Miyamoto, M., T. Fujita, Y. Kimura, M. Maruyama, H. Harada, Y. Sudo, T. Miyata, and T. Taniguchi.** 1988. Regulated expression of a gene encoding a nuclear factor, IRF-1, that specifically binds to the IFN- β gene regulatory elements. *Cell* **54**:903-913.
139. **Miyamoto, S., P. J. Chiao, and I. M. Verma.** 1994. Enhanced I κ B α degradation is responsible for constitutive NF- κ B activity in mature murine B-cell lines. *Mol. Cell Biol.* **14**:3276-3282.
140. **Moore, P. A., S. M. Ruben, and C. A. Rosen.** 1993. Conservation of transcriptional activation functions of the NF- κ B p50 and p65 subunits in mammalian cells and *Saccharomyces cerevisiae*. *Mol. Cell. Biol.* **13**:16661-11674.
141. **Moore, P. S., C. Boshoff, R. A. Weiss, and Y. Chang.** 1996. Molecular mimicry of human cytokine and cytokine response pathway genes by KSHV. *Science* **274**:1739-1744.

142. **Müller, U., U. Steinhoff, L. F. Reis, S. Hemmi, J. Pavlovic, R. M. Zingernagel, and M. Aguet.** 1994. Functional role of type I and type II interferons in antiviral defense. *Science* **264**:1918-1921.
143. **Nagata, S., N. Mantei, and C. Weissmann.** 1980. The structure of one of the eight or more distinct chromosomal genes for human interferon- α . *Nature* **287**:401-408.
144. **Nelson, N., M. S. Marks, P. H. Driggers, and K. Ozato.** 1993. Interferon consensus sequence binding protein, a member of the interferon regulatory factor family, suppresses interferon-induced gene transcription. *Mol. Cell Biol.* **13**:588-599.
145. **Neri, A., C. -C. Chang, L. Lombardi, M. Salina, P. Corradini, A. T. Maiolo, R. S. K. Chaganti, and R. Dalla-Favera.** 1991. B cell lymphoma-associated chromosomal translocation involves candidate oncogene *lyt-10*, homologous to NF- κ B p50. *Cell* **67**:1075-1087.
146. **Nguyen, H., R. Lin, and J. Hiscott.** 1997. Activation of multiple growth regulatory genes following inducible expression of IRF-1 or IRF/RelA fusion proteins. *Oncogene* **15**:1425-1435.
147. **Nolan, G. P., T. Fujita, K. Bhatia, C. Huppi, H. -C. Liou, M. L. Scott, and D. Baltimore.** 1993. The *bcl-3* proto-oncogene encodes a nuclear I κ B-like molecule that preferentially interacts with NF- κ B p50 and p52 in a phosphorylation-dependent manner. *Mol. Cell Biol.* **13**:3557-3566.
148. **Nolan, G. P., S. Ghosh, H. -C. Liou, P. Tempst, and D. Baltimore.** 1991. DNA binding and I κ B inhibition of the cloned p65 subunit of NF- κ B, a *rel*-related polypeptide. *Cell* **64**:961-969.
149. **Nonkwello, C., I. K. Ruf, and J. Sample.** 1997. Interferon-independent and -induced regulation of Epstein-Barr Virus EBNA-1 gene transcription in Burkitt lymphoma. *J. Virol.* **71**:6887-6897.
150. **Nonkwello, C., I. K. Ruf, and J. Sample.** 1997. The Epstein-Barr Virus EBNA-1 promoter Q μ requires an initiator-like element. *J. Virol.* **71**:354-361.
151. **Nourbakhsh, M., K. Hoffman, and H. Hauser.** 1993. Interferon- β promoters contain a DNA element that acts as a position-dependent silencer on the NF- κ B site. *EMBO J.* **12**:451-459.
152. **Ozawa, H., T. Matsuyama, T. W. Mak, S. Aizawa, T. Tokino, M. Oren, and T. Taniguchi.** 1996. Cooperation of the tumour suppressors IRF-1 and p53 in response to DNA damage. *Nature* **382**:816-818.

153. **Palombella, V. and T. Maniatis.** 1992. Inducible processing of interferon regulatory factor-2. *Mol. Cell. Biol.* **12**:3325-3336.
154. **Palombella, V. J., O. J. Rando, A. L. Goldberg, and T. Maniatis.** 1994. The ubiquitin-proteasome pathway is required for processing the NF- κ B1 precursor protein and the activation of NF- κ B. *Cell* **78**:773-785.
155. **Penninger, J. M. and T. W. Mak.** 1994. Signal transduction, mitotic catastrophies, and death in T-cell development. *Immunol. Rev.* **142**:231-272.
156. **Pepin, N., A. Roulston, J. Lacoste, R. Lin, and J. Hiscott.** 1994. Subcellular redistribution of HTLV-1-Tax protein by NF- κ B/Rel transcription factors. *Virology* **204**:706-716.
157. **Perkel, J. M. and M. L. Atchison.** 1998. A two-step mechanism for recruitment of Pip by PU.1. *J. Immunol.* **160**:241-252.
158. **Pine, R., A. Canova, and C. Schindler.** 1994. Tyrosine phosphorylated p91 binds to a single element in the ISGF2/IRF-1 promoter to mediate induction by IFN α and IFN β , and is likely to autoregulate the p91 gene. *EMBO J.* **13**:158-167.
159. **Pine, R., T. Decker, D. S. Kessler, D. E. Levy, and J. E. Darnell Jr..** 1990. Purification and cloning of interferon-stimulated gene factor 2 (ISGF2): ISGF2 (IRF-1) can bind to the promoters of both beta-interferon- and interferon-stimulated genes but is not a primary transcriptional activator of either. *Mol. Cell Biol.* **10**:2448-2457.
160. **Pinna, L. A.** 1990. Casein kinase II: An 'Eminence grise' in cellular regulation? *Biochim. Biophys. Acta.* **1054**:267-284.
161. **Pongubala, J. M. R., S. Nagulapalli, M. J. Klemsz, S. R. McKercher, R. A. Maki, and M. L. Atchison.** 1992. PU.1 recruits a second nuclear factor to a site important for immunoglobulin κ 3' enhancer activity. *Mol. Cell Biol.* **12**:368-378.
162. **Raj, N. B. and P. M. Pitha.** 1981. Analysis of interferon mRNA in human fibroblast cells induced to produce interferon. *Proc. Natl. Acad. Sci. USA* **78**:7426-7430.
163. **Reis, L. F. L., H. Harada, J. D. Wolchok, T. Taniguchi, and J. Vilcek.** 1992. Critical role of a common transcription factor, IRF-1, in the regulation of IFN- β and IFN-inducible genes. *EMBO J.* **11**:185-193.

164. **Reis, L. F. L., H. Ruffner, G. Stark, M. Aguet, and C. Weissmann.** 1994. Mice devoid of interferon regulatory factor 1 (IRF-1) show normal expression of type I interferon genes. *EMBO J.* **13**:4798-4806.
165. **Roulston, A., P. Beauparlant, N. R. Rice, and J. Hiscott.** 1993. Chronic human immunodeficiency virus type 1 infection stimulates distinct NF- κ B/rel DNA binding activities in myelomonoblastic cells. *J. Virol.* **67**:5235-5246.
166. **Ruben, S. M., P. J. Dillon, R. Schreck, T. Henkel, C. H. Chen, M. Maher, P. A. Baeuerle, and C. A. Rosen.** 1991. Isolation of a *rel*-related human cDNA that potentially encodes the 65-kD subunit of NF- κ B. *Science* **251**:1490-1493.
167. **Ruben, S. M., J. F. Klement, T. A. Coleman, M. Maher, C. -H. Chen, and C. A. Rosen.** 1992. I-rel: a novel *rel*-related protein that inhibits NF- κ B transcriptional activity. *Genes Dev.* **6**:745-760.
168. **Russo, J. J., R. A. Bohenzky, M. -C. Chien, J. Chen, M. Yan, D. Maddalena, J. P. Parry, D. Peruzzi, I. S. Edelman, Y. Chang, and P. Moore.** 1996. Nucleotide sequence of the kaposi sarcoma-associated herpesvirus (HHV8). *Proc. Natl. Acad. Sci. USA* **93**:14862-14867.
169. **Ryseck, R. -P., P. Bull, M. Takamiya, V. Bours, U. Siebenlist, P. Dobrzanski, and R. Bravo.** 1992. RelB, a new rel family transcription activator that can interact with p50-NF- κ B. *Mol. Cell. Biol.* **12**:674-684.
170. **Régnier, C., H. Y. Song, X. Gao, D. V. Goeddel, Z. Cao, and M. Rothe.** 1997. Identification and characterization of an I κ B kinase. *Cell* **90**:373-383.
171. **Schaefer, B. C., E. Paulson, J. L. Strominger, and S. H. Speck.** 1997. Constitutive activation of Epstein-Barr Virus (EBV) nuclear antigen 1 gene transcription by IRF1 and IRF2 during restricted EBV latency. *Mol. Cell Biol.* **17**:873-886.
172. **Schafer, S. L., R. Lin, P. A. Moore, J. Hiscott, and P. M. Pitha.** 1998. Regulation of type 1 interferon gene expression by interferon regulatory factor 3. *J. Biol. Chem.* **273**:2714-2720.
173. **Schindler, C. and J. E. Darnell Jr..** 1995. Transcriptional responses to polypeptide ligands: the JAK-STAT pathway. *Ann. Rev. Biochem.* **64**:621-651.

174. **Schindler, C., K. Shuai, V. R. Prezioso, and J. E. Darnell.** 1992. Interferon-dependent tyrosine phosphorylation of a latent cytoplasmic transcription factor. *Science* **257**:809-813.
175. **Schmid, R. M., N. D. Perkins, C. S. Duckett, P. C. Andrews, and G. J. Nabel.** 1991. Cloning of an NF- κ B subunit which stimulates HIV transcription in synergy with p65. *Nature* **352**:733-736.
176. **Scott, M. L., T. Fujita, H. -C. Liou, G. P. Nolan, and D. Baltimore.** 1993. The p65 subunit of NF- κ B regulates I κ B by two distinct mechanisms. *Genes Dev.* **7**:1266-1276.
177. **Sharf, R., A. Azriel, F. Lejbkowitz, S. S. Winograd, R. Ehrlick, and B. -Z. Levi.** 1995. Functional domain analysis of interferon consensus sequence binding protein (ICSBP) and its association with interferon regulatory factors. *J. Biol. Chem.* **270**:13063-13069.
178. **Sharf, R., D. Meraro, A. Azriel, A. M. Thornton, K. Ozato, E. F. Petricoin, A. C. Lerner, F. Schaper, H. Hauser, and B. -Z. Levi.** 1997. Phosphorylation events modulate the ability of interferon consensus sequence binding protein to interact with interferon regulatory factors and to bind DNA. *J. Biol. Chem.* **272**:9785-9792.
179. **Shockett, P., M. Difilippantonio, N. Hellman, and D. G. Schatz.** 1995. A modified tetracycline-regulated system provides autoregulatory, inducible gene expression in cultured cells and transgenic mice. *Proc. Natl. Acad. Sci. USA* **92**:6522-6526.
180. **Shuai, K., C. Schindler, V. R. Prezioso, and J. E. Darnell.** 1992. Activation of transcription by IFN-gamma: tyrosine phosphorylation of a 91-kD DNA binding protein. *Science* **258**:1808-1812.
181. **Shuai, K., G. R. Stark, I. M. Kerr, and J. E. Darnell.** 1993. A single phosphotyrosine residue of STAT91 required for gene activation by interferon- γ . *Science* **261**:1744-1746.
182. **Sims, S. H., Y. Cha, M. F. Romine, P. -Q. Gao, K. Gottlieb, and A. B. Deisseroth.** 1993. A novel interferon-inducible domain: structural and functional analysis of the human interferon regulatory factor 1 gene promoter. *Mol. Cell Biol.* **13**:690-702.
183. **Squire, J., E. F. Meurs, K. L. Chong, N. A. J. McMillan, A. G. Hovanessian, and B. R. G. Williams.** 1993. Localization of the human interferon-induced, dsRNA activated p68 kinase gene (PKR) to chromosome 2p21-p22. *Genomics* **16**:768-770.

184. **Steward, W. E., L. B. Gosser, and R. Z. Lockart Jr.** 1971. The effect of priming with interferon on interferon production by two lines of L cells. *J. Gen. Virol.* **15**:85-87.
185. **Sun, S. -C., P. A. Ganchi, D. W. Ballard, and W. C. Greene.** 1993. NF- κ B controls expression of inhibitor I κ B α : evidence for an inducible autoregulatory pathway. *Science* **259**:1912-1915.
186. **Suyang, H., R. Phillips, I. Douglas, and S. Ghosh.** 1996. Role of unphosphorylated, newly synthesized I κ B β in persistent activation of NF- κ B. *Mol. Cell Biol.* **16**:5444-5449.
187. **Taki, S., T. Sato, K. Ogasawara, T. Fukuda, M. Sato, S. Hida, G. Suzuki, M. Mitsuyama, T. Furuta, S. Kojima, T. Taniguchi, and Y. Asano.** 1997. Multistage regulation of Th1-type immune responses by the transcription factor IRF-1. *Immunity* **6**:1-20.
188. **Tal-Singer, R., W. Podrzucki, T. M. Lasner, A. Skokotas, J. J. Leary, N. W. Fraser, and S. L. Berger.** 1998. Use of differential display reverse transcription-PCR to reveal cellular changes during stimuli that result in herpes simplex virus type 1 reactivation from latency: upregulation of immediate-early cellular response genes TIS7, interferon, and Interferon Regulatory Factor-1. *J. Virol.* **72**:1252-1261.
189. **Tamura, T., M. Ishihara, M. S. Lamphier, N. Tanaka, I. Oishi, S. Aizawa, T. Matsuyama, T. W. Mak, S. Taki, and T. Taniguchi.** 1995. An IRF-1-dependent pathway of DNA damage-induced apoptosis in mitogen-activated T-lymphocytes. *Nature* **376**:596-599.
190. **Tan, R. S., T. Taniguchi, and H. Harada.** 1996. Identification of the lysyl oxidase gene as target of the antioncogenic transcription factor, IRF-1, and its possible role in tumor suppression. *Cancer Res.* **56**:2417-2421.
191. **Tanaka, H. and C. E. Samuel.** 1994. Mechanism of interferon action: Structure of the mouse PKR gene encoding the interferon-inducible RNA-dependent protein kinase. *Proc. Natl. Acad. Sci. USA* **91**:7995-7999.
192. **Tanaka, N., M. Ishihara, M. Kitagawa, H. Harada, T. Kimura, T. Matsuyama, M. S. Lamphier, S. Aizawa, T. W. Mak, and T. Taniguchi.** 1994. Cellular commitment to oncogene-induced transformation or apoptosis is dependent on the transcription factor IRF-1. *Cell* **77**:829-839.
193. **Tanaka, N., M. Ishihara, and T. Taniguchi.** 1994. Suppression of *c-myc* or *fos-B*-induced cell transformation by the transcription factor IRF-1. *Cancer lett.* **83**:191-196.

194. **Taniguchi, T., M. S. Lamphier, and N. Tanaka.** 1997. IRF-1: the transcription factor linking the interferon response and oncogenesis. *Biochim. Biophys. Acta Rev. Cancer* (in press)
195. **Thanos, D. and T. Maniatis.** 1992. The high mobility group protein HMG I(Y) is required for NF- κ B dependent virus induction of the human IFN- β gene. *Cell* **71**:777-789.
196. **Thanos, D. and T. Maniatis.** 1995. Virus induction of human IFN β gene expression requires the assembly of an enhanceosome. *Cell* **83**:1091-1100.
197. **Thanos, D. and T. Maniatis.** 1995. Identification of the rel family members required for virus induction of the human beta interferon gene. *Mol. Cell Biol.* **15**:152-164.
198. **Thompson, J. E., R. J. Phillips, H. Erdjument-Bromage, P. Tempst, and S. Ghosh.** 1995. I κ B- β regulates the persistent response in a biphasic activation of NF- κ B. *Cell* **80**:573-582.
199. **Thompson, R. C. and K. Ohlsson.** 1986. Isolation, properties, and complete amino acid sequence of human secretory leukocyte protease inhibitor, a potent inhibitor of leukocyte elastase. *Proc. Natl. Acad. Sci. USA* **83**:6692-6696.
200. **Thornton, A. M., R. M. L. Buller, A. L. DeVico, I. -M. Wang, and K. Ozato.** 1996. Inhibition of human immunodeficiency virus type I and vaccinia virus infection by a dominant negative factor of the interferon regulatory factor family expressed in monocytic cells. *Proc. Natl. Acad. Sci. USA* **93**:383-387.
201. **Thornton, A. M., V. V. Ogryzko, A. Dent, R. Sharf, B. -Z. Levi, Y. Kanno, L. M. Staudt, B. H. Howard, and K. Ozato.** 1996. A dominant negative mutant of an IFN regulatory factor family protein inhibits both type I and type II IFN-stimulated gene expression and antiproliferative activity of IFNs. *J. Immunol.* **157**:5145-5154.
202. **Traenckner, E. B., H. L. Phal, T. Henkel, N. K. Schmidt, S. Wilk, and P. A. Baeuerle.** 1995. Phosphorylation of human I κ B α on serines 32 and 36 controls I κ B α proteolysis and NF- κ B activation in response to diverse stimuli. *EMBO J.* **14**:2876-2883.
203. **Tran, K., . M. Merika, and D. Thanos.** 1997. Distinct functional properties of I κ B α and I κ B β . *Mol. Cell Biol.* **17**:5386-5399.

204. **Uegaki, K., M. Shirakawa, T. Fujita, T. Taniguchi, and Y. Kyogoku.** 1993. Characterization of the DNA binding domain of the mouse IRF-2 protein. *Protein Eng.* **6**:195-200.
205. **van Lint, C., C. A. Amella, S. Emilani, M. John, T. Jie, and E. Verdin.** 1997. Transcription factor binding sites downstream of the human immunodeficiency virus type 1 transcription start site are important for virus infectivity. *J. Virol.* **71**:6113-6127.
206. **Vaughan, P. S., F. Aziz, A. J. van Wijnen, S. Wu, H. Harada, T. Taniguchi, K. J. Soprano, J. L. Stein, and G. S. Stein.** 1995. Activation of a cell-cycle-regulated histone gene by the oncogenic transcription factor IRF-2. *Nature* **377**:362-365.
207. **Vaughan, P. S., C. M. J. van der Meijden, F. Aziz, H. Harada, T. Taniguchi, A. J. van Wijnen, J. L. Stein, and G. S. Stein.** 1998. Cell cycle regulation of histone H4 gene transcription requires the oncogenic factor IRF-2. *J. Biol. Chem.* **273**:194-199.
208. **Veals, S. A., T. Santa Maria, and D. E. Levy.** 1993. Two domains of ISGF3 γ that mediate protein-DNA and protein-protein interactions during transcription factor assembly contribute to DNA-binding specificity. *Mol. Cell Biol.* **13**:196-206.
209. **Veals, S. A., C. Schindler, D. Leonard, X. -Y. Fu, R. Aebersold, J. E. Darnell Jr., and D. E. Levy.** 1992. Subunit of an alpha-interferon-responsive transcription factor is related to interferon regulatory factor and myb families of DNA-binding proteins. *Mol. Cell Biol.* **12**:3315-3324.
210. **Vilcek, J. and G. Sen.** 1996. Interferons and other cytokines. In *Virology*. B. Fields, D. M. Knipe, and P. M. Howley, editors. Lippincott-Raven, Philadelphia. 375-399.
211. **Vinson, C. C. R., P. B. Sigler, and S. L. McKnight.** 1989. Scissors-grip model for DNA recognition by a family of leucine zipper proteins. *Science* **246**:911-916.
212. **Visvanathan, K. V. and S. Goodbourn.** 1989. Double-stranded RNA activates binding of NF- κ B to an inducible element in the human β -interferon promoter. *EMBO J.* **8**:1129-1138.
213. **Vogelmeier, C., A. Gillisen, and R. Buhl.** 1996. Use of secretory leukoprotease inhibitor to augment lung antineutrophil elastase activity. *Chest* **110**:261S-266S.

214. **Wahl, S. M., P. Worley, W. Jin, T. B. McNeely, S. Eisenberg, C. Fasching, J. M. Orenstein, and E. N. Janoff.** 1997. Anatomic dissociation between HIV-1 and its endogenous inhibitor in mucosal tissues. *Am. Journ. Path.* **150**:1275-1284.
215. **Wan, J. S., S. J. Sharp, G. M. -C. Poirier, P. C. Wagaman, J. Chambers, J. Pyati, Y. -L. Hom, J. E. Galindo, A. Huvar, P. A. Peterson, M. R. Jackson, and M. G. Erlander.** 1996. Cloning differentially expressed mRNAs. *Nat. Biotech.* **14**:1685-1691.
216. **Wang, I. -M., J. C. G. Blanco, S. Y. Tsai, M. -J. Tsai, and K. Ozato.** 1996. Interferon regulatory factors and TFIIB cooperatively regulate interferon-responsive promoter activity *in vivo* and *in vitro*. *Mol. Cell Biol.* **16**:6313-6324.
217. **Watanabe, N., J. Sakakibara, A. G. Hovanessian, T. Taniguchi, and T. Fujita.** 1991. Activation of IFN- β element by IRF-1 requires a post-translational event in addition to IRF-1 synthesis. *Nucl. Acid Res.* **19**:4421-4428.
218. **Weaver, B. K., K. P. Kumar, and N. C. Reich.** 1998. Interferon regulatory factor 3 and CREB-binding protein/p300 are subunits of double-stranded RNA-activated transcription factor DRAF1. *Mol. Cell Biol.* **18**:1359-1368.
219. **Weisz, A., P. Marx, R. Sharf, E. Appella, P. H. Driggers, K. Ozato, and B. -Z. Levi.** 1992. Human interferon consensus sequence binding protein is a negative regulator of enhancer elements common to interferon-inducible genes. *J. Biol. Chem.* **267**:25589-25596.
220. **White, L. C., K. L. Wright, N. J. Felix, H. Ruffner, L. F. Reis, R. Pine, and J. P. Ting.** 1996. Regulation of LMP2 and TAP1 genes by IRF-1 explains the paucity of CD8⁺ T cells in IRF-1^{-/-} mice. *Immunity* **5**:365-376.
221. **Whiteside, S. T., J. C. Epinat, N. R. Rice, and A. Israel.** 1997. I kappa B epsilon, a novel member of the I kappa B family, controls RelA and c-Rel NF-kappa B activity. *EMBO J.* **16**:1413-1426.
222. **Whiteside, S. T., P. King, and S. Goodbourn.** 1994. A truncated form of the IRF-2 transcription factor has the properties of a postinduction repressor of interferon- β gene expression. *J. Biol. Chem.* **269**:27059-27065.

223. **Whiteside, S. T., K. V. Visvanathan, and S. Goodbourn.** 1992. Identification of novel factors that bind to the PRDI region of the human β -interferon promoter. *Nucl. Acid Res.* **20**:1531-1538.
224. **Willman, C. L., C. E. Sever, M. G. Pallavicini, H. Harada, N. Tanaka, M. L. Slovak, H. Yamamoto, K. Harada, T. C. Meeker, A. F. List, and T. Taniguchi.** 1993. Deletion of IRF-1, mapping to chromosome 5q31.1, in human leukemia and preleukemic myelodysplasias. *Science* **259**:968-971.
225. **Wong, A., N. Tam, Y. -L. Yang, A. Cuddhidy, S. Li, S. Kirchhoff, H. Hauser, T. Decker, and A. E. Koromilas.** 1997. Physical association between STAT1 and the IFN-inducible protein kinase PKR and implications for IFN and double-stranded RNA signalling pathways. *EMBO J.* 1291-1304.
226. **Woronicz, J. D., X. Gao, Z. Cao, M. Rothe, and D. V. Goeddel.** 1997. I κ B kinase- β : NF- κ B activation and complex formation with I κ B kinase- α and NIK. *Science* **278**:866-869.
227. **Yamagata, T., J. Nishida, T. Tanaka, R. Sakai, K. Mitani, M. Yoshida, T. Taniguchi, Y. Yazaki, and H. Hirai.** 1996. A novel interferon regulatory factor family transcription factor, ICSAT/Pip/LSIRF, that negatively regulates the activity of interferon-regulated genes. *Mol. Cell Biol.* **16**:1283-1294.
228. **Yamamoto, H., M. S. Lamphier, T. Fujita, T. Taniguchi, and H. Harada.** 1994. The oncogenic transcription factor IRF-2 possesses a transcriptional repression and a latent activation domain. *Oncogene* **9**:1423-1428.
229. **Yie, J., S. Liang, M. Merika, and D. Thanos.** 1997. Intra- and intermolecular cooperative binding of high-mobility-group protein I(Y) to the beta-interferon promoter. *Mol. Cell Biol.* **17**:3649-3662.
230. **Yoneyama, M., W. Suhara, Y. Fukuhara, M. Fukada, E. Nishida, and T. Fujita.** 1998. Direct triggering of the type I interferon system by virus infection: activation of a transcription factor complex containing IRF-3 and CBP/p300. *EMBO J.* **17**:1087-1095.
231. **Yoneyama, M., W. Suhara, Y. Fukuhara, M. Sato, K. Ozato, and T. Fujita.** 1996. Autocrine amplification of type I interferon gene expression mediated by interferon stimulated gene factor 3 (ISGF3). *J Biochem.* **120**:160-169.

232. **Zandi, E., D. M. Rothwarf, M. Delhase, M. Hayakawa, and M. Karin.** 1997. The IkappaB kinase complex (IKK) contains two kinase subunits, IKKalpha and IKKbeta, necessary for IkappaB phosphorylation and NF-kappaB activation. *Cell* **91**:243-252.
233. **Zhang, J. J., U. Vinkemeier, W. Gu, D. Chakravarti, C. M. Horvath, and J. E. Darnell.** 1996. Two contact regions between STAT1 and CBP/p300 in interferon gamma signalling. *Proc. Natl. Acad. Sci. USA* **93**:15092-15096.
234. **Zhang, L. and J. S. Pagano.** 1997. IRF-7, a new interferon regulatory factor associated with Epstein Barr Virus latency. *Mol. Cell. Biol.* **17**:5748-5757.
235. **Zimring, J. C., S. Goodbourn, and M. K. Offerman.** 1998. Human herpesvirus 8 encodes an interferon regulatory factor (IRF) homolog that represses IRF-1-mediated transcription. *J. Virol.* **72**:701-707.